NOTE TO USERS

This reproduction is the best copy available.

INTERDEPENDENCY OF SECURITY-CONSTRAINED ELECTRICITY AND NATURAL GAS INFRASTRUCTURES

BY

CONG LIU

DEPARTMENT OF ELECTRICAL AND COMPUTER ENGINEERING

Submitted in partial fulfillment of the
requirements for the degree of
Doctor of Philosophy in Electrical Engineering
in the Graduate College of the
Illinois Institute of Technology

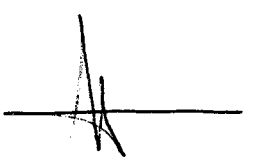

Approved _____
Adviser

Chicago, Illinois
July 2010

ACKNOWLEDGEMENT

I would like to express my deep and sincere gratitude to my supervisor, Bodine Professor Mohammad Shahidehpour, Ph.D., Chair of the Department of Electrical and Computer Engineering at Illinois Institute of Technology. His wide knowledge, logic ways of thinking and diligent spirit have been of great value for me. His understanding, encouraging and personal guidance have provided an excellent basis for the present thesis.

I wish to express my warm and sincere thanks to Associate Professor Zuyi Li, Dr. Lei Wu, Dr. Yong Fu, Dr. Jianhui Wang. Their extensive discussions around my work and valuable advices have been very helpful for this study. I warmly thank Professor Xifan Wang at Xi'an Jiaotong University for previous instructions before my Ph.D. study and his friendly encourage during my Ph.D. study.

I owe my loving thanks to my parents Yiwu Liu and Ling Zhang and my grand father and mother Wenhan Liu and Xiumei Zhang. They have lost a lot due to my research abroad. Without their encouragement and understanding it would have been impossible for me to finish this work.

TABLE OF CONTENTS

LIST OF TABLES

LIST OF FIGURES

LIST OF SYMBOLS

Chapter	Symbol	Definition
2	i	Index for units
2	j	Index for CTs
2	k	Index for STs
2	s	Index for segments
2	t	Time in sheducling period
2	x, y	Index for modes
2	f, g, h	Denoting fuel-MW curve, MW-generated steam curve, and consumed steam-MW curve, respectively.
2	hp, lp	Denoting high pressure and low pressure steam turbines, respectively, in a CCGT unit with two STs
2	I	Binary indicator for commitment of a unit, a mode, a CT, or an ST
2	I^{aug}	Binary indicator for power augmentation of a CT
2	I^{DB}	Binary indicator for duct burners
2	OR	Operating reserve (MW)
2	SR	Spinning reserve (MW)
2	P	Generation output (MW)
2	Px	Generation of a segment in a piecewise linear curve for a mode in the mode model or for a CT when the CT operates in the base area in the component model (MW)
2	Px^{aug}	Additional generation when a CT operates in the power augmentation area (MW)
2	TF	Transition fuel (MBtu)
2	Y	Binary indicator for startup
2	Z	Binary indicator for shutdown
2	δ	Binary variable indicating whether the generation of a segment reaches its maximum value
2	CTF	Transition fuel between two modes (MBtu)

Chapter	Symbol	Definition
2	CUR, CDR	Ramping up and ramping down limits between two modes, respectively (MW/h)
2	ef^{DB}	Burning efficiency of duct burners
2	F^0	Minimum fuel consumption in a piecewise linear fuel consumption curve (MBtu)
2	$F^{0,aug}$	Additional fuel consumption needed for a CT to operate in the power augmentation area (MBtu)
2	IF	Slope of a segment in a piecewise linear fuel consumption curve (MBtu/MWh)
2	IF^{aug}	Incremental fuel consumption when a CT operates in the power augmentation area (MBtu/MWh)
2	M	Large number used in MIP formulation
2	MSR	Maximum sustained ramping rate of a mode or a component (MW/min)
2	$MaxCTN1^{on}$	Maximum number of on-line CTs for a CCGT unit when all STs are off
2	$MaxCTN2^{on}$, $MaxCTN3^{on}$	Maximum number of on-line CTs for a CCGT unit when only HPST or LPST is on, respectively
2	$MaxCTN1^{sd}$, $MaxCTN2^{sd}$, $MaxCTN3^{sd}$	Maximum number of CTs that can be shut down simultaneously for a CCGT unit when its ST is kept on previous status, started up, or shut down respectively
2	$MaxCTN1^{su}$, $MaxCTN2^{su}$, $MaxCTN3^{su}$	Maximum number of CTs that can be started up simultaneously for a CCGT unit when its ST is kept on previous status, started up, or shut down respectively
2	$MinCTN1^{on}$	Minimum number of on-line CTs for a CCGT unit to operate all STs
2	$MinCTN2^{on}$	Minimum number of on-line CTs for a CCGT unit to start the first ST
2	$MinCTN3^{on}$, $MinCTN4^{on}$	Minimum number of on-line CTs for a CCGT unit to operate only HPST or LPST, respectively
2	$MinCTT^{on}$	Minimum number of hours the CTs of a CCGT unit must have been on before operating a ST

Chapter	Symbol	Definition
2	$MinHPT^{on}$	Minimum number of hours the HPST of a CCGT unit must have been on before operating a LPST
2	NCT, NST	Number of CTs and STs of a CCGT unit, respectively
2	NFT	Total Number of feasible transitions for a CCGT
2	NM	Number of modes of a CCGT unit
2	NS	Number of segments in a piece-wise linear curve
2	NT	Number of scheduling periods
2	$P_{\min}, P_{\max}$	Minimum and maximum generation of a mode or a component, respectively (MW)
2	$P_{\min}^{DB}$	Minimum generation output of a CCGT unit when the duct burner is on (MW)
2	$P_{\max}^{aug}$	Maximum generation output when a CT operates in the power augmentation area (MW)
2	$P_{\max}^{base}$	Maximum generation output when a CT operates in the base area without power augmentation (MW)
2	$Px_{\max}$	Maximum generation of a segment in a piecewise linear fuel consumption curve (MW)
2	QSC	Quick start capacity (MW)
2	SD, SU	Startup and shutdown fuels of a mode or a component, respectively (MBtu)
2	$T_{\min}^{on}, T_{\min}^{off}$	Minimum on or minimum off time of a mode or component, respectively
2	UR, DR	Ramping up and ramping down limits of a mode or a component, respectively (MW/h)
2	UT, DT	Number of hours a mode or a component would need to remain on or off initially, respectively
2	$X_{\text{ini}}^{on}, X_{\text{ini}}^{off}$	Number of hours a mode or a component has been initially on or off, respectively
2	ρ_f	Fuel price ($/MBtu)
2	CCS	Set of CCGT units
2	CTS, STS	Set of CTs and STs of a CCGT unit, respectively
2	FS, IFS	Feasible and infeasible mode transition sets of a CCGT unit

Chapter	Symbol	Definition
3, 4, 5	i, j	Index of power unit
3, 4, 5	ξ	Index of power plant
3, 4, 5	cm	Index of compressor
3, 4, 5	η	Index of natural gas supply contract
3, 4, 5	k	Index of iterations
5	n	Index of discrete point along pipeline z
3, 4, 5	gi	Index of gas supplier including gas wells, storages and liquefied natural gas tanks
3, 4, 5	el, gl	Index of electricity load and residual gas load
3, 4, 5	a, b	Index of bus in power system
3, 4, 5	na, nb	Index of node in gas network
3, 4, 5	l	Index of branch in power system
3, 4, 5	I	Status indicator of generating unit
3, 4	Y, Z	Startup and shutdown indicator of unit
3, 4, 5	P	Generation of unit
3, 4, 5	SR	Spinning reserve of unit
3, 4, 5	SU, SD	Start up and Shut down cost of unit
3, 4, 5	$X_{it}^{on}, X_{it}^{off}$	Up/down time of unit i at hour t
4	GI	Status indicator of gas well
4	GI^o, GI^I	Indicator of releasing status and charging status of storage
3, 4, 5	GP	Net output of gas well, storage
4	GP^o, GP^I	Releasing and charging gas flow of storage
3, 5	W	Cost of natural gas contract
3, 5	W_o	Cost of take-or-pay natural gas contract
3, 4, 5	$F_{ec,}()$	Unit's production cost function
3, 4, 5	$F_{gc,}()$	Gas supplier's production cost function
3, 4, 5	$F_{ef}, ()$	Natural gas consumption of a gas-fired unit or a contract
3, 4, 5	$F_{cf,}()$	Natural gas consumption of compressor

Chapter	Symbol	Definition
4	$F_{h,}()$	Power-water discharge function
3, 5	$F_{o,\eta}$	Contracted amount of take or pay gas contract
3, 4	SV, HV	Volume of gas storage and hydro reservoir
3, 4, 5	ELS, GLS	Not served electricity and gas load
3, 5	SL	Slack variable
3, 4, 5	GL	Gas load
3, 4, 5	pf_b	Power flow through branch b
3, 4, 5	π	Pressure of node in gas system
3, 4, 5	Gf, Pf	Gas flow, power flow through a branch
3, 4, 5	CH	Horsepower of compressor
3, 4, 5	γ	Control angel of phase shifter
3, 4, 5	θ	Bus voltage angle
4	q	Water discharge of hydro unit
4	s	Spillage of hydro unit
4	τ	Step size to update Lagrangian multiplier
4	w	Natural in flow to the reservoir of hydro unit
5	ρ	Gas density
5	h	Specific enthalpy
5	v	Gas axial velocity
5	z	Mileage of pipeline
5	e	Specific internal energy of gas pipeline
5	Ω	Rate of heat transfer per unit time and unit mass of the gas
5	Z	Compressibility factor of gas in pipeline
5	T	Temperature of gas in pipeline
3, 4, 5	λ, μ	Lagrangian multiplier or dual variable
3, 4, 5	ω	Penalty factor
3, 4, 5	$\boldsymbol{\chi}$	Vector of unknown variables
3, 4, 5	$\Delta\boldsymbol{\chi}$	Difference vector of unknown variables between two iterations

Chapter	Symbol	Definition
3, 4, 5	x, y	Vector of variables in power and natural gas systems
3, 4, 5	x_c, y_c	Sub-vector of x, y representing variables in coupling constraints
3, 4, 5	$e(x_c), g(y_c)$	Functions in coupling constrains
3, 4, 5	ρ_{gas}	price of gas contract, gas wellhead, charging gas storage or releasing gas storage
3, 4, 5	$w()$	Objective function of natural gas and power transmission check subproblems
3, 4, 5	a_{cm}, b_{cm}, c_{cm}	Parameters of gas consuming function of compressor cm
3, 4, 5	$k1_{cm}, k2_{cm}, k3_{cm}$	Parameters of gas flow equation of compressor cm
3, 4, 5	M	A large number
3, 4, 5	σ	Price of not served electricity and gas load
4	α, β	Parameters of augmented LR
5	α	Elevation angle of gas pipeline
5	R_g	Gas constant
5	g_e	Gravitation acceleration
3, 4, 5	x_{ab}	Reactance between bus a and b
5	$K1, K2$	Parameter in transient state model of gas pipeline
3, 4	C	Parameter in steady state model of gas pipeline
5	L	Length of pipeline
5	f_c	Fenning fraction factor of gas pipeline
5	d	Diameter of pipeline
5	Z_{avg}	Average gas compressibility factor
5	T_{avg}	Average temperature of gas in pipeline
3, 4, 5	$Pf_{l,\max}$	Power flow limits of branch l
3, 4, 5	EL, GL	Estimated electricity and residual gas load
3, 4, 5	SR_D	Required spinning reserve of system
3, 4, 5	P_{Loss}	Power transmission loss
3, 4, 5	GU	Set of gas-fired units

Chapter	Symbol	Definition
3, 4, 5	UR, DR	Max ramp up/down rate
3, 4, 5	T^{on}, T^{off}	Min on/off time of unit
3, 4, 5	$P_{\min}, P_{\max}$	Min/Max capacity of a unit
3, 4, 5	$GP_{\min}, GP_{\max}$	Max/Min net output of gas well and storage
3, 4, 5	$GL_{\min}, GL_{\max}$	Max/Min gas load
3, 4, 5	$PN_{\min}, PN_{\max}$	Max/Min pressure
3, 4, 5	$SV_{\max}, SV_{\min}$	Upper, lower volume limit of hydro reservoir
3, 4, 5	$HV_{\max}, HV_{\min}$	Upper, lower volume limits of storage
3, 4, 5	$PR_{\min}, PR_{\max}$	Max/Min pressure ratio of compressor
3, 4, 5	$CH_{\min}, CH_{\max}$	Max/Min horsepower of compressor
5	N	Number of discrete point of pipeline
3, 4, 5	NGS	Number of gas suppliers
3, 4, 5	NGL	Number of natural gas loads
3, 4, 5	NN	Number of nodes in gas transmission system
3, 4, 5	NT	Scheduling period
3, 4, 5	NC	Number of compressors
3, 4, 5	NB	Number of buses in power tramnsmission
3, 4, 5	$N\eta(\xi)$	Number of gas contracts of power plant ξ
3, 4, 5	$GC(na)$	Set of nodes connected with na
3, 4, 5	$\boldsymbol{J}, \boldsymbol{K}$	Jacobian matrix
3, 4, 5	$\boldsymbol{A}$	Bus-generator incidence matrix
3, 4, 5	$\boldsymbol{B}$	Bus-electrical load incidence matrix
3, 4, 5	$\boldsymbol{C}$	Bus-branch incidence matrix
3, 4, 5	$\boldsymbol{GA}$	Node-gas supplier incidence matrix
3, 4, 5	$\boldsymbol{GB}$	Node-gas load incidence matrix
3, 4, 5	$\boldsymbol{GK}$	Node-gas branch incidence matrix
3, 4, 5	$\boldsymbol{GD}$	Gas withdrawing node-compressor incidence matrix
3, 4, 5	$\boldsymbol{GE}$	Gas load-power unit index incidence matrix

Chapter	Symbol	Definition
3, 5	$\boldsymbol{SL}$	Vectors of slack variables
3, 4, 5	$g_{na}()$	Gas mismatch of node na

ABSTRACT

The electric power generation relies increasingly on the natural gas supply system as additional natural gas-fired power plants are installed in restructured power systems. In this context, the economics and the reliability of electric power and natural gas systems will impact one another. This dissertation addresses the interdependency of electricity and natural gas systems and proposes integrated approaches for the operation and the scheduling of the coupled energy systems.

This dissertation considers combined-cycle gas turbine units (CCGTs) as key elements for linking electric power and natural gas systems and proposes mode and component models for representing CCGTs. The two models are used in scheduling of CCGTs by mixed-integer programming (MIP).

This dissertation proposes two integrated short-term scheduling models. The first one is from the viewpoint of the ISO (Independent System Operator) which proposes a security-based methodology for the unit commitment solution when considering the natural gas transmission system and contracts. The proposed solution applies a Benders decomposition method to incorporate the natural gas transmission feasibility check subproblem in the security-constrained unit commitment (SCUC) solution. The second integrated model considers a joint-operator for the coordinated scheduling of the interdependent power and natural gas systems. The integrated operator utilizes an augmented Lagrangian relaxation (LR) based model for the coordinated least-cost allocation of natural gas resources to individual gas loads and power plants.

The natural gas flow exhibits remarkable differences from the electric power flow because of the slow response of the former system and storage nature of pipelines. This

dissertation also proposes an integrated short-term scheduling model with the transient state natural gas flow formulations which is represented by a group of partial differential equations and nonlinear algebraic equations. The implicit finite difference method is adopted to approximate partial differential equations into algebraic difference equations. The scheduling coordination problem is described as a bilevel programming formulation. The objective of the upper-level problem is to minimize the operating cost of the electric power system while the lower-level optimal natural gas scheduling problem is nested as a constraint. Based on Benders decomposition methodology, a coordination scheme is proposed and corresponding optimization algorithm is developed.

CHAPTER 1

INTRODUCTION

1.1 Research Background

Environmental and economic factors play ever-increasing roles in the energy production, transportation, and consumption. The development of sustainable, affordable, and clean sources of energy are generally considered as a prerequisite for today's economic strength and will benefit the tomorrow's society. Under the impetus of competition in the energy industry, the unbundling of electricity sector has introduced new technologies for the generation and the delivery of electricity which signify less pollutant, highly efficiency, and less costly ways of supplying the electricity. Such technologies would highlight the applications of gas-fired combined cycle plants and renewable sources of energy.

In recent years, a new trend in power generation has emerged as combined cycle gas turbine units (CCGTs) have been introduced to power systems and installed in increasing numbers throughout the world. CCGTs demonstrate their advantages based on four principles [Boy02 Cha Keh91 Lu04]. First, gas-fired generating units have lower environmental impacts. NOx, CO2, and SO2 emissions from a CCGT could be reduced to be significantly less than those of other types of thermal plants. Second, CCGTs demonstrate higher economic competitiveness over fossil units. CCGTs integrate two thermal cycles for improving the total energy conversion efficiency. Third, CCGTs can be quite instrumental in hedging rapid fluctuations in electricity and fuel markets because of their fast ramping and quick start capabilities. Fourth, CCGTs have relatively lower investment costs and require shorter installation periods. The natural

gas has been the primary choice for expanding the fossil fuel power generation. The trend is expected to continue over the next several years by further increasing the proportion of natural gas power generation in the electricity industry.

Besides natural gas-fired power generation, renewable sources of energy such as wind and solar have become more common in electric power systems. Especially, the wind energy in the United States is projected to represent 20% of consumption by 2030 [Dep08]. The large scale integration of volatile and intermittent renewable units into power systems would require additional reserves and fast response generating capacity, while the installed coal and nuclear units continue to supply the base load. Natural gas-fired generating units including CCGTs, single gas-turbine units and fuel-switching units have a remarkable fast response performance. Thereby, the natural gas-fired generation units will continue to play an indispensable role in power systems with volatile renewable power generation units.

According to the published data in United States by the Energy Information Administration (EIA) [Eia], natural gas-fired units generated 496,058 Gigawatt hours in 1995. The number increased to 920,378 Gigawatt hours in 2009 accounting for 23.3% of the total U.S. electricity consumption. Figure 1.1 shows the generation proportion by different sources in the last 15 years, which indicates the continuing and the rapid growth of natural gas used for electricity production. In certain U.S. regions (i.e., New England, New York, Texas, California-Arizona-Southern Nevada, and Alaska), the dependency on natural gas is much higher. For instance, the gas-fired generating units in ERCOT and Florida exceed 60% and 51% [Nor07] of the total capacity. The ISO New England installed 11,705 MW gas-fired units prior to 2008 that accounted for 38% of its total

installed generation capacity [ISO08a]. From the natural gas sector's view, power plants are considered as the fastest growing customer in U.S. In 2008, the natural gas used for the electric power generation account for almost one third of the total consumptions as shown in Table 1.1 [Eia].

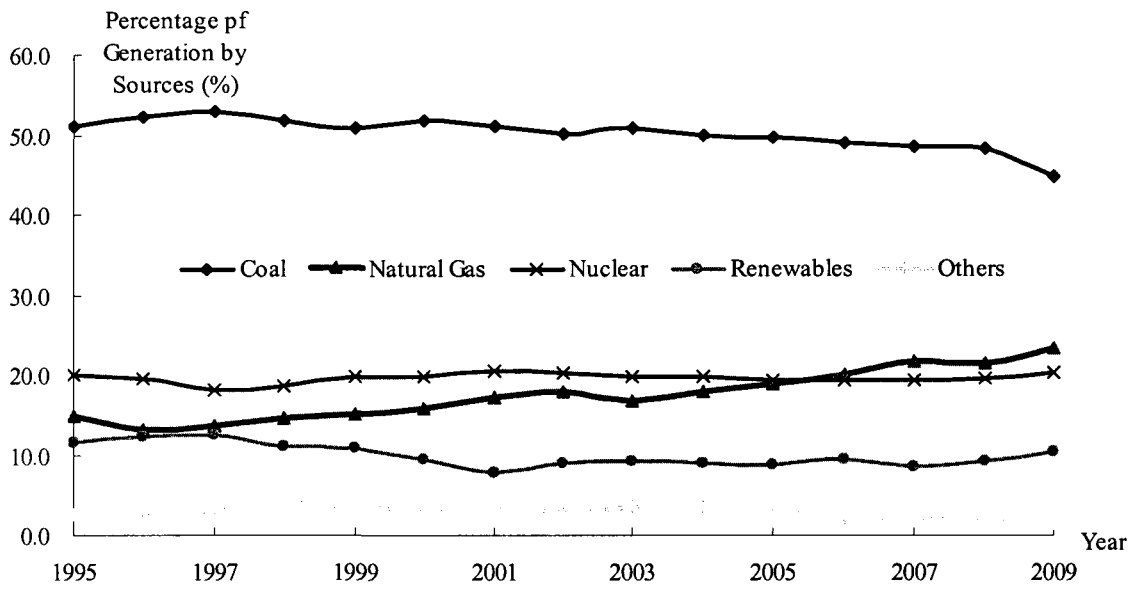

Figure 1.1. Annual Percentage of Resources for Generation in 1995-2009 in U.S.

Around the world, natural gas-fired power plants represent a comparatively rapidly increasing capacity. Especially in Europe and South America, natural gas-fired power plants account for a half of the new installed capacity from 1990 to 2004 [Rub08]. In 2005, more than 26% of the total gas consumed in South American countries was used to generate electricity. More than 90% of the natural gas supply is delivered to power plants in Argentina, Brazil, Chile, Colombia and Venezuela [Iea07].

It is evident that the electric power sector relies highly on the natural gas supply to maintain its reliability and pursue economic operations. Besides, the natural gas system

supplies an increasing level of demand in electric power systems.

Table 1.1. U.S. Natural Gas Consumption in 2004-2008 (Billion Cubic Feet/Day)

Consumption Sector	2004	2005	2006	2007	2008
Residential and Commercial	21.84	21.44	19.72	21.15	21.88
Industrial	19.79	18.07	17.84	18.21	18.17
Electric Power	**14.93**	**16.08**	**17.05**	**18.74**	**18.2**
Lease and Plant Fuel	3	3.05	3.13	3.36	3.34
Pipeline Use	1.55	1.6	1.6	1.7	1.77
Vehicle Use	0.06	0.06	0.07	0.07	0.08
Total Consumption	61.17	60.3	59.41	63.28	63.44

1.2 Electric Power and Natural Gas Systems

1.2.1 Coupled Infrastructures. Electric power and natural gas infrastructures have common features but also pose significant differences. Both energy infrastructures can be divided into four major sectors including supply, transmission, distribution and consumption. Table 1.2 lists components of different sectors in each system and show their corresponding relationships.

Power plants produce electricity by converting different primary sources of energy to electric power. In natural gas systems, gas wells are main suppliers which are commonly located at remote sites which are far from load centers. After processing, the natural gas is injected into the pipeline network. Unlike electricity, natural gas can be stored in large ungrounded storage facilities or metal tanks as liquid state. During the peak demand hours, the gas storage located near loads, and liquefied natural gas (LNG) can supplement suppliers in natural gas system.

Table 1.2. Structures of Electric Power and Natural Gas Systems

Sectors	Natural gas system	Electric power system
Supply	Gas wells, storages and LNG injection terminal	Power plants (Coal, natural gas, nuclear, renewable)
Transmission	Higher pressure network (Interstate pipelines, compressors, valves)	Higher voltage network (Transmission lines, underground cables, transformers, breakers)
Distribution	Lower pressure network (Intrastate pipelines, regulators, valves)	Lower voltage network (Transmission lines, underground cables, transformers, breakers)
Consumption	Large and small consumers	Large and small consumers

The transportation network can be classified into transmission and distribution sectors according to their pressure level and voltage level, respectively. The transmission network delivers bulk energy into regional demands or large customers. The distribution part mostly owned by utility links small customers to junctions of the transmission network. In electric power systems, a network consists of transmission lines, cables, breakers, and transformers, while a natural gas network is represented by pipelines, valves, and compressors. The network components can be modeled as either distributed or lumped parameters.

The load sectors in both electric power and natural gas systems include large and small customers. Most of residential and commercial customers are supplied by distribution networks. Industrial customers are usually large which are linked directly to transmission networks.

Natural gas-fired power plants are linkages between the two infrastructures as shown in Figure 1.2. They belong to the load sector in the natural gas system while represent suppliers in the electric power system.

The most distinctive difference between the two energy infrastructures is the traveling speed of energy flow through the respective networks. Electricity moves at the speed of light. However, natural gas travels much slower through pipelines. In addition, pipelines themselves can store natural gas which relates to line pack resource for maintaining the above normal pressure in pipelines.

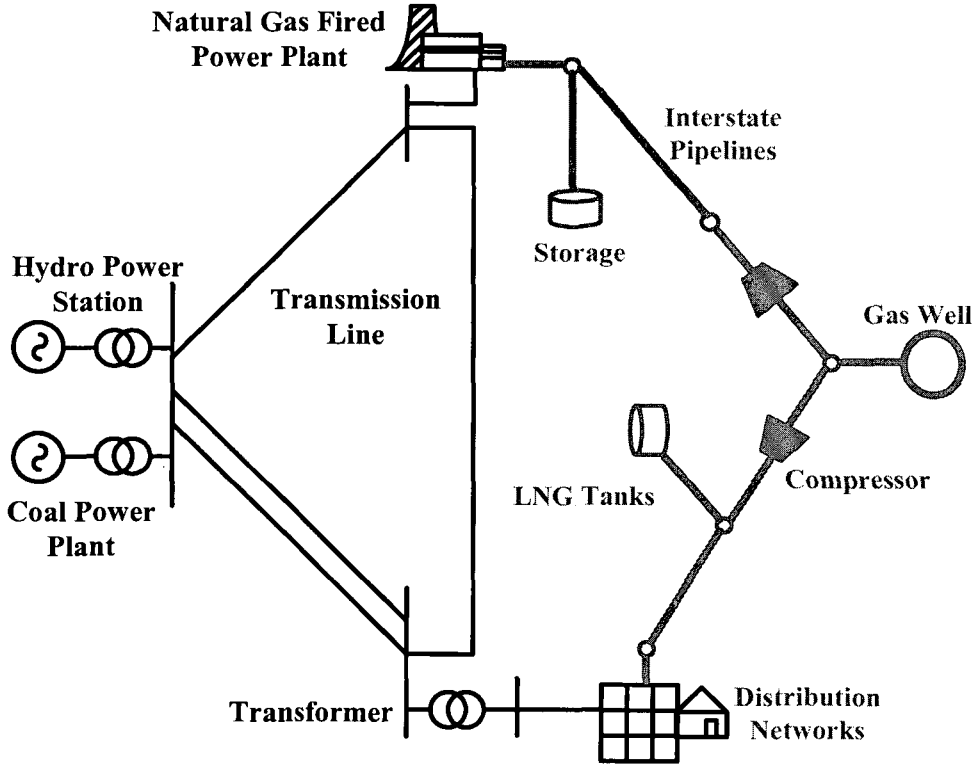

Figure 1.2. Coupled Electricity and Natural Gas Infrastructures

1.2.2 Competitive Market and Restructured Environment. Electric power systems are rapidly becoming market-driven. In a competitive electricity market, the traditional

vertically integrated monopolies are restructured into generation, transmission and distribution entities as shown in Figure 1.3 and competition is introduced through open access. The introduction of restructuring is to reduce energy charges through competition, provide customers with more choices by creating open access, price different levels of service reliability for customers, and create more business opportunities for new products and services. However, restructuring is not synonymous with deregulation. The self-interested entities including GENCOs (Generation companies), TRANSCOs (Transmission companies) and DISCOs (Distribution companies) constitute optimal strategies to maximize their profits by performing price-based unit commitment and scheduled maintenance outage planning based on forecasted market prices of energy and ancillary services.

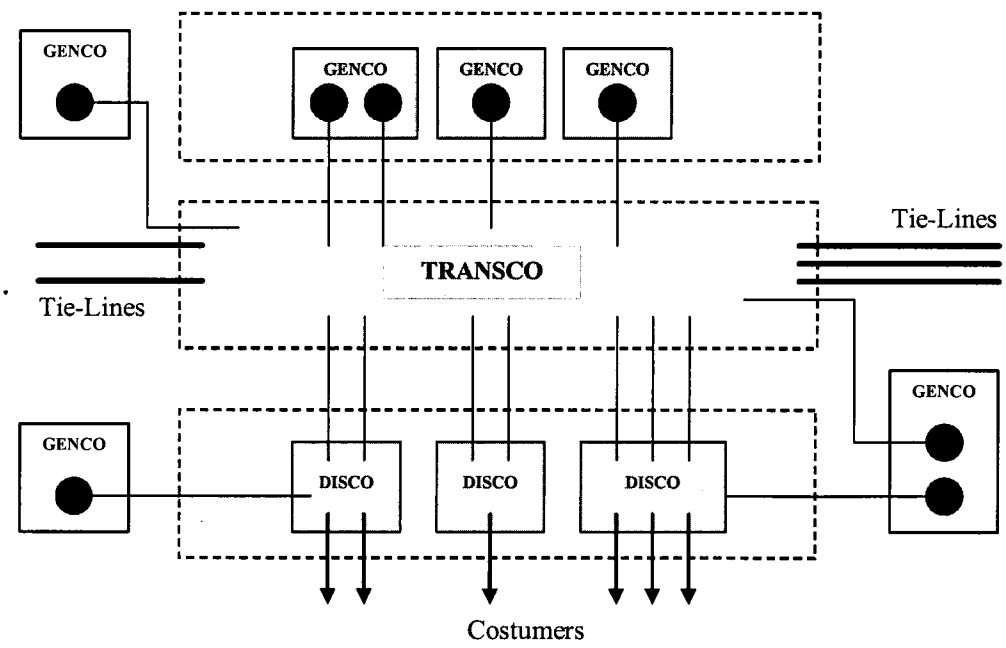

Figure 1.3. Restructured Electric Power Systems

An ISO (independent system operator) coordinates market participants for supplying the real-time load demand, and satisfying limited fuel and other resource constraints, environmental constraints, and transmission security requirements [Sha01, Sha02, Sha03].

In competitive electricity markets, customers expect a least-cost and high-quality supply of electric energy that requires the solution of security-constrained unit commitments and other sophisticated techniques executed by the ISO (such as the PJM ISO or the New York ISO) to minimize the system operation cost and enhance the power systems reliability. Security-constrained unit commitment refers to the strategic choice for determining the ON/OFF status and dispatch of available generators with minimum cost for all available generators while preserving the network security and satisfying the load demand forecasted by an ISO.

In general, the electricity energy market operated by ISO includes a Day Ahead Market (DAM) and a Real Time Market (RTM) as well as bilateral contracts arranged independent of RTM and DAM. The DAM is an hourly forward market for scheduling electricity demands and resources. To ensure the reliability of power systems the production and consumption of electric power would have to be balanced in real time. The RTM is designed to compensate differences between the day-ahead scheduled electricity and the actual real-time load requirements.

There is also reserve market (ancillary service market) where reserve products are cleared and procured through a system-wide or zonal-based auction to prevent the loss of system reliability due to contingencies. Besides, certain ISOs operate a forward capacity market for long-term reliability and a financial transmission right market to deal with

transmission congestion.

Market participants either pay or are paid the real-time locational marginal price (LMP). LMP is a price incentive for capturing the impact on operating cost of locational variations in supply, demand, and transmission limits at related bus in power systems. [Sha02]

Under the Natural Gas Wellhead Decontrol Act (NGWDC) of 1989, the natural gas supply is a deregulated business which allows the market to determine the price of natural gas at the wellhead. There is a remarkable difference between the electricity and natural gas markets. The electricity market has hourly and real time pricing in DAM and RTM. In contrast, the natural gas market is based on daily pricing of its commodity with nominations for transportation.

Natural gas transmission sectors are regulated by two entities. Interstate gas pipelines are regulated by the Federal Energy Regulatory Commission (FERC) while intrastate pipelines are regulated by State Public Utility Commissions. In 1985 and 1987 respectively, the U.S. FERC issued "Open Access Orders" 436 and 500 that took the first step toward allowing pipeline customers the choice in the purchase of natural gas and only transportation services. The interstate pipelines were regulated to offer nondiscriminatory services to all transportation requests. The transportation service gradually became the primary function and business of interstate pipelines. The FERC Order No. 636 took further steps towards unbundling of transportation and sales so that all pipeline customers could select their gas sales, transportation, and storage services from any provider in any quantity. A variety of gas purchase and transportation patterns appeared during market evolutions.

There are different classes of gas transportation services that are defined by [ISO08a]:

No-Notice: The customer can use gas whether nominated or not on a daily basis up to its firm entitlement without incurring any balancing or scheduling penalties.

Primary Firm: The customer should have no interruptions (except for force majeure) but is responsible for paying the penalties for using more gas then their nominated amount. This service can bump interruptible customers.

Secondary Firm: Similar to Primary Firm except the customer nominates at a location other than the primary point that was specified in their contract or nominates at a value that was greater than what they were entitled to at specific points.

Interruptible: The customer can be interrupted with little notice and can be bumped by higher priority services.

With unbundling environment and competition, however, the natural gas transmission sectors are no longer responsible for assuring sufficient supplies on interstate pipeline for noncore interruptible customers such as electric generators. These customers will have to acquire interstate pipeline capacity while locational gas distribution companies (LDCs) or utilities are responsible for assuring that the intrastate gas system is adequate to draw the flow from the interstate pipelines.

Natural gas sectors usually run an optimization program to make short term or long term schedule for natural gas system operation. The objective function is usually to minimize energy consumed cost of compressors, gas allocation cost, or maximize their revenues while satisfying premium of network constraints and pressure requirements of receiving points.

1.3 Electricity/Natural Gas Interdependencies

Natural gas-fired power plants erect a bridge between the electric power system and the natural gas system. The interdependent relationship between the two systems is examined and described as follows.

1.3.1 Market. The natural gas price fluctuation profile in gas markets is a key driver of electricity price movements in electricity markets. Natural gas-fired units usually serve intermediate and peak electricity demands, so a gas price hike could push up their marginal cost of generating electricity. In a competitive environment, the gas price will directly affect a GENCO's bidding strategies which is one of factors in market clearing. Figure 1.4 shows the monthly average electricity and natural gas prices at the New England region in the day-ahead market in 2006 and 2007.

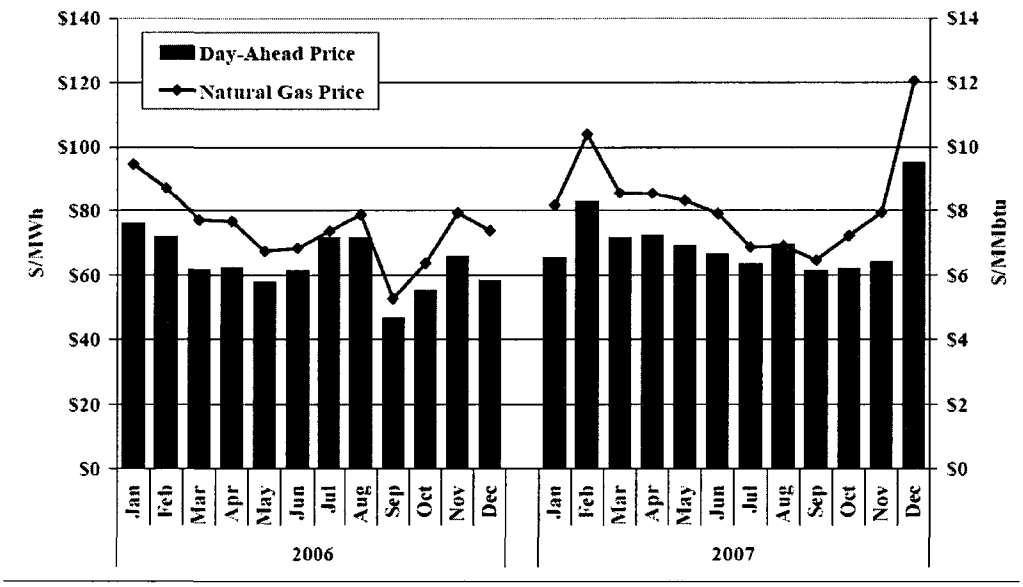

Figure 1.4. Monthly Average Electricity and Natural Gas Prices in New England 2006 - 2007 [Iso08b]

Another important price factor in electricity markets is natural gas supply disruptions during critical gas operating hours or seasons. Gas LDCs traditionally sign a no-notice or firm transportation service contracts to guarantee the supply of their core customers. In some regions during the winter, LDCs buy almost the entire capacity of pipelines in order to supply space heating demands of residual and commercial customers. However, most of gas-fired generators do not utilize firm transportation contracts for economic reasons because the expected price in electricity markets is relatively low. Interruptible natural gas transportation contracts could lead to bumps or delays of ongoing natural gas supply and the disruption of electricity generation by gas-fired units. To balance electricity generation and demands, the electric market would need to switch from gas-fired units to less efficient units which utilize other types of fuel such as coal and oil, which would translate into higher market prices for electricity.

The gas-fired units participate in both the electricity market and the natural gas market. On the one hand, GENCOs can seek to arbitrage the price difference between electric and gas markets in real-time at particular locations. When the market implies higher natural gas prices and lower electricity prices, the power generator could buy electricity, rather than producing it, and sell natural gas to the spot market [Che07, Iso08a]. On the other hand, the risk management for gas-fired units is likely more complicated than those units with other types of fuel, because gas-fired units face a gas consumption balancing issue in the real time generation, gas nomination in dynamic forward natural gas market, and gas transportation via pipelines. Owners or operators of gas-fired generation units must constantly deal with hourly, daily, weekly or monthly imbalance resolutions. In the winter, uncertainty threat of gas supply in gas markets and

gas transportation may impact the market participants' profit and behavior when they play in DAM, RTM and reserve markets.

1.3.2 Operation. Gas fuel adequacy and availability will directly affect a generation unit's commitment, dispatch, and generation cost. Gas adequacy has two components, supply (gas well and storage) and the infrastructure to transport it. Thus, the natural gas transmission congestion or the gas well maximum output can impact the schedule and the operating status of power systems.

In natural gas operating center, gas-fired units with interruptible transportation contract are usually treated as the top curtailment candidate. Once the congestion has occurred in natural gas transmission systems or the gas well has reached its maximum output, the natural gas drawn by gas-fired units with non-firm transportation contracts are expected to be limited or bumped. Moreover, operating new gas turbine units or CCGT usually depends on high gas pressure based on their specific design, so electric generators are more susceptible to the pressure drops in their delivery point than other gas load. Even gas delivery service priority of gas-fired units is same as other gas loads, weaker bearing ability of pressure drops make gas curtailment of gas-fired units more possibly happened.

From another point of view, the scheduling of natural gas transmission systems will be based on the unit commitment and the dispatch of gas-fired units in electric power systems. Gas-fired units usually serve intermediate or peak electrical loads, which would lead to fluctuating gas consumptions. The natural gas system would have to schedule compressors, line-pack resources as well as gas wells in advance to satisfy the constraints on gas-fired units and other gas loads within a reasonable pressure range.

It is inevitable that forced outages occur in both power and natural gas systems. In contingency cases, potential interactions between the two systems are expected to be strengthened. There are two scenarios to be considered as follows:

1) Contingencies in power systems. Direct loss of a gas-fired generating unit would result in a step change in gas demand, while the power system frequency would drop. Then, the other power system units will be rescheduled to pick up the lost power. The loss of non-gas-fired units or transmission lines will also call on reserves to maintain the security and to balance the power in real time. Lines pack resource in a pipeline is crucial to deal with large swings in gas demand. To ensure the integrity of gas pipelines in winter, some pipelines will not allow gas-fired units to come online to absorb their curtail line pack resource unless their fuel nomination has been confirmed. This in effect, turns these quick start gas-fired units into the ones with longer response times and can prevent them from providing quick spinning and operating reserves to power systems.
2) Contingencies in natural gas systems. Due to the proliferation of new gas-fired units supplied by a common source or regional gas pipelines, the sudden loss of a gas supply, compressor or pipeline may cause the loss of several gas-fired generators. This case may be beyond the traditional N-1 planning standards and could seriously jeopardize the security of power systems. The electrical load shedding may possibly happen in order to balance the real time demand and maintain the security of power system. When a contingency occurs, certain gas units can quickly switch to burn and others without dual-fuel capacities must be taken off the online to switch burners.

1.3.3 Maintenance and Planning. The midterm and long-term economics and reliability of power systems are impacted by the installation of new generation resources, transportation network expansions, long-term load profile, scheduled outages as well as unscheduled outages.

The addition of new component will impact the natural gas supply system. For instance, a new interstate pipeline could alleviate the burden on existing pipelines. In such cases, the curtailment of natural gas supply to power generation units may be diminished and the reliability of power system could be enhanced, even if gas-fired units still hold interruptible contracts that are subordinate to residual and commercial gas loads. On the contrary, the scheduled outage of a compressor may reduce the natural gas transportation capacity and result in a lower reliability of power system if the supply to gas-fired units is interrupted.

In addition, the planning of additional gas-fired power plants in electric power systems would require an adequate supply of natural gas. In general, the pipeline expansion which is in response to the load growth is regulated by FERC. FERC will generally not authorize new pipelines or facilities to improve the existing capacity unless customers are already obliged to such expansions. Thus, in an optimal situation, the gas-fired power plant planning should be bundled with the gas pipeline expansion planning.

1.4 Integrated Modeling of Interdependent Systems

In the previous section, we discussed the interdependency of electricity and natural gas. For pursuing the economic efficiency and increasing the reliability, it is of paramount necessity to incorporate the natural gas system model into the reliability evaluation, operation, and optimization of electric power systems. In this regard, new

integrated models and novel solution methodologies would be required.

1.4.1 Literature Review. The reliability assessment report [Nor02] put forward in 2002 the interdependency of electricity and natural gas. In [Nor04, Sha05], the security of interdependent gas and electricity infrastructures were addressed. [Rub08] surveyed the interdependency of electricity and gas systems in South American and analyzed the latest research and development on this topic. [ISO08a] introduced a case study on the interactions of electricity market and natural gas market in New England. These reports and chapters focus on the proposed problem but lack much of detailed models and analytical solutions.

In [An03, Uns07a] a nonlinear continuous optimization model was proposed by merging the traditional optimal power flow and the natural gas optimal flow. However, the model is based on a single hour horizon. The objective function of [An03] is to maximize the social welfare. The case studies show the difference between the independent model for the two systems and the proposed integrated model. The natural gas pipelines are modeled as non-linear components at steady state, but the compressor station is not included. [Mel06 Mun03] present the two-phase integrated models to calculate the maximum generation output of an electric power plant subject to natural gas system constraints. Active and passive arcs are used to represent natural gas pipelines and compressors.

The short-term scheduling of hydrothermal power systems with linear gas transmission constraints was considered in [Uns07b] where the problem is formulated as a multi-stage scheduling in which the objective function is to minimize the total operating cost to meet electricity demand forecasts. The heat-rate curve of gas-fired units is based

on the simple proportional function. The unit commitment problem was decomposed into subproblems for each unit by relaxing the electricity load balance and reserve constraints. Linear natural gas transmission constraints with a pipeline loss factor are modeled into subproblems for gas-fired units. In [Li08], a security-constrained unit commitment (SCUC) model with hourly and daily natural gas usage limits, instead of gas network constraints, are proposed. The detailed mixed-integer programming formulation of combined-cycle gas units and fuel switching units are incorporated into the unit commitment (UC) model. [Sha05] also gave a SCUC model with relatively simple gas network considerations. The piecewise linear approximation of nonlinear gas flow-pressure is modeled in the UC problem [Urb07]. [Gei07] introduces a general optimization approach for power dispatch that included multiple energy carriers such as electricity, natural gas, and district heating. Additionally, the optimality conditions for the multiple energy carrier dispatch were derived for a simplified natural gas transmission system.

For a long-term model, [Gil03] proposed multi-period generalized network flow model of the U.S integrated energy system with natural gas, coal, and power infrastructures. [Que06 Que07] further developed this model by proposing nodal prices in an integrated energy system. The application focused on long-term macroscopic analyses for the national economic and large-scale disruptions. However, this model is an approximate because of assumptions on virtual infrastructure topology and linear network flows. [Bez06] presented a methodology that modeled the natural gas supply, demand and transmission network in the stochastic hydrothermal scheduling. The objective function is to minimize the expectation of operating cost for a several year horizon. The

natural gas is also modeled as linear equations, and storage facilities are not taken into account.

A stochastic optimization model for electric utility was proposed in [Che07]. The model maximizes utility benefits by considering financial risks associated with the gas supply portfolio of electricity utility. The impact of natural gas transmission system on power markets was discussed in [Mor03].

The long-term integrated planning is analyzed in [Hec01 Uns07c] as decisions are highly interdependent in natural gas and power transmission systems. These approaches are based on a multi-period deterministic optimization in which the objective function is to minimize the gas-electricity investment and operating costs. However, gas prices are stated as input parameters, while in the practice they exhibit a stochastic nature and would depend on the gas pipeline expansion decisions.

1.4.2 Challenges and Unsolved Problems. The integrated modeling of interdependent electricity and natural gas systems is relatively new and previous models discussed earlier are imperfect. There are several unresolved problems and difficult modeling issues that we would need to address:

1) Modeling of natural gas-fired units. Natural gas-fired units represent key linkages between natural gas and electricity infrastructures. In the new operating environment, natural gas-fired units may generate electricity and heat products with flexible operating modes by burning either gas or oil. The modeling of such systems especially for newly emerged CCGTs would require further investigations.
2) Natural gas steady state model. From the literature review, the natural gas

transmission network in most existing models is considered as a linear system or simplified nonlinear equations. In power systems, simplified linear power flow equations are applicable because branch flows are approximated as a linear function of the voltage angel difference between two linked buses. However, the simplified natural gas flow model lacks a similar theoretical support. In addition, unlike power systems, there are storages facilities in natural gas systems which can not be ignored. Thus, the exact nonlinear steady-state model of natural gas system should be adopted which may introduce more difficulties in the solution of the integrated model.

3) Natural gas transient. Since natural gas flows travel slowly and some of interstate pipelines have line pack capacity, the steady-state flow assumption may lead to inaccurate results. Rigorously, in short-term integrated operation model, it is required to consider pipeline distributed parameters and a transient model.
4) Coordination schemes. Different coordination schemes between natural gas and electric power sectors may bring about different objective functions and model structures. For instance, electric power and natural gas systems can be modeled as an integrated system to pursue their overall benefits. Also, two systems can be considered individually with respective contracts and constraints. An iterative coordination and communications is executed until they obtain respective feasible solutions acceptable by both systems. For diversity, further research on different coordination schemes would be needed.
5) Algorithms and decomposition strategies. The integrated model is frequently a mixed-integer nonlinear programming problem with large-scale complex

transmission network constraints. It is hard to solve the entire system as one piece. Most references do not concentrate on developing appropriate algorithms to solve the integrated model. Their studied cases are usually small and simple. Optimization techniques applied to the operation and planning of a single energy carrier system have been well developed. It is convenient to utilize decomposition techniques to separate the integrated model into several subproblems which can be handled more easily.

6) Integrated model in midterm and long term time scale. Midterm and long-term integrated models require stochastic representations and appropriate simplifications based on the short-term model. More research is required on this subject.

1.5 Proposed Research

This dissertation focuses on short-term studies and deals with standing issues described earlier. The outline of this dissertation and its main contributions are presented as follows.

First of all, natural gas-fired units consist of traditional single-cycle gas turbine units, fuel switching units and combined-cycle gas turbine units. Either single-cycle gas turbines or fuel switching units can be considered as special forms of CCGTs with simplified configurations. We develop mode and component models of CCGTs based on the mixed-integer linear programming (MIP) formulation in Chapter 1. Cogeneration and various enhancement tools can also be represented by the proposed model.

Second, the natural gas transmission system is modeled by various methods in this dissertation. Chapter 3 presents the steady-state nonlinear natural gas transmission

model which is based on the node and branch topology and the nodal mass flow balance. Gas wells, LNG, pipelines, compressors as well as storages are represented as nonlinear equations and inequalities. Moreover, Chapter 4 adds discrete variables to the gas transmission model presented in Chapter 3 which would result in a more reasonable representation of practical natural gas system operations. Chapter 5 adopts a natural gas transient model to instead steady state model due to considerations of line pack of pipelines and slow traveling speed of gas flow. Transient model is a group of partial differential equations and nonlinear algebraic equations. Partial differential equations are transformed into difference equations by introducing implicit numerical methods.

Third, coordination schemes in Chapters 3 and 5 are different from that in Chapter 4. Chapter 3 presents a security-based methodology from the ISO viewpoint for the solution of SCUC when considering the impact of natural gas transmission system and respecting gas contracts. The objective function of the model is to minimize the operating cost of a power system. Chapter 5 further develops the coordination scheme. Based on the SCUC solution, the ISO would submit gas fuel demands to gas transmission sectors. The gas transmission operator examines the feasibility by checking gas network constraints and gas transportation contracts. If there are no violations, the natural gas sector will confirm the gas demand level and optimize its operation schedule based on the confirmed gas usage. Otherwise, the natural gas sector will return energy constraints generated by sensitivity analyses to the ISO. A distinct coordination scheme for a comprehensive scheduling of gas and electric operations is presented in Chapter 4, where the objective function is to minimize the social cost or maximize the social welfare during the time horizon. The social cost that is the sum of operating costs of natural gas

system and electric power system. The integrated operator will coordinate its operation schedules and allocate natural gas resources optimally to either serve gas loads or generate electric power.

Furthermore, the dissertation applies Benders decomposition and dual decomposition based on the augmented Lagrangian relaxation to solve different integrated models respectively. The Benders decomposition method separates the natural gas transmission feasibility check subproblem and the power transmission feasibility check subproblem from the hourly UC in the master problem. The subproblems are nonlinear continuous optimization models which are solved by successive linear programming. The Lagrangian dual decomposition separates the optimization problem into a SCUC subproblem and the gas allocation subproblem. Both subproblems can be mixed-integer nonlinear programming problem. The related formulations can be found in Chapter 3 and Chapter 4.

Finally, the proposed models in this dissertation will provide a foundation for long-term reliability and planning studies.

CHAPTER 2

MODE AND COMPONENT MODEL FOR SHORT-TERM SCHEDULING OF COMBINED-CYCLE UNITS

2.1 Introduction

Benefiting from a quick start-up capability in competitive markets and public outcry for cleaner energy production, CCGTs have mushroomed in the past 20 years and become an important generation technology in today's power system operation.

A CCGT consisting of multiple combustion turbines (CTs) and steam turbines (STs) can operate at multiple operating modes. Figure 2.1 depicts a CCGT with 2 CTs and 1 ST. The scheduling of CCGTs will determine the hourly on/off status of CTs and STs based on operating constraints of individual components and combined modes. Accordingly, the scheduling of CCGTs becomes a cumbersome and more complicated optimization problem when compared to the scheduling of traditional thermal units.

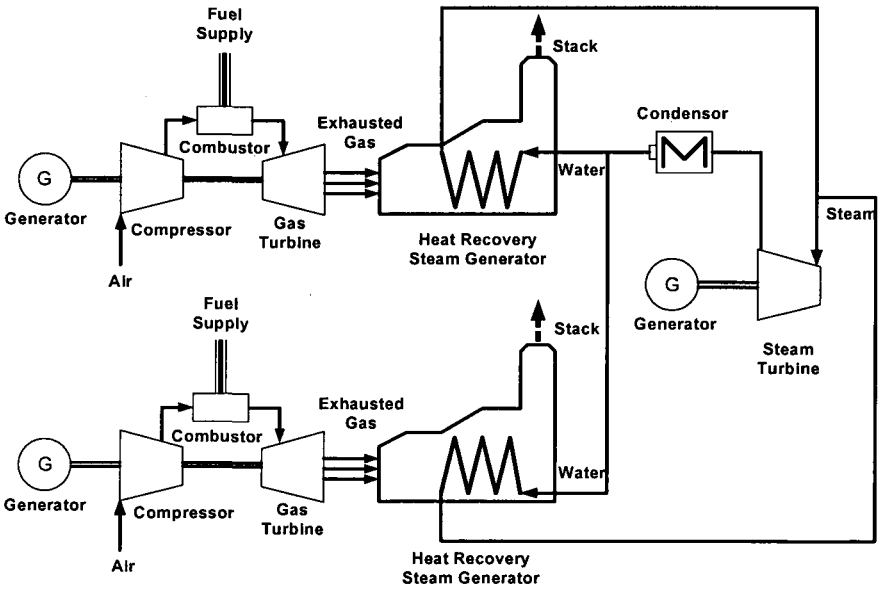

Figure 2.1. CCGT with 2 CTs and 1 ST

The combined-cycle mode (CCM) model for scheduling problem includes a certain number of modes based on operating practices and constraints. The combined-cycle mode (CCM) model includes a certain number of modes based on operating practices and constraints. The CCM model was applied in [Lu04 Li05] to solve the unit commitment of CCGTs in which the problem was to find the optimal operating mode for minimizing operating costs. Each mode was considered as a pseudo unit with its own characteristics and parameters such as minimum on/off time and ramping constraints. There were additional constraints for transitions between certain modes. In this case, the scheduling of CCGT was equivalent to the scheduling of multiple pseudo units with coupling constraints. Previous unit commitment studies applied Lagrangian relaxation to the scheduling of CCGTs which was decomposed into a set of subproblems for representing individual modes [Bje00 Coh96 Lu04]. The individual subproblems were solved by dynamic programming to calculate the optimal hourly commitment based on state transition diagrams. The mixed-integer programming (MIP) formulation of CCGT and fuel switching units, based on the mode model, was given in [Li05].

In this chapter, we present a combined-cycle component (CCC) model for the unit commitment of CCGTs, and compare the results with those of the CCM model. The basic idea in the CCC representation is to model each CT and ST individually in the optimization problem rather than lumping them into modes. We apply the MIP approach to model and solve the unit commitment problem because of its advantages over the LR approach including global optimality, direct measure of the optimality of a solution, and more flexible and accurate modeling capabilities [Bix07 Str05 Wil99].

The rest of the chapter is organized as follows. The characteristics of CCGTs are

given in Section 2.2. Section 2.3 presents the MIP formulations of CCM and CCC models. Comparison between the two models is also given in Section 2.4. Section 2.5 gives illustrative numerical examples. The conclusions are provided in Section 2.6.

2.2 Characteristics of CCGTs

2.2.1 Components of CCGT. Most combined-cycle plants represent the integration of Brayton cycle gas turbine and Rankine cycles steam turbine for achieving efficient, flexible, reliable, and economic power generation and cogeneration. The Brayton cycle is a topping cycle with a higher temperature and the Rankine cycle is a bottoming cycle with a lower temperature. After the integration of two cycles, the total energy conversion efficiency of combined-cycle plants can reach 55% which is 20%-30% higher than that of traditional single-cycle thermal plants [Keh91].

A CT consists of an axial compressor, combustion chambers, and a turbine. At the initial stage, air is drawn into the compressor and compressed air from the compressor is mixed with natural gas in a combustion chamber, where the combustion process takes place. The hot gas resulting from the combustion process is expanded through a turbine to drive the generator and the compressor. The ST in most combined-cycle applications is similar to that in a conventional steam plant, transferring the energy of steam to kinetic energy. As large CCGT plants frequently generate steam at multiple pressure levels, STs could include dual or triple pressure sections so as to operate at a higher thermal efficiency level [Boy02 Pou03].

In order to reach a higher thermal efficiency and utilize the total enthalpy produced by the combustion process in Brayton cycle, a heat exchange takes place between the two cycles. Therefore, the two cycles are coupled by a linking component

called heat recovery steam generator (HRSG), which can effectively transfer a part of the energy in the exhaust gas emitted by CTs to produce steam for STs [Keh91].

2.2.2 Multiple operating modes. The operating flexibility is another paramount advantage of CCGT plants over traditional thermal units [Cha]. Most CCGT plants can operate in several modes by configuring CT and ST components. Generally, distinct modes have their own parameters and generation characteristics. A CCGT plant optimizes its modes in real-time. However, a limited number of CT and ST combinations will represent feasible modes. Usually, CTs can operate without STs, while STs cannot operate independently. Figure 2.2 shows the possible modes and state transitions diagram for the CCGT with 2 CTs and 1 ST depicted in Figure 2.1. In this case, mode 1 would transit to either mode 2 or 3 before its transition to mode 4.

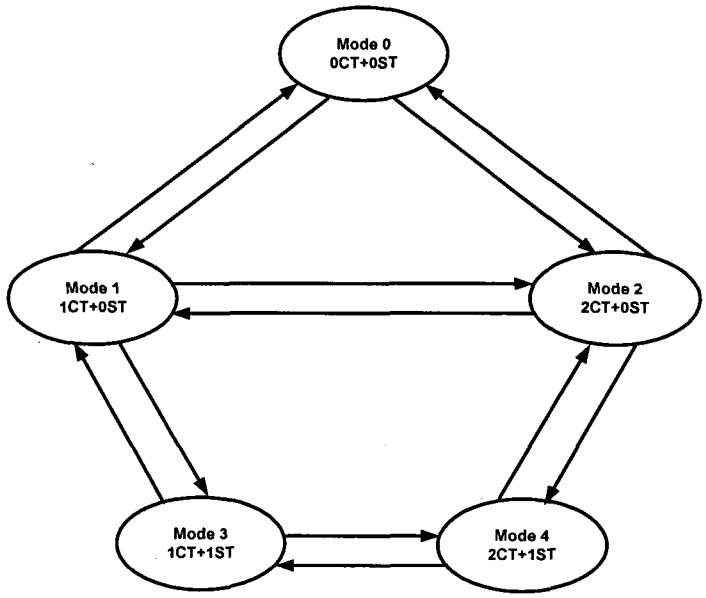

Figure. 2.2. State Transition Diagram for CCGT with 2 CTs and 1 ST

2.2.3 Power enhancement and cogeneration. The power enhancement for CCGT plants will increase the capability of the plant to provide additional power above its base capacity during peak hours. A variety of methods are available for enhancing the peak power output of CCGT plants [Jon].

The output of a CT corresponds to the mass flow rate and firing temperature. Therefore, there are two ways to enhance the output of CT. First, inlet cooling methods, which include the installation of foggers and injection steam, are useful options for power enhancement as they decrease the air flow temperature and increase the mass flow rate. In addition, CTs operating in a peak firing mode can increase their firing temperature above the base rating despite shorter inspection cycles and increased maintenance [Jon]. It is noted that CT enhancements can influence the output of bottoming ST cycle.

The exhaust from CT contains a certain level of oxygen for the bottoming cycle which is not consumed in the combustion process. Duct burners increase the ST output by supplementary fuel firing before or within HRSG for increasing the steam production rate [Boy02 Jon].

CCGT plants can operate as cogeneration plants which produce electricity and supply heat to industrial or domestic facilities at the same time [Gao05]. In most combined-cycle cogeneration plants, the supplementary firing equipment such as duct burners are installed in HRSG in order to control the steam production process and increase the thermal efficiency by regulating the fuel input to duct burners [Boy02]. According to the required steam pressure and temperature, the low pressure steam extracted from ST and HRSG can be sold out.

2.3 Modeling of CCGTs.

2.3.1 CCM model. .

1) Operating cost of CCGT. The objective of short-term scheduling problem is to minimize the total operating costs. For CCGTs, the operating cost is composed of production cost and mode transition costs as shown in (2.1).

$$\sum_{i\in CCS}\sum_{t=1}^{NT}\rho_f\cdot[F_{f,it}+TF_{it}] \tag{2.1}$$

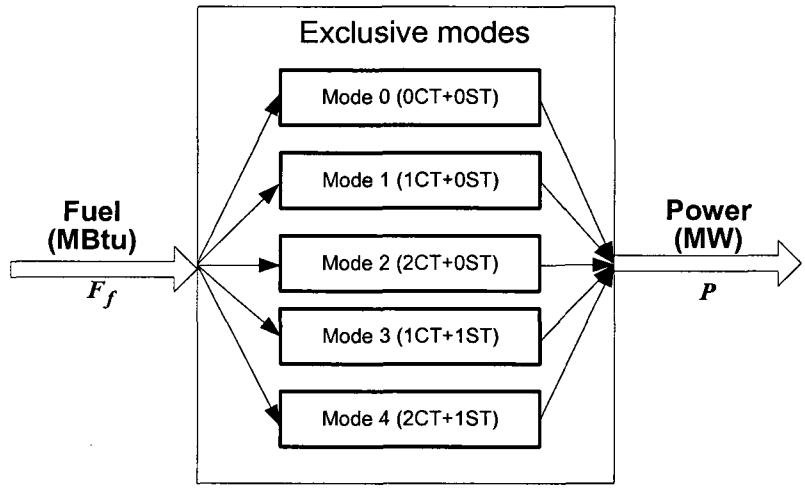

Figure 2.3. CCM Model for A CCGT with Five Exclusive Modes

In Figure 2.3, each exclusive mode is modeled as a pseudo unit. The fuel consumption of CCGT unit i at hour t, when the fuel-MW curve is defined as a convex piecewise linear function, is represented as (2.2) and (2.3). For a non-convex fuel-MW curve, (2.4) will be included in the CCM model.

$$F_{f,it}=\sum_{x\in NM_i,x\neq 0}[F^0_{f,ix}\cdot I_{ixt}+\sum_{s=1}^{NS_{ix}}(IF^s_{f,ix}\cdot Px^s_{ixt})] \tag{2.2}$$

$$P_{ixt}=P_{\min,ix}\cdot I_{ixt}+\sum_{s=1}^{NS_{ix}}Px^s_{ixt}\qquad \forall i,\forall x\neq 0,\forall t \tag{2.3}$$

$$\begin{cases} Px^{s}_{\max,ix} \cdot \delta^{s}_{ixt} \le Px^{s}_{ixt} \le Px^{s}_{\max,ix} \cdot I_{ixt} & s = 1 \\ Px^{s}_{\max,ix} \cdot \delta^{s}_{ixt} \le Px^{s}_{ixt} \le Px^{s}_{\max,ix} \cdot \delta^{s-1}_{ixt} & 2 \le s \le NS_{ix} \end{cases} \tag{2.4}$$

In (2.4), δ^{s}_{ixt} is equal to 1 if Px^{s}_{ixt} has reached $Px^{s}_{\max,ix}$; otherwise, δ^{s}_{ixt} equals to 0.

2) Transition fuel constraints. When the CCGT unit operation would transit from one mode to another, the transition fuel consumption from mode x at hour $t-1$ to feasible mode y at hour t is enforced as

$$TF_{it} - CTF_{i,xy} \ge -M \cdot [2 - I_{ix(t-1)} - I_{iyt}] \qquad \forall x, y \in FS_{ix}, \forall t \tag{2.5}$$

In (2.5), M is a large number so that constraint (2.5) for given modes x, y can be relaxed if $I_{ix(t-1)}$ or I_{iyt} is zero. The value of M should also be small for a good MIP formulation [Wil99]. In this case, M is set to $CTF_{i,xy}$ for a given pair of modes x, y. Each feasible transition defined by the state transition diagram such as Figure 2.3 should correspond to one constraint (2.5) at each hour.

3) Transition and state coupling constraints. The CCGT modes (pseudo units) are mutually exclusive. So

$$\sum_{x \in MS_i} I_{ixt} = 1 \qquad \forall i, \forall t \tag{2.6}$$

As illustrated in Figure 2.3, the mode x of unit i at hour t can only transit to a set of feasible modes defined by FS_{ix} at the next hour. It is noted that mode x itself is included in FS_{ix}. The feasible transition rule is formulated as

$$1 - \sum_{y \in FS_{ix}} I_{iy(t+1)} + \sum_{y \in IFS_{ix}} I_{iy(t+1)} \le 2[1 - I_{ixt}] \qquad \forall i, \forall x, \forall t \tag{2.7}$$

4) Ramping constraints. Ramping constraints in the CCM model is divided into two cases: ramping within a mode and ramping between modes. The ramping constraints within the same mode are represented as

$$P_{ix(t+1)} - P_{ixt} \le UR_{ix} + M \cdot [2 - I_{ixt} - I_{ix(t+1)}] \qquad \forall i, \forall x \ne 0, \forall t \qquad (2.8)$$

$$P_{ixt} - P_{ix(t+1)} \le DR_{ix} + M \cdot [2 - I_{ixt} - I_{ix(t+1)}] \qquad \forall i, \forall x \ne 0, \forall t \qquad (2.9)$$

In (2.8) and (2.9), M is a large number so that constraints can be relaxed if I_{ixt} or $I_{ix(t+1)}$ is zero. In this case, M can be set to $P_{\max,ix}$ which is the maximum generating capacity of mode x.

Ramping constraints between hours t and $t+1$ for transiting from mode x to mode y are represented as

$$P_{iy(t+1)} - P_{ixt} \le CUR_{ixy} + M \cdot [2 - I_{ixt} - I_{iy(t+1)}] \quad \forall i, \forall x, y \in FS_{ix} \text{ and } y \ne x, \forall t \quad (2.10)$$

$$P_{ixt} - P_{iy(t+1)} \le CDR_{ixy} + M \cdot [2 - I_{ixt} - I_{iy(t+1)}] \quad \forall i, \forall x, y \in FS_{ix} \text{ and } y \ne x, \forall t \quad (2.11)$$

In (2.10) and (2.11), M is a large number for relaxing constraints if I_{ixt} or $I_{iy(t+1)}$ is zero. In this case, M can be set to $P_{\max,i}$ which is the maximum generating capacity of CCGT unit i.

5) Minimum on/off time constraints. The minimum on time constraint of a mode is formulated in (2.12)-(2.14), which is similar to that for a conventional thermal unit.

$$\sum_{t=1}^{UT_{ix}} (1 - I_{ixt}) = 0 \qquad \forall i, \forall x, \forall t \qquad (2.12)$$

$$\sum_{\tau=t}^{t+T^{on}_{\min,ix}-1} I_{ix\tau} \ge T^{on}_{\min,ix} \cdot Y_{ixt} \quad \forall i, \forall x, \forall t = UT_{ix}+1, \ldots, NT - T^{on}_{\min,ix}+1 \qquad (2.13)$$

$$\sum_{\tau=t}^{NT}(I_{ix\tau} - Y_{ixt}) \geq 0 \quad \forall i, \forall x, \forall t = NT - T^{on}_{\min,ix} + 2, ..., NT \tag{2.14}$$

where $UT_{ix} = \max\{0, \min[NT, (T^{on}_{\min,ix} - X^{on}_{ini,ix})I_{ix0}]\}$

The minimum off time constraints is formulated similarly.

6) Generation and reserve constraints.

$$P_{ixt} + SR_{it} \cdot I_{ixt} \leq P_{\max,ix} \cdot I_{ixt} \qquad \forall i, \forall x \neq 0, \forall t \tag{2.15}$$

$$SR_{it} \leq 10 \sum_{x \in MS_i, x \neq 0}(MSR_{ix} \cdot I_{ixt}) \qquad \forall i, \forall t \tag{2.16}$$

$$OR_{it} - SR_{it} \leq QSC_i \cdot [1 - \sum_{x \in MS_i, x \neq 0} I_{ixt}] \qquad \forall i, \forall t \tag{2.17}$$

$$\sum_{x \in MS_i} P_{ixt} = P_{it} \qquad \forall i, \forall t \tag{2.18}$$

7) Startup and shutdown indicators. (2.19)-(2.20) represents the relationship among unit status, startup and shutdown indicators.

$$Y_{ix(t+1)} - Z_{ix(t+1)} = I_{ix(t+1)} - I_{ixt} \qquad \forall i, \forall x, \forall t \tag{2.19}$$

$$Y_{ix(t+1)} + Z_{ix(t+1)} \leq 1 \qquad \forall i, \forall x, \forall t \tag{2.20}$$

2.3.2 CCC model. The CCC model represents CTs and STs as individual components instead of considering them in modes. Each CT and ST in the CCC model is regarded as a single unit with its own unit parameters, such as ramping rate limits, minimum on/off time limits, and startup/shutdown costs. A CCC model is depicted in Figure 2.4 for a CCGT unit with 2 CTs and 1 ST. Three input-output curves of components are included in the CCC model. Each CT has a fuel-MW curve, and a MW-generated steam curve which represents the amount of steam that will be produced by HRSG when the CT generates a certain MW of electricity. Each ST has a consumed steam-MW curve

representing the amount of electricity generated by the ST given a certain amount of steam. Steam coupling constraints between CT and ST components as well as state transition constraints specified as simply explainable constraints are included in the CCC model. Power enhancement, duct burners, and cogeneration are appropriately considered in the CCC model. The MIP formulation of CCC model is presented as follows.

In Figure 2.4, $F_{f,CT}(P_{CT})$ represents the fuel-MW curve of CT; $F_{g,CT}(P_{CT})$ represents the MW-generated steam curve of CT; $F_{h,ST}(P_{ST})$ represents the consumed steam-MW curve of ST.

1) Operating cost of CCGT. It is shown in (2.21) that the total operating cost of a CCGT unit i is a function of production fuel consumption for generating power and startup/shutdown fuel of CTs. The fuel consumed by duct burners is also accounted for in the total fuel consumption.

$$\sum_{i\in CCS}\sum_{t=1}^{NT}\rho_f\cdot\left[\sum_{j\in CTS_i}F_{f,ijt}+\sum_{j\in CTS_i}SU_{f,ij}\cdot Y_{ijt}+\sum_{j\in CTS_i}SD_{f,ij}\cdot Z_{ijt}+F_{f,it}^{DB}\right] \quad (2.21)$$

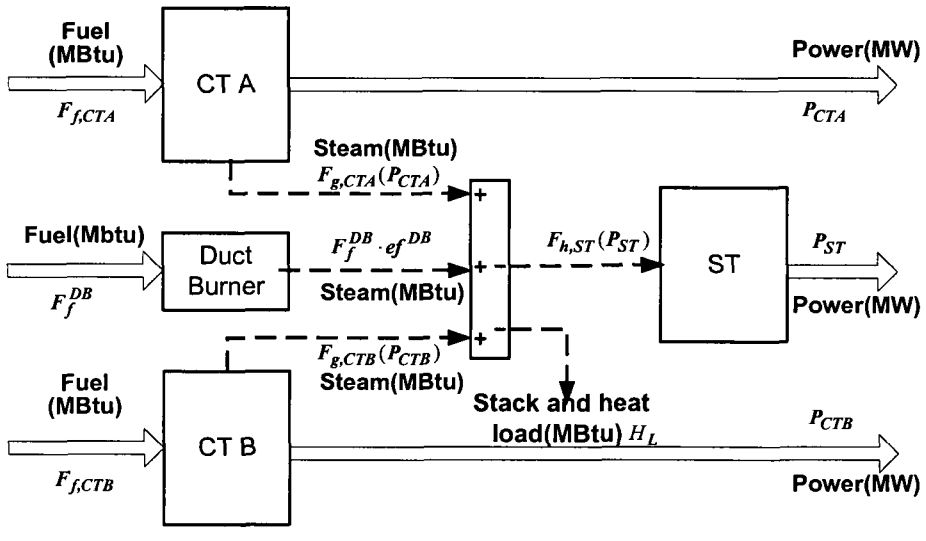

Figure 2.4. CCC model with 2 CTs and 1 ST

The linearized fuel-MW curve of a CT is shown in Figure 2.5, with the power augmentation of CT. The curve is divided into two parts with different generation regions. Normally, a CT operates in the base area where the generation is less than $P_{\max,ij}^{base}$. At peak hours, foggers and peak firing supplements can enhance the CT output above the base loading. Here, $F_{f,ij}^{0,aug}$ represents the additional cost for operating foggers or peak-firing.

The fuel consumption for operating a CT is represented as

$$F_{f,ijt} = \sum_{j \in CTS_i} [F_{f,ij}^{0} \cdot I_{ijt} + \sum_{s=1}^{NS_{ij}} (IF_{f,ij}^{s} \cdot Px_{ijt}^{s}) + F_{f,ij}^{0,aug} \cdot I_{ijt}^{aug} + Px_{ijt}^{aug} \cdot IF_{f,ij}^{aug}] \tag{2.22}$$

$$P_{ijt} = P_{\min,ij} \cdot I_{ijt} + \sum_{s=1}^{NS_{ij}} Px_{ijt}^{s} + Px_{ijt}^{aug} \quad \forall i, \forall j, \forall t \tag{2.23}$$

$$\begin{cases} Px_{\max,ij}^{s} \cdot \delta_{ijt}^{1} \le Px_{ijt}^{s} \le Px_{\max,ij}^{s} \cdot I_{ijt} & s = 1 \\ Px_{\max,ij}^{s} \cdot \delta_{ijt}^{s} \le Px_{ijt}^{s} \le Px_{\max,ij}^{s} \cdot \delta_{ijt}^{s-1} & 2 \le s \le NS_{ij} \end{cases} \tag{2.24}$$

$$0 \le Px_{ijt}^{aug} \le I_{ijt}^{aug} \cdot (P_{\max,ij}^{aug} - P_{\max,ij}^{base}) \quad \forall i, \forall j, \forall t \tag{2.25}$$

(2.22)-(2.25) applies to both convex and non-convex fuel-MW curve. The MW-generated steam curve of a CT, corresponding to its fuel-MW output curve, which represents the steam produced by HRSG is given in (2.26).

$$F_{g,ijt} = \sum_{j \in CTS_i} [F_{g,ij}^{0} \cdot I_{ijt} + \sum_{s=1}^{NS_{ij}} (IF_{g,ij}^{s} \cdot Px_{ijt}^{s}) + F_{g,ij}^{aug} \cdot I_{ijt}^{aug} + IF_{g,ij}^{aug} \cdot Px_{ijt}^{aug}] \tag{2.26}$$

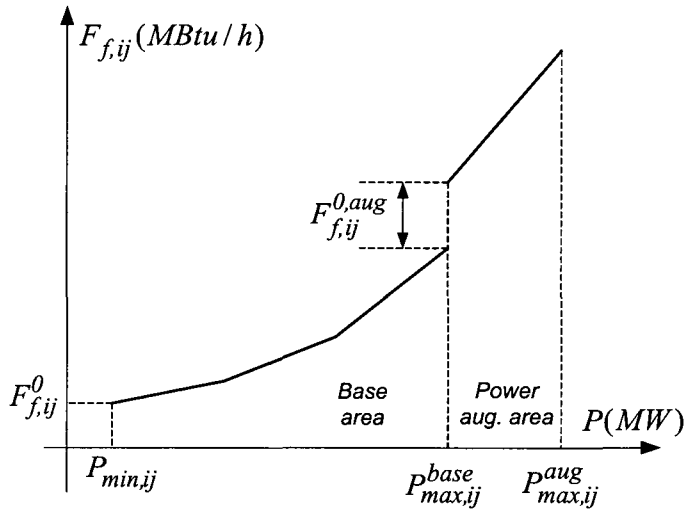

Figure 2.5. Piecewise linear fuel-MW curve of a CT

2) Steam coupling constraints. The exhaust gas from a CT can be utilized by STs, or released through the stack when the CT operates without STs (e.g. 1CT - 0ST mode). (2.27) simulates the heat exchange between CT-HRSGs and STs. The first term in the left hand side of (2.27) represents the amount of steam used by ST for producing electricity and the second term represents the MBtu heat load. The right hand side of (2.27) denotes the potential amount of steam that can be generated from the exhaust gas emitted by CTs (the first term) and duct burners (the second term). In (2.27), ef_i^{DB} represents the burning efficiency of duct burners.

$$\sum_{k \in STS_i} F_{h,ikt} + HL_{it} \leq \sum_{j \in CTS_i} F_{g,ijt} + F_{f,it}^{DB} \cdot ef_i^{DB} \qquad \forall i, \forall t \qquad (2.27)$$

The steam consumed by ST will not be included in the objective function since no additional fuel is needed for producing steam. The ST steam consumption is represented in (2.28) and (2.29) when the consumed steam-MW

curve is convex. For a non-convex consumed steam-MW curve, (2.30) will include additional integer variables.

$$F_{h,ikt} = \sum_{k \in STS_i} [F^0_{h,ik} \cdot I_{ikt} + \sum_{s=1}^{NS_{ik}} (IF^s_{h,ik} \cdot Px^s_{ikt})] \tag{2.28}$$

$$P_{ijt} = P_{\min,ik} \cdot I_{ikt} + \sum_{s=1}^{NS_{ik}} Px^s_{ikt} \qquad \forall i, \forall j, \forall t \tag{2.29}$$

$$\begin{cases} Px^s_{\max,jk} \cdot \delta^s_{ikt} \le Px^s_{ikt} \le Px^s_{\max,jk} \cdot I_{ikt} & s = 1 \\ Px^s_{\max,jk} \cdot \delta^s_{ikt} \le Px^s_{ikt} \le Px^s_{\max,jk} \cdot \delta^{s-1}_{ikt} & 2 \le s \le NS_{ik} \end{cases} \tag{2.30}$$

3) Generation and reserve constraints. The 10-minute spinning reserve of a CT or ST is the unloaded synchronized generation that can provide sustainable upward ramp in 10 minutes, which cannot exceed the difference between its maximum capacity and current generation, as modeled by (2.31) for CT and (2.33) for ST. It is also limited by the 10-minute maximum sustained ramping rate, as modeled by (2.32) for CT and (2.34) for ST.

Generation and spinning reserve constraints for each component are

$$P_{ijt} + SR_{ijt} \le P^{base}_{\max,ij} \cdot I_{ijt} + P^{aug}_{\max,ij} \cdot I^{aug}_{ijt} \qquad \forall i, \forall j, \forall t \tag{2.31}$$

$$SR_{ijt} \le 10 \cdot MSR_{ij} \cdot I_{ijt} \qquad \forall i, \forall j, \forall t \tag{2.32}$$

$$P_{ikt} + SR_{ikt} \le P_{\max,ik} \cdot I_{ikt} \qquad \forall i, \forall k, \forall t \tag{2.33}$$

$$SR_{ikt} \le 10 \cdot MSR_{ik} \cdot I_{ikt} \qquad \forall i, \forall k, \forall t \tag{2.34}$$

Generation, spinning reserve, and operating reserve for a CCGT unit are modeled as

$$\sum_{j \in CTS_j} P_{ijt} + \sum_{k \in STS_i} P_{ikt} = P_{it} \qquad \forall i, \forall t \tag{2.35}$$

$$\sum_{j \in CTS_j} SR_{ijt} + \sum_{k \in STS_i} SR_{ikt} = SR_{it} \qquad \forall i, \forall t \qquad (2.36)$$

$$OR_{it} - (\sum_{j \in CTS_i} SR_{ijt} + \sum_{k \in STS_i} SR_{ikt}) \le QSC_i \cdot (1 - I_{it}) \qquad \forall i, \forall t \qquad (2.37)$$

The commitment status of the CCGT unit I_{it} is related to the commitment status of all CTs of the CCGT plant I_{ijt}, as in (2.38)

$$NCT_i \cdot (I_{it} - 1) \le \sum_{j \in CTS_i} I_{ijt} \qquad \forall i, \forall t \qquad (2.38)$$

4) Ramping constraints. Ramping up/down limits for are enforced as (2.39) for CT and (2.40) for ST.

$$-DR_{ij} \le P_{ij(t+1)} - P_{ijt} \le UR_{ij} \qquad \forall i, \forall j, \forall t \qquad (2.39)$$

$$-DR_{ik} \le P_{ik(t+1)} - P_{ikt} \le UR_{ik} \qquad \forall i, \forall k, \forall t \qquad (2.40)$$

5) Minimum on/off time constraints. The minimum on/off time constraints for each component (CT or ST) can be expressed in the same ways as in the mode model.

6) Transition and state coupling constraints. The transitions between different operating modes of a CCGT unit can be specified as a group of simple constraints that depend on the specific characteristics of the unit. In this chapter, we consider two types of CCGTs: CCS_1 represents the set of CCGT units with multiple CTs and one ST (nCT-1ST); CCS_2 represents the set of CCGT units with multiple CTs and two STs (nCT-2ST) including one high pressure steam turbine (HPST) and one low pressure steam turbine (LPST). The formulations of the two sets are given as follows.

For both CCS_1 and CCS_2:

Maximum number of CTs that can be started up simultaneously

$$\sum_{j\in CTS_i} Y_{ijt} \le MaxCTN1_{ik}^{su}\cdot(1-Y_{ikt}-Z_{ikt})+MaxCTN2_{ik}^{su}\cdot Y_{ikt} + MaxCTN3_{ik}^{su}\cdot Z_{ikt} \qquad \forall i,\forall k,\forall t \tag{2.41}$$

Maximum number of CTs that can be shut down simultaneously

$$\sum_{j\in CTS_i} Z_{ijt} \le MaxCTN1_{ik}^{sd}\cdot(1-Y_{ikt}-Z_{ikt})+MaxCTN2_{ik}^{sd}\cdot Y_{ikt} + MaxCTN3_{ik}^{sd}\cdot Z_{ikt} \qquad \forall i,\forall k,\forall t \tag{2.42}$$

Minimum number of CTs that must be on for running all STs

$$\sum_{j\in CTS_i} I_{ijt} \ge MinCTN1_i^{on}\cdot[\sum_{k\in STS_i} I_{ikt} - NST_i + 1] \quad \forall i,\forall t \tag{2.43}$$

Maximum number of CTs that can be on without operating any STs

$$\sum_{j\in CTS_i} I_{ijt} \le MaxCTN1_i^{on} + NCT_i \cdot \sum_{k\in STS_i} I_{ikt} \quad \forall i,\forall t \tag{2.44}$$

A required number of CTs that must be on for a minimum number of hours before starting the first ST (HPST of nCT-2ST)

$$\sum_{j\in CTS_i} I_{ij\tau} \ge Y_{ikt}\cdot M\text{inCTN2}_i^{on} \qquad \forall i,\forall t,k=1,\tau=t-MinCTT_i^{on},\ldots,t-1 \tag{2.45}$$

For CCS_2:

Minimum number of CTs that must be on for operating the HPST alone is

$$\sum_{j\in CTS_i} I_{ijt} \ge MinCTN3_i^{on}\cdot[I_{i(hp)t} - I_{i(lp)t}] \quad \forall i\in CCS_2,\forall t \tag{2.46}$$

Maximum number of CTs that can be on for operating the HPST alone is

$$\sum_{j\in CTS_i} I_{ijt} \le MaxCTN2_i^{on} + NCT_i\cdot[1-I_{i(hp)t}+I_{i(lp)t}] \quad \forall i\in CCS_2,\forall t \tag{2.47}$$

Minimum number of CTs that must be on for operating the LPST alone is

$$\sum_{j \in CTS_i} I_{ijt} \geq MinCTN4_i^{on} \cdot [I_{i(lp)t} - I_{i(hp)t}] \qquad \forall i \in CCS_2, \forall t \quad (2.48)$$

Maximum number of CTs that can be on for operating the LPST alone is

$$\sum_{j \in CTS_i} I_{ijt} \leq MaxCTN3_i^{on} + NCT_i \cdot [1 - I_{i(lp)t} + I_{i(hp)t}] \quad \forall i \in CCS_2, \forall t \quad (2.49)$$

HPST must be operated for a minimum number of hours (at least 1) before starting LPST

$$\sum_{\tau=t-CTT_{\min,i}^{on}}^{t-1} I_{i(hp)\tau} \geq MinHPT_i^{on} \cdot Y_{i(lp)t} \qquad \forall i \in CCS_2, \forall t \quad (2.50)$$

HPST and the LPST cannot be started up and shut down at the same hour

$$Y_{i(lp)t} + Z_{i(lp)t} + Y_{i(hp)t} + Z_{i(hp)t} \leq 1 \qquad \forall i \in CCS_2, \forall t \quad (2.51)$$

7) Others. The relationship among status, startup and shutdown indicators of each component can be modeled in the same ways as in the mode model. To run duct burners, the CCGT generation must be larger than a minimum value.

$$I_{it}^{DB} \cdot P_{\min,i}^{DB} \leq \sum_{j=1}^{NCT_i} P_{ijt} + \sum_{k=1}^{NST_i} P_{ikt} \qquad \forall i, \forall t \qquad (2.52)$$

2.3.3 Comparison of CCC and CCM models. CCM and CCC models represent two distinct ways of modeling CCGT units for solving the short-term scheduling problem. In this section, we present a comparison between the two models.

1) Operating cost. The operating cost of a CCGT unit, as listed in (2.1) and (2.21), indicates different compositions in CCM and CCC models.

The transition cost between modes in the CCM model is equivalent to the sum of startup and shutdown costs of the related components in the CCC model. Both costs depend on commitment rather than dispatch. However, if the startup

cost of a component is considered as a function of its shutdown time [Car06], it will be difficult to model the transition cost in the CCM model. In such cases, the modeling of transition cost may need some approximation startup and shutdown costs of related components.

The production cost of a CCGT unit depends on the input-output curves and the generation dispatch of each mode or component. As discussed below, the inaccuracy of CCM input-output mode curves and component dispatch may lead to higher production costs.

2) Input-output curves. There are three kinds of curves in the CCC model including fuel-MW curve for each CT, MW-generated steam curve for each CT, and consumed steam-MW for each ST. In comparison, a fuel-MW curve is considered for each CCM mode.

The CCM fuel-MW curves are obtained by fuel consumption-power output tests, which are usually updated for major modes. During the test, a non-optimal generation dispatch among components could result in an upward shift of fuel-MW curves (assuming MW on the horizontal axis and fuel consumption on the vertical axis). Accordingly, the CCGT scheduling based on these curves will result in higher production costs. In addition, CCGT operators would still have to map the total power dispatch into individual ST and CT dispatch. The dispatch is usually done based on operators' experience or a dispatch table obtained during the above-mentioned test.

Successful applications of the proposed CCC model require similar tests to be performed for individual components, including CTs, CT-associated HRSGs,

and STs. Since individual component tests can be performed independently, it is more likely to obtain accurate component curves. In addition, individual component dispatch will be based on optimization results (unit commitment and economic dispatch) rather than operators' experience or pre-fabricated CCM dispatch tables.

Obviously, it is not easy to deduce component curves from mode curve. However, if CCC component curves are known, we can obtain fuel-MW CCM curves and the corresponding dispatch.

3) Minimum on/off time and ramp rate limits. CTs and STs, operating in different thermal cycles, usually have different ramp rates and minimum on/off time limits. These operating parameters for components can be expressed very accurately in the CCC model, as presented in Section 2.3.2 of this chapter. The application of CCM model with only mode variables for modeling these operating parameters may prove to be difficult.

Additional modes could be considered for a more accurate modeling of minimum on/off time constraints in the CCM model. Accordingly, the optimization problem will be larger in terms of number of variables and constraints. Consider a simple example where the minimum on/off time limits of both CTs and STs are 2 hours. Figure 2.6 shows that we would have to double the number of existing modes and expand the state transition diagram. Dashed lines in Fig. 6 indicate that the occurrence of corresponding transitions is conditional, depending on not only the modes in current and next hours, but also the modes in last several hours. Obviously, if the number of components is large (e.g. CCGT

unit with 4CT & 1ST) or the minimum on/off times are longer, the number of modes will be much higher and the complexity of state transition diagram will increase considerably.

It is even more difficult to accurately model the ramping constraints of CCM components because ramp rates relate to the component commitment and dispatch. Accordingly, the mode ramping rate constraints and minimum on/off time constraints will unavoidably introduce conservative approximations and probably lead to higher operation costs.

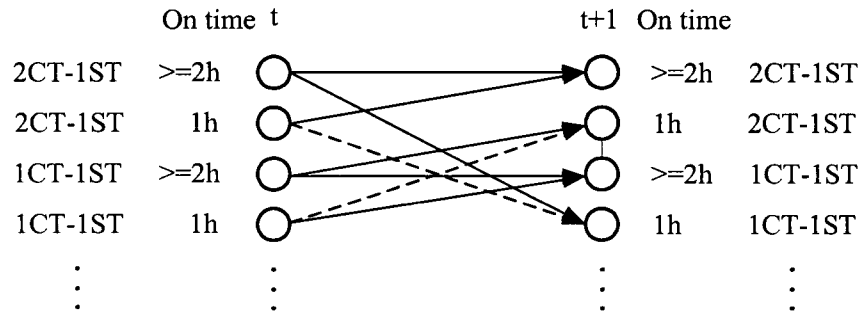

Figure 2.6. State transition diagram considering online hours

4) Inclusion of special operating conditions. According to section 2.3.2, it is convenient to model power augmentation, duct burners, and cogeneration using the CCC model. It would be difficult or inefficient to model those conditions in the CCM model as explained below. Firstly, the CCM model requires the introduction of many new modes and the expansion of state transition diagram. Secondly, it is hard to test and determine input-output curves for new added modes. For example, when cogeneration is considered, traditional fuel-MW curves in the CCM model are not adequate for describing production costs because the fuel consumption is a function of both power and heat output.

Additionally, it is more convenient to deal with component maintenance or deration in the CCC model. For instance, in the case that components are derated, both models have to reset maximum capacities of related components or modes. The CCC model can still ensure an optimal solution without changing the input-output curves, whereas the CCM model using the old fuel-MW curves may result in suboptimal or incorrect dispatch among components.

5) State transition diagram and transition constraints. As presented above as well as in [Coh96] and [Bje00], the CCM state transition diagram can include additional modes for improving the CCM model accuracy. However, the expansion cannot fundamentally avoid the limitations or disadvantages of CCM model which lead to suboptimal solutions. Furthermore, the expansion will significantly increase the size of the MIP-based optimization problem due to considerable increases in the number of integer variables and constraints resulting from the addition of new modes and more complex state transition diagram.

   In the CCM model, uniform transition constraints as (2.6) can be applicable to any given state transition diagrams. In the CCC model, mode transitions are specified as constraints such as (2.41)-(2.49). Some of these constraints are commonly applicable to CCGT units whereas the others can only be used for certain types of CCGT units.

6) Size of the MIP-based optimization problem. The numbers for integer variables including continuing variables and constraints for different types of CCGTs are shown in Table 2.1 based on the proposed MIP formulations in Sections 2.3.1 and 2.3.2. It is assumed here that non-convex input-output curves are linearized into 5

pieces. No special operating conditions are included in either model. All minimum on/off time parameters are assumed to be 2 hours and the impact of initial unit status is ignored. The scheduling period is 24 hours. State transition diagrams for 4CT-1ST and 6CT-2ST units are the same as those used for the case study 2.4.3.

Table 2.1. Dimensions of MIP Formulations for Different Types of CCGTS Based on CCC Model and CCM Model

Dimensions of MIP Formulations	CCGT (2CT-1ST)		CCGT (4CT-1ST)		CCGT (6CT-2ST)	
	CCC	CCM	CCC	CCM	CCC	CCM
Integer Variables	600	840	984	1032	1560	1992
Continuous Variables	528	696	864	864	1368	1704
Equality Constraints	144	240	240	192	384	672
Inequality Constraints	1572	2716	2476	3768	3976	6868

7) Summary. In summary, the CCC model would be more accurate than the CCM model in the modeling of CCGT units since it relates more closely to the physical representations of CTs and STs, which could also demonstrate a lower operation cost for CCGTs. In comparison, the CCGT unit scheduling by the traditional CCM model would have to consider certain approximations on ramping limits, minimum on/off, transition cost, among others. It is possible for the CCM model to improve the modeling accuracy of CCGTs, however, by expanding the state transition diagrams at the cost of increasing the size of the model.

Normally, the number of variables and constraints of MIP formulation, based on the CCC model, is smaller than that of the CCM model. However,

generation variables in the CCM model do not have very tight coupling relations since different modes are exclusive. In comparison, component variables based on the CCC model in the same CCGT unit are highly coupled. One consequence of such coupling is that CTs with identical parameters in the CCC model may have an adverse impact on the convergence of MIP-based optimization problem.

2.3.4 Inclusion of CCC and CCM models into SCUC. The objective of short-term security-constrained unit commitment (SCUC) is to minimize the system operating cost while satisfying the prevailing constraints such as power balance, system spinning and operating reserve requirements, unit minimum on/off time limits and ramping up/down limits, limits on state and control variables including real and reactive power generation, controlled voltages, settings of tap-changing and phase-shifting transformers, branch flows, bus voltages, and so on. Reference [Fu05 Fu07] presented a MIP-based formulation of SCUC including generating units with multiple operating modes. The proposed CCC and CCM models for CCGTs and the operating cost (2.1) or (2.21) will be included in SCUC. For large-scale systems, the SCUC problem is decomposed into the master UC problem and network security check subproblems. The subproblems mitigate network violations and iterate with UC via power transfer distribution factor (PTDF) or Benders decomposition method. The incorporation of the proposed CCC or CCM models does not change the overall SCUC solution strategy.

2.4 Case Studies

Three examples are presented to illustrate the advantages and efficiency of the proposed CCC model. Example A compares CCC and CCM models when scheduling a single CCGT. Example B demonstrates that the proposed CCC model can deal with

power enhancement and cogeneration in the SCUC solution. Example C shows that the proposed CCC model is effective in solving a relatively large system with multiple types of CCGTs. All numerical examples are run on a Pentium-4 2.6 GHz personal computer. The MIP problem is solved using CPLEX 9.0.

2.4.1 Scheduling of one CCGT based on CCC and CCM models. We first consider a single CCGT which is labeled as CC1 in this example. Both CCC and CCM models are used to solve the scheduling problem of CC1. The basic unit characteristics of CC1 are shown in Table 2.2 in which "IniT" represents the number of hours that the unit has been on (positive) or of (negative). Unit CC1 consists of 2 identical CTs and 1 ST which can operate in 5 modes as shown in Figure 2.2 The parameters for transition coupling constraints in the CCC model are shown in Table 2.3. Other component parameters are given in Table 2.4. The quadratic input-output curve coefficients of each component are given in Table 2.5. In order to simulate experience-based or test-based curves in the CCM model as mentioned in Section 2.3, we form the input-output curve of each mode based on the given curves for CTs and STs and the assumption that CT A and CT B generate at the same dispatch level. First, we select a set of feasible generation dispatch for a single CT:

$$P_{CT}^{(1)}, P_{CT}^{(2)}, \ldots\ldots, P_{CT}^{(n)}$$

According to the fuel-MW output curve and the MW-generated steam curve of CT, we determine the fuel consumption as well as the steam generation corresponding to the above generation dispatch levels.

$F_{f,CT}^{(1)}, F_{f,CT}^{(2)}, \ldots, F_{f,CT}^{(n)}$ for fuel consumption

$F_{g,CT}^{(1)}, F_{g,CT}^{(2)}, \ldots, F_{g,CT}^{(n)}$ for steam generation

Table 2.2. Parameters of Single CCGT Unit

Unit	Mode Num	CT Number	ST Number	IniT (Hour)	Ini Mode	Identical CT
CC1	5	2	1	3	0	Yes

Table 2.3. Parameters of Single CCGT Unit in the CCC Model (Hours)

$MaxCTN1^{on}$	2	$MaxCTN1^{su}$	2
$MinCTN1^{on}$	1	$MaxCTN2^{su}, MaxCTN3^{su}$	0
$MinCTN2^{on}$	1	$MaxCTN1^{sd}$	2
$MinCTT^{on}$	2	$MaxCTN2^{sd}, MaxCTN3^{sd}$	0

Table 2.4. Parameters of Components of Single CCGT Unit

Component	Min On (h)	Min Off (h)	Pmin (MW)	Pmax (MW)	Ramp Up (MW/h)
CT	2	2	40	141.5	100
ST	2	2	40	180	100
Component	**Ramp Down (MW/h)**	**St (MBtu)**	**Sd (MBtu)**	**MSR (MW/min)**	**IniT (Hour)**
CT	100	60	0	5	-3
ST	100	0	0	5	-3

Table 2.5. Input-output Curves of CCC and CCM Models of Single CCGT Unit

Component Curve		a (MBtu/MW2h)	b (MBtu/MWh)	c (MBtu)
CT Fuel-MW Curve		0.001534	7.10787	509.781
ST Steam-MW Curve		0.021575	5.92653	245.894
CT MW-Steam Curve		0.001028	4.62012	331.357
Index	Mode	a (MBtu/MW^{2}h)	b (MBtu/MWh)	c (MBtu)
0	0 CT and 0 ST	0	0	0
1	1 CT and 0 ST	0.001534	7.10787	509.781
2	2 CT and 0 ST	0.000767	7.10787	1019.562
3	1 CT and 1 ST	0.0019	4.2010e	448.1889
4	2 CT and 1 ST	0.0011	4.5902	741.2075

We then determine the generation level of ST by solving an algebraic equation which results from the consumed steam-MW curve of ST.

Solve $F_{h,ST}(P_{ST}^{(1)}) = 2F_{g,CT}^{(1)}$ for $P_{ST}^{(1)}$

Solve $F_{h,ST}(P_{ST}^{(2)}) = 2F_{g,CT}^{(2)}$ for $P_{ST}^{(2)}$

...

Solve $F_{h,ST}(P_{ST}^{(n)}) = 2F_{g,CT}^{(n)}$ for $P_{ST}^{(n)}$

We now have a set of fuel input and the corresponding power output as shown in Table 2.6. We can either directly use Table 2.6 as the fuel-MW curve of the modes or calculate the coefficients of quadratic polynomials by the polynomial curve fitting method. By the above method, we can at least make sure that the ST is always working on the most efficient way based on the fact that the ST utilizes all steams generated by

CT-HRSGs. The fitted quadratic curves of modes are list in Table 2.5. Other parameters in the CCM model are given in Table 2.7. In this example, all curves are linearized into 10 pieces. The 24-hour system load and generation schedules are listed in Table 2.8. The social cost for the CCC model is $49,523 with a higher cost of $51,839 for the CCM model.

Table 2.6. Fuel Input-Power Output of Modes

Fuel Input (MBtu)	Power Output (MW)
$2F_f^{(1)}$	$2P_{CT}^{(1)} + P_{ST}^{(1)}$
$2F_{f,i}^{(2)}$	$2P_{CT}^{(2)} + P_{ST}^{(2)}$
...	...
$2F_{f,i}^{(n)}$	$2P_{CT}^{(n)} + P_{ST}^{(n)}$

Table 2.7. Parameters of Modes of of Single CCGT Unit

Mode #	Min On	Min Off	Pmin (MW)	Pmax (MW)	Ramp Up (MW)	Ramp Down (MW)
0	2	2	0	0	0	0
1	2	2	40	141.5	100	100
2	2	2	80	283	200	200
3	2	2	81	236	155	155
4	2	2	180	463	285	285

Table 2.8. Load Data and Dispatch of Single CCGT based on CCC and CCM Model

Hour	Load (MW)	UC and Dispatch based on CCC Model				UC based on CCM Model
		CT A (MW)	CT B (MW)	ST (MW)	Mode Index	Mode Index
1	145.3	74.85	70.45	0	2	2
2	126.6	66.3	60.3	0	2	2
3	60.4	0	60.4	0	1	1
4	138.9	0	78.74	60.16	3	1
5	203	0	119.08	83.92	3	3
6	206.7	0	121.51	85.19	3	3
7	144.8	0	81.06	63.74	3	3
8	401	100	137.64	163.36	4	4
9	372.1	105.71	111.05	155.34	4	4
10	404.2	118.8	121.2	164.2	4	4
11	423.6	122.82	131.35	169.43	4	4
12	367.8	100	113.64	154.16	4	4
13	216.8	0	128.22	88.58	3	3
14	209.5	0	123.35	86.15	3	3
15	312.1	82.93	90.75	138.42	4	4
16	396.6	113.3	121.2	162.1	4	4
17	457.4	123.41	131.35	169.64	4	4
18	464.1	131.35	133.45	173.3	4	4
19	478.2	131.35	138.65	175.2	4	4
20	410.7	121.2	123.52	165.98	4	4
21	327.5	90.75	93.94	142.81	4	4
22	254.6	62.56	70.45	121.59	4	2
23	135.7	75.19	0	60.51	3	2
24	58.8	58.8	0	0	1	1

By comparing the hourly commitments in Table 2.8, we find that CCGT can operate at more efficient modes at hours 4, 22, and 23 based on the CCC model because the minimum on/off time constraints are calculated differently in the CCC and CCM models. In the CCC model, we know exactly the minimum number of CTs that should be on for a minimum number of hours before starting a ST. There is at least 1 CT at hour 4 which has already been on for 2 hours and thus the ST can startup at hour 4. However, the minimum on time constraint for the CCM model requires CC1 to stay at mode 1 at hour 4. Obviously, mode 1 is more costly than mode 3 for generating the same amount of power.

The hourly load drops from 327.5 MW at hour 21 to 58.8 MW at hour 24. Hence CC1 switches from mode 4 to mode 1 which reduces the commitment cost in the CCC model. In comparison, the hourly UC solution based on the CCM model indicates that CC1 should operate in the more expensive mode 2 at hours 22-23 as shown in Table IX. Accordingly, the approximate minimum on/off time of the CCM mode will increase the operation cost particularly during the upward/ downward transition hours.

As discussed in section 2.3, the CCC scheduling not only indicates the hourly on/off schedules but also determines the component dispatch economically when considering ramping constraints. From hour 7 to 8, the load increases sharply and CC1 would switch from mode 3 to 4. Since the ramping up rate of CT and ST is 100 MW/hour, CT A starts to run at hour 8 and reaches its maximum feasible generation level of 100 MW while CT B is dispatched at 137.64 MW. The generation dispatch of CT B is more than that of CT A. A similar instance occurs at hour 12 when the hourly load decreases sharply. The CCM model indicates that the composite MW is dispatched optimally at

hours 8 and 12, which may result in a non-optimal dispatch of components. In this case, the assumption that CT A and CT B should have the same MW dispatch before fitting the fuel-MW curve of mode 4, is not cost-effective at hours 8 and 12.

The assumption that committed CTs in a single CCGT should generate the same level of generation dispatch is not always optimal. The case given in Figure 2.7 shows that both CTs in a CCGT have the same fuel-MW and MW-generated steam curves.

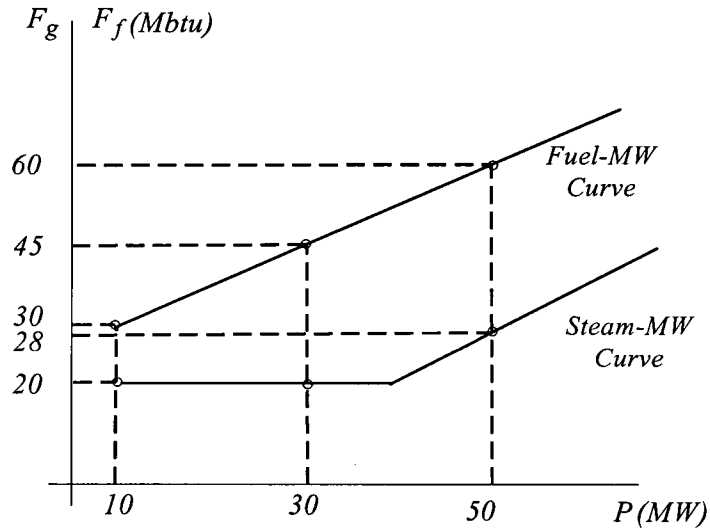

Figure 2.7. Fuel-MW and MW-generated steam curves of CT

Table 2.9 shows that different hourly dispatches of CTs may result in the same fuel consumption but different levels of generated steam. More steam will lead to more ST generation. Therefore, even if we ignore ramping and minimum on/off constraints of components, the CCC model will dispatch CTs at different generation levels. So it is clear that the CCM model is an approximated model and engineers working in such power plants will still need to dispatch the CCGT generation to CT and ST component levels.

Table 2.9. Fuel Consumption and Steam Generated with CT Dispatch

CT Dispatch	Fuel Consumption (MBtu)	Generated Steam (MBtu)
CTA 10MW - CTB 50MW	90	48
CTA 30MW - CTB 30MW	90	40

2.4.2 Power enhancement and cogeneration based on the CCC model. An 8-bus system shown in Fig. 8 is used to illustrate the way the proposed CCC model can deal with power enhancement. Larger CCGTs with power enhancement are cheaper than thermal units for supplying the load. Power enhancement is also utilized at peak hours for mitigating congestion. The CCC model can also be used to model CCGTs as cogeneration units. This 8-bus system has 3 CCGTs and 3 thermal units as described in http://motor.ece.iit.edu/Data/ CCC_Data1.pdf. All curves are linearized into 5 pieces. The hourly electricity load and spinning reserve are given in Table 2.10. In addition, steam is extracted from CC3 at certain hours to supply a constant heat load of 300 MBtu.

The system is tested for 24 hours with a peak load of 2040 MW. Four cases are studied to illustrate the new CCC model and the impact of duct burners, peak firing, and foggers.

- Case 0: Calculate the hourly UC solution without network constraints. No duct burners, foggers or peak-firing are installed.
- Case 1: Consider the DC network security constraints in Case 0.
- Case 2: In Case 0, utilize peak firing and foggers for CC1 and CC2 and supplementary firing by duct burners for CC3.
- Case 3: Consider the DC network security constraints in Case 2.

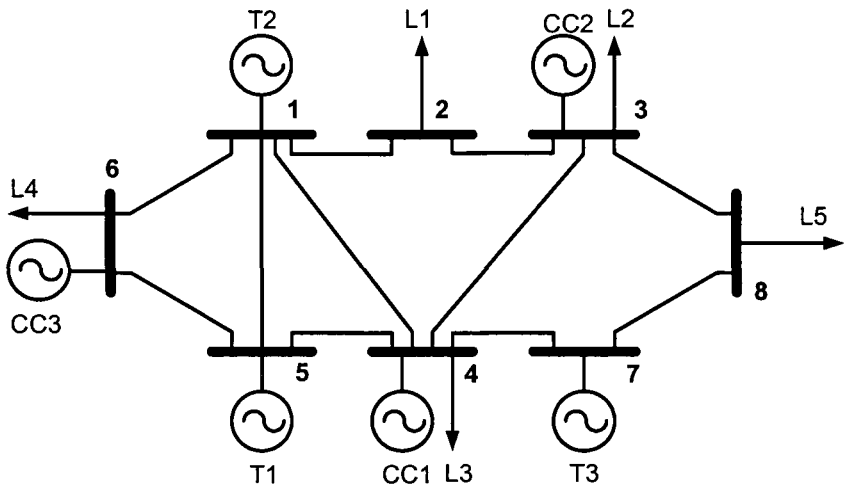

Figure 2.8. One-line diagram of the 8-bus system

Table 2.10. Hourly Electrical Load, Reserve, and Heat Load of 8-bus system

Hour	E. Load (MW)	Reserve (MW)	H. Load (MBtu)	Hour	E. Load (MW)	Reserve (MW)	H. Load (MBtu)
1	1382.88	69.14	0	13	1726.15	86.31	0
2	1294.62	64.73	0	14	1639.85	81.99	0
3	1078.85	53.94	0	15	1898.77	94.94	0
4	863.08	43.15	0	16	1941.92	97.10	0
5	1078.85	53.94	300	17	1834.04	91.70	300
6	1294.62	64.73	300	18	1920.35	96.02	300
7	1510.38	75.52	300	19	2020.38	101.02	300
8	1683.00	84.15	300	20	2030.19	101.51	300
9	1769.31	88.47	300	21	2040.00	102.00	300
10	1898.77	94.94	300	22	1990.96	99.55	300
11	1920.35	96.02	300	23	1877.19	93.86	300
12	1812.46	90.62	0	24	1769.31	88.47	300

In Case 0, CC2, T2 and T3 are initially on. The hourly schedule is presented in Table 2.11 with a daily generation cost of $264,073. We run the Case 1 which is shown in Figure 2.9 as the congestion occurs in branch 10 between buses 7 and 8 at hours 10-12 and 15-23. The solution of Case 1 shows that the violation of branch 10 is mitigated when the generation of cheaper unit T3 is decreased and the expensive unit T1 is committed at peak hour 19-22 as shown in Table 2.12. The daily production cost is $269,765. Table 2.13 lists the hourly commitment of units and the status of peak firing, foggers and duct burners in Case 2. The daily production cost is $263,458 which is cheaper than that in Case 0.

Table 2.11. Schedules of CCGTs and Thermal Units in Case 0

Unit	Hours (0-24)																								
CC1	0	1	1	3	3	3	3	4	4	4	4	4	4	4	4	4	4	4	4	4	4	4	4	4	4
CC2	4	4	4	4	4	4	4	4	4	4	4	4	4	4	4	4	4	4	4	4	4	4	4	4	4
CC3	0	0	0	0	1	1	2	4	4	4	4	4	4	4	4	4	4	4	4	4	4	4	4	4	4
T1	0	0	0	0	0	0	0	0	0	0	0	0	0	0	0	0	0	0	0	0	0	0	0	0	0
T2	1	1	1	0	0	0	0	1	1	1	1	1	1	1	1	1	1	1	1	1	1	1	1	1	1
T3	1	1	1	1	1	1	1	1	1	1	1	1	1	1	1	1	1	1	1	1	1	1	1	1	1

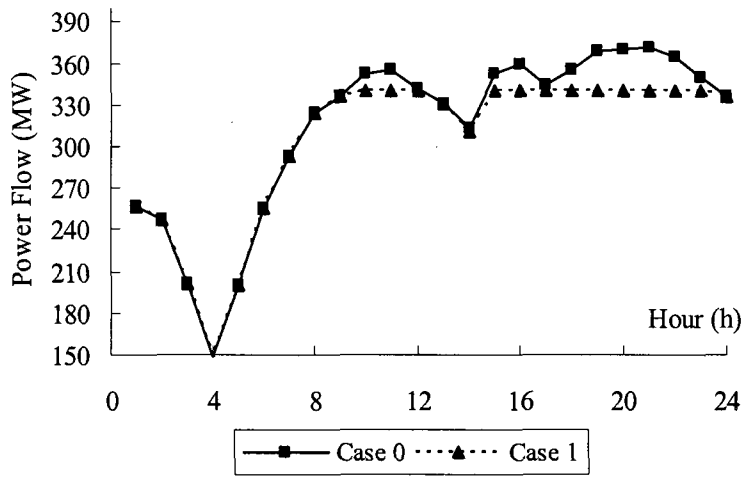

Figure 2.9. Power flow of branch 10 (between Bus 7 and 8) in Cases 0 and 1

Table 2.12. Schedules of CCGTs and Thermal Units in Case 1

Unit	Hours (0-24)
CC1	0 1 1 3 3 3 3 4 4 4 4 4 4 4 4 4 4 4 4 4 4 4 4 4
CC2	4 4 4 4 4 4 4 4 4 4 4 4 4 4 4 4 4 4 4 4 4 4 4 4
CC3	0 0 0 0 1 1 2 4 4 4 4 4 4 4 4 4 4 4 4 4 4 4 4 4
T1	0 0 0 0 0 0 0 0 0 0 0 0 0 0 0 0 0 0 0 1 1 1 1 0 0
T2	1 1 1 0 0 0 0 0 1 1 1 1 1 1 1 1 1 1 1 1 1 1 1 1
T3	1 1 1 1 1 1 1 1 1 1 1 1 1 1 1 1 1 1 1 1 1 1 1 1

Table 2.13. Schedules of CCGTs and Thermal Units in Case 2

Unit	Hours (0-24)
CC1	0 1 1 3 3 3 3 4 4 4 4 4 4 4 4 4 4 4 4 4 4 4 4 4
Peak-firing CT1	0 0 0 0 0 0 1 0 1 0 1 1 0 0 0 0 1 0 1 1 1 1 1 1 0
Peak-firing CT2	0 0 0 0 0 0 0 0 0 0 1 1 0 0 0 1 1 0 1 1 1 1 1 1 0
CC2	4 4 4 4 4 4 4 4 4 4 4 4 4 4 4 4 4 4 4 4 4 4 4 4
Fogger CT1	0 0 0 0 0 0 0 0 1 0 0 0 0 0 0 0 0 0 0 1 1 1 1 0 0
Fogger CT2	0 0 0 0 0 0 0 0 0 0 0 0 0 0 0 0 0 0 0 1 1 1 1 0 0
CC3	0 0 0 0 1 1 2 4 4 4 4 4 4 4 4 4 4 4 4 4 4 4 4 4
Duct Burners	0 0 0 0 0 0 0 0 1 0 0 0 0 0 0 0 0 0 0 0 0 0 0 0
T1	0 0 0 0 0 0 0 0 0 0 0 0 0 0 0 0 0 0 0 0 0 0 0 0
T2	1 1 1 0 0 0 0 0 0 1 1 1 1 1 1 1 1 1 1 1 1 1 1 1
T3	1 1 1 1 1 1 1 1 1 1 1 1 1 1 1 1 1 1 1 1 1 1 1 1

It is noted that peak firing and fogging are available to a single CT or both CTs. Figure 2.10 shows that by including peak firing, both CTs and ST of CC1 would generate additional hourly power. CC2 and CC3 behave similarly at certain hours by operating foggers and duct burners. Power enhancement will increase the generation cost of CCGTs; however, hourly schedule of CCGT will still be more competitive than that of expensive thermal units.

In Case 3, the hourly schedules are listed in Table 2.14. Figure 2.11 shows that CCGTs would generate a higher hourly power than that in Case 1. In addition, the most expensive thermal unit T1 will no longer be scheduled at hours 19-22 which reduces the daily generation cost by 1.59% to $265,483. In Case 3, CC1 cannot include peak firing at

certain hours as in Case 2 for mitigating the congestion on branch 10. So CC2 has a better opportunity to operate forgers to compensate the reduction of CC1. Furthermore, the duct burner of CC3 provides more steam to HRSG to generate additional power.

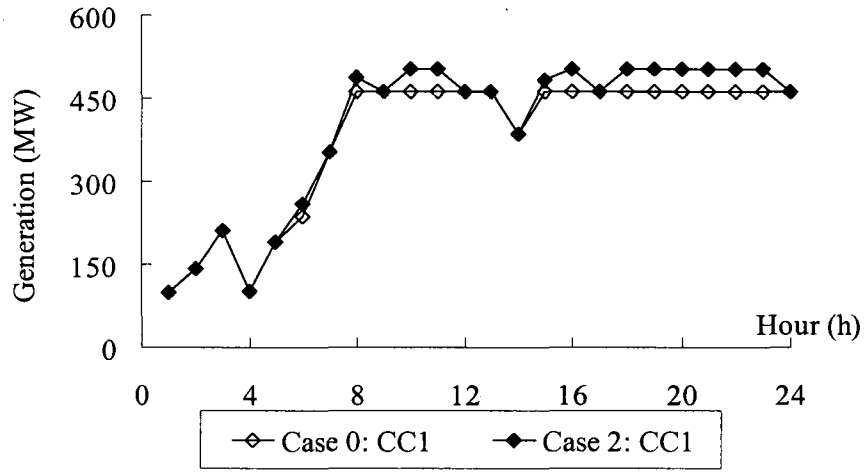

Figure 2.10. Hourly generation of CC1 in Cases 0 and 2

Table 2.14. Schedules of CCGTs and Thermal Units in Case 3

Unit	Hours (0-24)																								
CC1	0	1	1	3	3	3	3	4	4	4	4	4	4	4	4	4	4	4	4	4	4	4	4	4	4
Peak-f CT1	0	0	0	0	0	0	1	0	1	0	0	0	0	0	0	0	0	0	0	0	0	0	0	0	0
Peak-f CT2	0	0	0	0	0	0	0	0	0	0	0	0	0	0	0	0	0	0	0	0	0	1	0	0	0
CC2	4	4	4	4	4	4	4	4	4	4	4	4	4	4	4	4	4	4	4	4	4	4	4	4	4
Fogger CT1	0	1	0	0	0	0	0	0	1	0	1	1	1	0	1	1	1	1	1	1	1	1	1	1	0
Fogger CT2	0	0	0	0	0	0	0	0	0	0	1	1	0	0	1	1	1	1	1	1	1	1	1	1	0
CC3	0	0	0	0	1	1	2	4	4	4	4	4	4	4	4	4	4	4	4	4	4	4	4	4	4
Duct Burners	0	0	0	0	0	0	0	0	1	0	0	0	0	0	0	0	0	0	0	1	1	1	0	0	0
T1	0	0	0	0	0	0	0	0	0	0	0	0	0	0	0	0	0	0	0	0	0	0	0	0	0
T2	1	1	1	0	0	0	0	0	0	1	1	1	1	1	1	1	1	1	1	1	1	1	1	1	1
T3	1	1	1	1	1	1	1	1	1	1	1	1	1	1	1	1	1	1	1	1	1	1	1	1	1

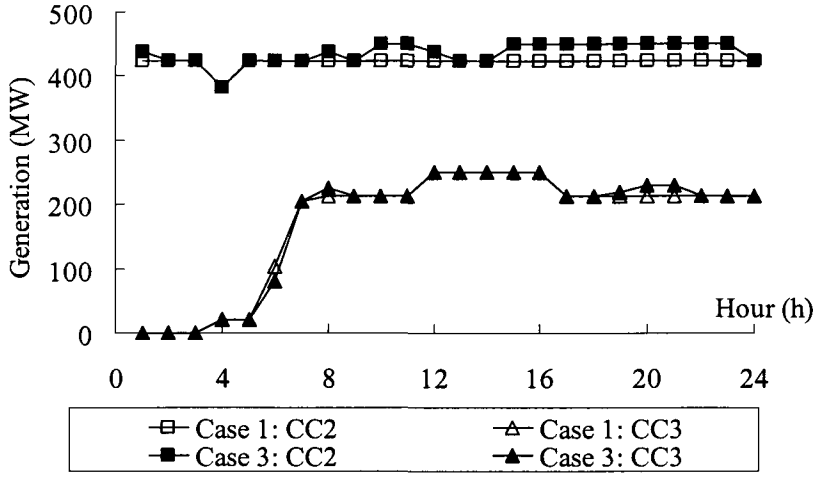

Figure 2.11. Hourly generation of CC2 and CC3 in Cases 1 and 3

2.4.3 IEEE 118-Bus System. Table 2.15 lists the general information on the test system, while the detailed unit data including their state transition diagrams in the test system are given in http://motor.ece.iit.edu/Data/CCC_Data2.pdf. The 12 CCGT units installed in this system have multiple types including 2CT-1ST, 4CT-1ST and 6CT-2ST. The 6CT-2ST unit is composed of 6 identical CTs, 1 HPST and 1 LPST, which can switch between 11 differen modes. All curves in this system are linearized into 5 pieces. Since all the curves of the ST are convex, corresponding integer variables with segment are not required for modeling the ST. A total of 8640 binary variables are included in the MIP formulations for this system. The daily generation cost is $1,908,377 and the computing time is 30s.

Base coal units such as 1004, 1005 and 1010 are committed in 24 hours. Single cycle gas or oil units can start or ramp up/down quickly. However, most of them remain off in this system to provide generation reserves. The hourly schedules of 2CT-1ST CCGTs are given in Table 2.16 by indicating their mode index. Since units 4002, 4005,

and 4010 can operate in several modes, we provide their component schedules in Table 2.17, Table 2.18 and Table 2.19. Compared to single-cycle units, CCGTs demonstrate higher efficiency and lower cost per unit of power generation.

Table 2.15. Modified IEEE 118-bus test system

Modified IEEE 118-Bus Power System	
Buses	118
Branches	186
Thermal Units	53
CCGTs with 2CT-1ST	9
CCGTs with 4CT-1ST	2
CCGTs with 6CT-2ST	1

Table 2.16. Schedule of 2CT-1ST CCGTs

Units	Hours (0-24)
4001	0 0 0 0 0 1 1 3 3 4 4 4 4 4 4 4 4 4 4 4 4 4 4 4 3
4003	0 0 0 1 1 3 3 3 3 3 3 3 3 3 3 3 3 3 3 3 3 3 3 3 3
4004	0 1 1 3 3 4 4 4 4 4 4 4 4 4 4 4 4 4 4 4 4 4 4 4 4
4006	0 0 0 0 0 0 1 1 3 3 4 4 4 4 4 4 4 4 4 4 4 4 4 4 4
4007	0 0 0 1 1 3 4 4 4 4 4 4 4 4 4 4 4 4 4 4 4 4 4 4 4
4008	0 0 0 1 1 3 4 4 4 4 4 4 4 4 4 4 4 4 4 4 4 4 4 4 4
4009	0 0 0 1 1 3 4 4 4 4 4 4 4 4 4 4 4 4 4 4 4 4 4 4 4
4011	0 0 0 0 1 1 3 4 4 4 4 4 4 4 4 4 4 4 4 4 4 4 4 4 4
4012	0 0 0 0 0 0 0 0 0 0 0 0 0 0 0 0 0 0 0 0 0 0 0 0 0

Table 2.17. Schedules of 4CT-1ST CCGTS (4005)

4005	Hours (0-24)
CT 1	0 0 0 0 0 1 1 1 1 1 1 1 1 1 1 1 1 1 1 1 1 1 1 1 1
CT 2	0 0 0 0 0 0 0 1 1 1 1 1 1 1 1 1 1 1 1 1 1 1 1 1 1
CT 3	0 0 0 0 0 0 0 0 0 0 1 1 1 1 1 1 1 1 1 1 1 1 0 0
CT 4	0 0 0 0 0 0 0 0 0 0 0 0 0 0 0 0 0 0 0 0 0 0 0 0 0
ST	0 0 0 0 0 0 0 0 0 1 1 1 1 1 1 1 1 1 1 1 1 1 1 1 1

Table 2.18. Schedules of 4CT-1ST CCGTS (4010)

4010	Hours (0-24)
CT 1	0 0 0 1 1 1 1 1 1 1 1 1 1 1 1 1 1 1 1 1 1 1 0 0 0
CT 2	0 0 0 1 1 1 1 1 1 1 1 1 1 1 1 1 1 1 1 1 1 1 1 1 1
CT 3	0 0 0 0 0 0 1 1 1 1 1 1 1 1 1 1 1 1 1 1 1 1 1 1 1
CT 4	0 0 0 0 0 0 0 0 0 0 0 0 0 0 0 0 0 0 0 0 1 1 1 1 1
ST	0 0 0 0 0 1 1 1 1 1 1 1 1 1 1 1 1 1 1 1 1 1 1 1 1

Table 2.19. Schedule of 6CT-2ST CCGT

4002	Hours (0-24)
CT 1	0 1 1 1 1 1 1 1 1 1 1 1 1 1 1 1 1 1 1 1 1 1 1 1 1
CT 2	0 1 1 1 1 1 1 1 1 1 1 1 1 1 1 1 1 1 1 1 1 1 1 1 1
CT 3	0 0 0 1 1 1 1 1 1 1 1 1 1 1 1 1 1 1 1 1 1 1 1 1 1
CT 4	0 0 0 0 0 0 1 1 1 1 1 1 1 1 1 1 1 1 1 1 1 1 1 1 1
CT 5	0 0 0 0 0 0 0 1 1 1 1 1 1 1 1 1 1 1 1 1 1 1 1 1 1
CT 6	0 0 0 0 0 0 0 1 1 1 1 1 1 1 1 1 1 1 1 1 1 1 1 1 1
HPST	0 0 0 1 1 1 1 1 1 1 1 1 1 1 1 1 1 1 1 1 1 1 1 1 1
LPST	0 0 0 0 0 0 0 1 1 1 1 1 1 1 1 1 1 1 1 1 1 1 1 1 1

2.5 Conclusions

This chapter presents a component model for the scheduling of CCGT by MIP. A CCGT unit is modeled by individual CTs and STs. The CCM model requires certain approximations in the modeling of input-output curves, transition costs, ramping limits, and minimum operating time. The system operators would also need to dispatch the composite generation of CCM to individual CT and ST units, which could mostly be based on the operators' experience. The proposed CCC model does not need any approximations and will optimally dispatch the output generation to individual CT and ST units. In the proposed CCC model, distinct characteristics and heat exchanges among components have already been taken into account. Moreover, the CCC model can be easily expanded to include special operating conditions for power augmentation and cogeneration. Test results verify that the CCC model can save operating costs. The IEEE

118-bus system with 12 CCGTs and various configurations (6CT-2ST, 4CT-1CT, and 2CT-1ST) is studied. Numerical results show that the proposed CCC model can be used successfully for representing CCGT units in the SCUC problem.

CHAPTER 3

SECUIRTY CONSTRAINTED UNIT COMMITMENT WITH STEADY STATE NATURAL GAS TRANSMISSION CONSTRAINTS

3.1 Introduction

Gas-fired power plants provide a linkage between natural gas transmission and power transmission systems. Natural gas transmission could affect the security and the economics of power transmission. From the economics point of view, natural gas contracts could affect the commitment, dispatch, and the operation of power systems. From the security point of view, pressure losses, pipeline contingencies, lack of storage or natural gas supply disruptions may lead to forced outgaes of multiple gas-fired unit or deration of generating capacity which could dramatically increase the operating costs and congestion, and jeopardize the security of power systems [Sha05]. Such conditions necessitate the solution of short-term unit commitment (UC) problem when integrating power transmission, natural gas contracts, as well as natural gas transmission systems as discussed in this chapter.

This chapter proposes an integrated model for SCUC with natural gas transmission constraints. The integrated model minimizes power system operating costs by taking into consideration power transmission constraints, natural gas transmission constraints, and natural gas contracts. Benders decomposition is applied to separate the natural gas transmission feasibility check subproblem from the master UC problem and the power transmission feasibility check subproblem as shown in Figure 3.1 Constraints related to natural gas contracts are directly included in the master UC problem. When an optimal UC schedule is obtained without violating power transmission constraints, hourly

natural gas demands of gas-fired units are then submitted to check the feasibility of natural gas transmission constraints. The natural gas transmission is modeled as a group of nonlinear equations for representing gas node pressures, which can be solved by a Newton-Raphson like method similar to the Newton-Raphson-based power flows solution. The natural gas transmission feasibility check is formulated as linear programming (LP) problem and solved iteratively. If any violations of natural gas transmission constraints are detected, corresponding energy constraints (Benders cuts) are formed and fed back to the master UC problem for the next iteration of calculation. The cut which represents shortages of natural gas supply or gas transmission congestions would limit the fuel consumption of a group of gas-fired units.

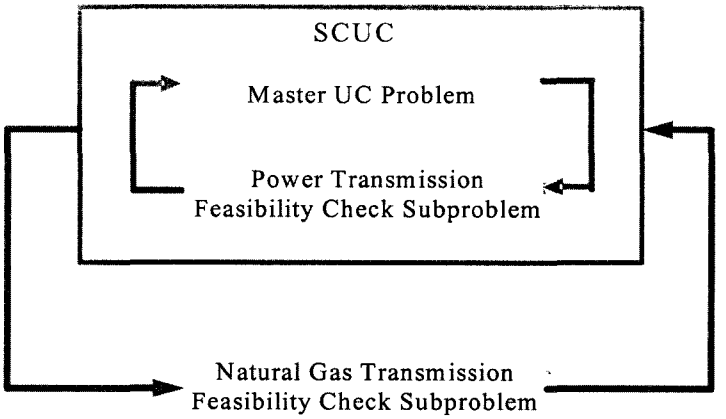

Figure 3.1. Decomposition strategy for natural gas and electricity

The proposed model is for the short-term operation of a large utility in the U.S. that has a large number of gas-fired and dual-fuel generating units. The same method can be applied to the ISO system. In regions where natural gas markets are heavily regulated but power systems are deregulated, natural gas transmission constraints imposed on power market participants such as generating companies (GENCOs) is submitted to electricity markets as energy constraints. In such cases, the proposed integrated SCUC

model is a very important tool for the daily scheduling and dispatch of generating units to meet the hourly system load. The proposed model can also be a foundation for the modeling of midterm or long-term operation of integrated natural gas and power transmission systems.

The rest of this chapter is organized as follows: Steady-state model of natural gas system is presented in section 3.2. SCUC model integrating constraints of natural gas system are formulated in section 3.3. Section 3.4 presents and in detail discusses a six-bus system and the IEEE 118-bus system. The conclusion drawn from the study is provided in Section 3.5.

3.2 Model of Natural Gas Transmission System

The natural gas transmission system is one of the largest and most complex nonlinear systems in the world, which is represented by its steady state and dynamic characteristics [Ber78, Sto72]. The steady-state mathematical model of natural gas transmission system comprised of a group of nonlinear algebraic equations is presented here for SCUC applications.

3.2.1 Key Component of Natural Gas System. Figure 3.2 depicts the natural gas transmission system from producers to end users that is comprised of natural gas wells, transmission and distribution pipelines, storage facilities, and compressors. From the mathematical modeling viewpoint, these components are categorized into nodes and branches. As state variables, gas pressure is associated with each node while the natural gas flow rate is associated with each branch.

1) Suppliers and loads in the gas transmission system. Natural gas may leave or enter the gas transmission system only through nodes, which represent delivery and

receipt points. Most of the gas is supplied from gas wells, which are commonly located at remote sites. Supplies are modeled as positive gas injections at related nodes. In this chapter, lower and upper limits of gas supply in each period are modeled as

$$GP_{gi,\min} \le GP_{gi} \le GP_{gi,\max} \tag{3.1}$$

The natural gas loads could be residential, commercial, or industrial. Gas-fired power plants represent the most important industrial gas loads, which link electric power and natural gas transmission systems. Gas loads are represented as negative gas injections at related nodes which are modeled as

$$GL_{gl,\min} \le GL_{gl} \le GL_{gl,\max} \tag{3.2}$$

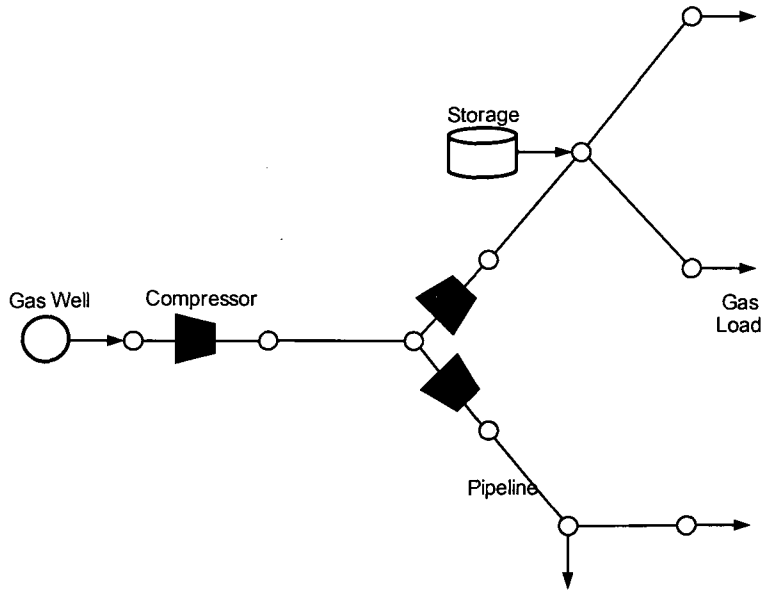

Figure 3.2. Natural gas transmission system

2) Gas storage. Unlike in electric power systems in which the electricity cannot be stored in large quantities, large sums of natural gas can be injected into natural gas storage facilities at off-peak periods and withdrawn during high demand

periods [Mer02]. This makes it possible to maintain a steady flow in a natural gas transmission pipeline even in peak periods or when contingencies occur.

Natural gas storage facilities are categorized based on their capacity and operating parameters that could balance gas transmission according to seasonal, monthly, and daily constraints [Pad08]. The scheduling of natural gas storage facilities is a midterm or long-term optimization problem with min/max storage capacity and injection/extraction rates represented as constraints. However, for the day-ahead scheduling of power systems, we either model a natural gas storage facility as a load or a supplier except for a self-owned storage facility of gas-fired power plants. Their operating status (decision variable that indicate if the storage works as injection or extraction facility) and other parameters (injection or extraction rate limits) as an input data in our model will be sent from a gas company based on its long-term or midterm operation plan.

3) Pipeline model. The power transmission depends on bus voltage conditions and parameters of transmission lines. By analogy, natural gas transmission, driven by pressures, are dependent on factors such as the length and the diameter of pipelines, operating temperatures and pressures, types of natural gas, altitude change over the transmission path, and the roughness of pipelines. Here, we present certain pipeline characteristics that are mostly used to design or optimize natural gas pipeline systems [Wol00, Ric79, Ouy96, Fu05]. The flow in a natural gas pipeline extending from gas node *na* to gas node *nb* is modeled as

$$Gf_{na\to nb} = \mathrm{sgn}(\pi_{na}, \pi_{nb}) \cdot C_{mn} \sqrt{\left|\pi_{na}^2 - \pi_{nb}^2\right|} \tag{3.3}$$

$$\text{sgn}(\pi_{na},\pi_{nb}) = \begin{cases} 1 & \pi_{na} \geq \pi_{nb} \\ -1 & \pi_{na} < \pi_{nb} \end{cases} \tag{3.4}$$

where C_{nanb} is the pipeline constant that depends on temperature, length, diameter, friction, and gas composition.

4) Compressor modeling. Pressure loss occurs when the natural gas flow encounters a pipeline resistance. In order to compensate for the pressure loss, compressor stations are installed at 50–100 mile intervals along pipelines. Compressor as a branch in the natural gas transmission system is analogous to a phase shifter or transformer in power systems. The natural gas flow through centrifugal compressor will be governed by

$$Gf_{na\to nb} = \text{sgn}(\pi_{na},\pi_{nb}) \frac{CH_{cm}}{k1_{cm} - k2_{cm}\left[\dfrac{\max(\pi_{na},\pi_{nb})}{\min(\pi_{na},\pi_{nb})}\right]^{k3_{cm}}} \tag{3.5}$$

where $k1_{cm}$, $k2_{cm}$ and $k3_{cm}$ are empirical parameters corresponding to the compressor design [An03, Ber78, Sto72]. CH_{cm} represents the power of compressor *cm* as a control variable, where

$$CH_{\min,cm} \leq CH_{cm} \leq CH_{\max,cm} \tag{3.6}$$

The pressure ratio in (3.5) is restricted within a feasible range in (3.7) which is based on compressor characteristics. Compressors would consume additional natural gas that can be withdrawn from either inlet or outlet of compressor to drive turbines as illustrated in Figure 3.3.

$$PR_{\min,cm} \leq \frac{\max(\pi_{na},\pi_{nb})}{\min(\pi_{na},\pi_{nb})} \leq PR_{\max,cm} \tag{3.7}$$

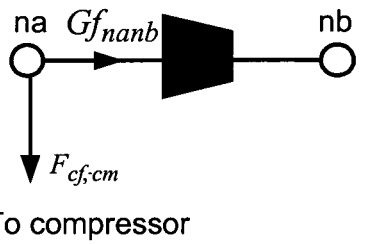

Figure 3.3. Modeling of a compressor

The part of natural gas consumed by compressors represents transmission losses of natural gas grid. The amount of consumed natural gas is related to power of compressors given in (3.8)

$$F_{cf,cm}(CH_{cm}) = c_{cm} + b_{cm} \cdot CH_{cm} + a_{cm} \cdot CH_{cm}^2 \tag{3.8}$$

3.2.2 Formulation of Node Flow Balance. A steady-state mathematical model of a natural gas transmission system is based on the nodal balance approach that indicates that the natural gas flow injected in a node is equal to the natural gas flowing out of the node. In other words, the natural gas flow mismatch at node na is equal to zero,

$$\begin{aligned} g_{na}(\boldsymbol{\pi}, \boldsymbol{CH}, \boldsymbol{GP}, \boldsymbol{GL}) = & \sum_{gi=1}^{NGS} GA_{na,gi} \cdot GP_{gi} - \sum_{gl=1}^{NGL} GB_{na,gl} \cdot GL_{gl} - \sum_{nb \in GC(na)} GK_{na,nb} \cdot Gf_{na \to nb} \\ & - \sum_{cm=1}^{NC} GD_{na,cm} \cdot F_{cf,cm}(CH_{cm}) = 0 \end{aligned} \tag{3.9}$$

By substituting (3.3),(3.5) and (3.8) into (3.9), a group of nonlinear equations with NN dimensions will be obtained in which there are $NN + NC + NGS + NGL$ variables involving node pressure, horsepower of each compressor, natural gas supply, and natural gas load.

3.3 Formulation of SCUC with Natural Gas Transmission System

SCUC with natural gas transmission constraints is to determine the hourly UC and

dispatch for minimizing the operating cost while meeting the prevailing electricity and natural gas constraints. The outline of the model is described as follows:

Min: System operating cost

s.t.

- Power balance and reserve constraints
- Individual generator constraints (Including min on/off time, min/max generation, startup/ shutdown characteristics, ramp rate limits, etc)
- Natural gas contract constraints
- Gas reserve constraints of gas-fired power plant
- Power transmission constraints
- Natural gas transmission constraints

Natural gas constraints are categorized into two types. The first type is modeled based on contracts between utility and natural gas providers. The other natural gas transmission constraints are derived according to natural gas transmission characteristics. The detailed modeling is presented as follows.

3.3.1 Objective function. The objective function (3.10) is composed of fuel costs (utilities) or bids (ISO) for producing electric power and startup and shutdown costs of individual units over the scheduling horizon.

$$Min\{\sum_{\eta} W_{o,\eta} + \sum_{t}\sum_{\eta} W_{\eta t} + \sum_{t}\sum_{i \notin GU}[F_{ec,i}(P_{it})\cdot I_{it} + SU_{it} + SD_{it}] + \sum_{t}\sum_{el}\sigma \cdot ELS_{elt}\} \qquad (3.10)$$

3.3.2 Natural gas contract constraints. Changes to natural gas regulations in the United States, which began in 1985, have offered new alternatives to natural gas transmission companies, locational distribution companies, and large end users [Ave92, Iso08a]. The changes have encouraged such companies to unbundle merchant services

which allow buyers to transport natural gas through pipelines. The natural gas transmission open access allows purchasers to buy natural gas directly from various sources such as natural gas producers and independent marketers. Large users may buy transportation services from natural gas transmission companies. Transportation services are divided into no-notice, firm, and interruptible. In general, natural gas supply contracts with interruptible transportation services can be interrupted with little notice and penalties [Iso08a]. The gas-fired generators have preferred interruptible transportation contracts which are more economical than firm services for supplying electricity at lower prices in competitive electricity markets. Therefore, natural gas supply contracts for gas-fired generating units are relatively less expensive with a lower service priority. Additionally, the gas turbine operation would require high gas pressure, electric generators are more susceptible than other gas loads to pressure losses. Hence, in emergencies, gas-fired generating units are curtailed first especially in winters when gas locational distribution companies would buy the majority of pipeline capacity for supplying their own customers.

In this chapter, we model natural gas supply contracts and transportation services together. A utility may sign up natural gas supply contracts with suppliers as take-or-pay or flexible contracts. Here we assume that each supply contract is corresponding to a priority level of service. The price of a natural gas supply contract has already included costs of transportation services. For take-or-pay natural gas supply contracts, the total cost is constant (3.11). Take-or-pay natural gas supply contracts are to be consumed regardless of cost.

$$W_{\eta} = W_{o,\eta} \tag{3.11}$$

The sum of natural gas usage cannot exceed the contracted amount stated as

$$\sum_t F_{ef,\eta t} \le F_{o,\eta} \tag{3.12}$$

For flexible natural gas supply contract price is usually higher than that of take-off-pay contact with the same transportation services. The total cost depends on the natural gas usage stated as

$$W_{\eta t} = \rho_{gas,\eta} \cdot F_{ef,\eta t} \tag{3.13}$$

Every natural gas contract is considered as a natural gas load with a certain service priority at hour t which is given as

$$GL_{glt} = F_{ef,\eta t} \tag{3.14}$$

3.3.3 Power System Constraints.

1) Power balance and reserve constraints.

$$\sum_i P_{it} \cdot I_{it} = P_{Loss,t} + \sum_{el} (EL - ELS_{elt}) \quad \forall t \tag{3.15}$$

$$\sum_i SR_{it} \ge SR_{D,t} \quad \forall t \tag{3.16}$$

2) Individual generator constraints. Generating units will have individual constraints for restricting ramp up/down, min up/down time, emission, max/min capacity and so on. A single-cycle natural gas unit is modeled as a thermal unit. Either the mode or the component model [Liu09a] may be used for modeling a combined-cycle unit. The model for fuel switching units is provided in [Lu05, Li08]. The detailed modeling of individual generating unit constraints is discussed in [Sha02].

3) Natural gas reserve constraints of gas-fired plants. Some gas-fired power plant may construct a self-owned storage tank so that it can reserve a few of natural gas to be used in peak hours. The natural gas balance constraint related to a gas

contract is given as

$$\sum_{i\in GU(\xi)} F_{ef,it} = SV_{t-1} - SV_t + \sum_{\eta=1}^{N\eta(\xi)} F_{ef,\eta t} \tag{3.17}$$

The self-owned storage is usually small which is scheduled by power plants. The volume of storage facility is governed by

$$SV_{\min} \le SV_t \le SV_{\max} \tag{3.18}$$

4) Power transmission constraints

$$\begin{aligned} &\boldsymbol{C}\cdot\boldsymbol{Pf} = \boldsymbol{A}\cdot\boldsymbol{P} - \boldsymbol{B}\cdot(\boldsymbol{EL} - \boldsymbol{ELS}) \\ &Pf_l = \frac{\theta_a - \theta_b - \gamma_{ab}}{x_{ab}} \quad (a,b \in l) \\ &\left|Pf_l\right| \le Pf_{l,\max} \\ &\gamma_{\min} \le \gamma \le \gamma_{\max} \\ &\theta_{ref} = 0 \end{aligned} \tag{3.19}$$

3.3.4 Natural gas tansmission constraints. See (3.1)-(3.9).

3.4 SCUC Solution with Natural Gas Transmission System

Figure 3.4 depicts the SCUC flowchart with natural gas transmission constraints. Benders decomposition is applied to decompose the original large-scale optimization problem into a master problem and several subproblems, based on the LP duality theory. The master problem is a mixed-integer program and subproblems are linear programs [Als90, Geo72]. The process is described as follows.

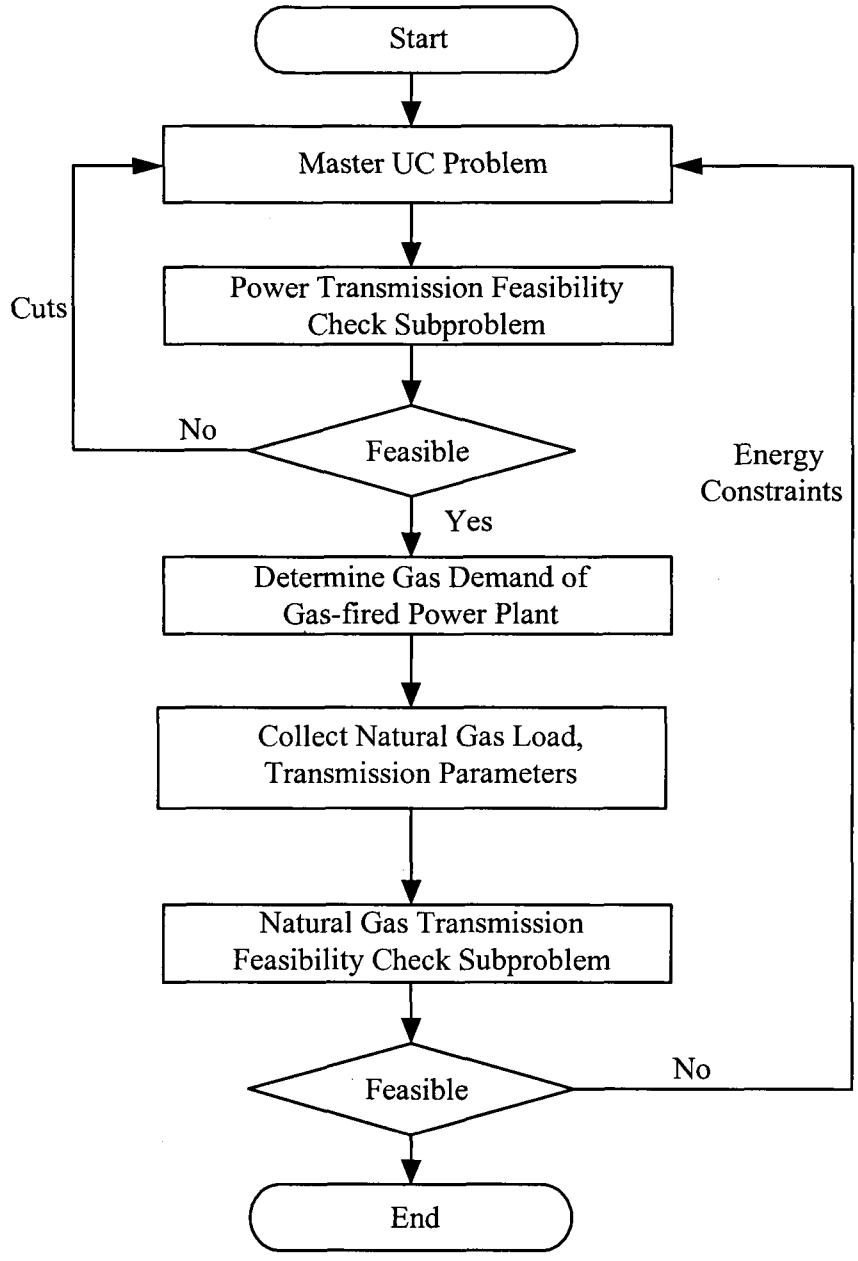

Figure 3.4. Flowchart of SCUC with Natural Gas Transmission Constraints

The ISO or the utility operator would execute the day-ahead SCUC to determine the UC schedule that would satisfy power transmission constraints. Meanwhile, natural gas transmission operators provide the ISO with the information on industrial and residential gas load forecasting with service priorities, natural gas transmission

parameters, and planned outage of natural gas pipelines. The ISO will check the feasibility of natural gas transmission system for serving expected natural gas loads based on available natural gas resources. If the natural gas check subproblem is infeasible, natural gas usage constraints for gas-fired power plants will be formed and added to the master UC problem for the daily UC rescheduling. The iterative process between UC and natural gas transmission feasibility check subproblem will continue until the feasibility of natural gas transmission flow is obtained. The ISO or utility will determine the hourly generation UC and dispatch in the day-ahead market accordingly. The corresponding natural gas consumption data will be transmitted to the natural gas company for evaluation.

3.4.1 Master UC Problem. It is represented by (3.10)-(3.18).

3.4.2 Power Transmission Check Subproblem. The subproblem for power transmission check conducts the security analysis based on the UC solution. The solution of subproblem may be parallelized because hourly power transmission constraints are not coupled. The power transmission model can be either DC or AC. The AC model is presented in [Fu05]. Here, for the sake of focusing on our proposed natural gas subproblem, we present a DC model. The subproblem minimizes the sum of bus power imbalances subjected to the relaxed DC transmission formulation (3.20). The subproblem mitigates transmission violations and iterates with UC via power transfer distribution factors (PTDFs) or Benders cuts.

The general Benders decomposition method will form both infeasibility and optimality cuts. We update upper and lower bounds until the gap between the bounds is less than a given value. For particular engineering applications, (3.10) will be fully

included in the master problem. The subproblems will check constraints (3.19) and produce infeasibility cuts (3.21) which are fed back to the master problem if any hourly values of objective function (3.20) are nonzero.

$$
\begin{aligned}
Min \quad & w(\hat{\boldsymbol{P}}) = \sum_{l=1}^{NB} (S1_l + S2_l) \\
S.t. \quad & \boldsymbol{C} \cdot \boldsymbol{pf} = \boldsymbol{A} \cdot \hat{\boldsymbol{P}} - \boldsymbol{B} \cdot \boldsymbol{EL} + \boldsymbol{S1} - \boldsymbol{S2} \qquad \lambda \\
& Pf_l = \frac{\theta_a - \theta_b - \gamma_{ab}}{x_{ab}} \quad (a,b \in l) \qquad \forall l \\
& Pf_{l,\max} \le Pf_l \le Pf_{l,\max} \qquad \forall l \\
& \gamma_{\min} \le \gamma \le \gamma_{\max} \\
& \theta_{ref} = 0
\end{aligned}
\tag{3.20}
$$

$$
w(\boldsymbol{P}) = w(\hat{\boldsymbol{P}}) + \sum_{i=1}^{NG} \lambda_{it} (P_{it} - \hat{P}_{it}) \le 0 \tag{3.21}
$$

3.4.3 Natural Gas Transmission Feasibility Check Subproblem. In the natural gas transmission (3.9) the number of variables is more than the number of equations and the solution would require fixing no more than $NC + NGS + NGL$ variables in iterative nonlinear optimization techniques. The Newton-Raphson method is applied to solve the nonlinear equations. If $\boldsymbol{\chi}$ represents the vector of unknown variables, the iterative equations are given as

$$
\begin{cases}
\boldsymbol{J}_k \Delta \boldsymbol{\chi}^{(k)} = -\boldsymbol{g}(\boldsymbol{\chi}^{(k)}) \\
\boldsymbol{\chi}^{(k+1)} = \boldsymbol{\chi}^{(k)} + \Delta \boldsymbol{\chi}^{(k)}
\end{cases}
\tag{3.22}
$$

where $\boldsymbol{J}^{(k)}$, the Jacobin matrix in the kth iteration, is given as

$$
\boldsymbol{J}^{(k)} = \boldsymbol{Dg}(\boldsymbol{\chi}^{(k)}) = \left. \frac{\partial \boldsymbol{g}}{\partial \boldsymbol{\chi}} \right|_{\boldsymbol{\chi}^{(k)}} \tag{3.23}
$$

The nonzero elements of Jacobian matrix are given as

$$\frac{\partial g_{na}}{\partial GP_{gi}} = GA_{na,gi} \tag{3.24}$$

$$\frac{\partial g_{na}}{\partial GL_{gl}} = GB_{na,gl} \tag{3.25}$$

$$\frac{\partial g_{na}}{\partial \pi_{na}} = -\sum_{nb \in na} \frac{\partial Gf_{na \to nb}}{\partial \pi_{na}} \tag{3.26}$$

$$\frac{\partial g_{na}}{\partial \pi_{nb}} = -\frac{\partial Gf_{na \to nb}}{\partial \pi_{nb}} \tag{3.27}$$

$$\frac{\partial g_{na}}{\partial CH_{cm}} = -\sum_{nb \in GC(na)} \frac{\partial Gf_{na \to nb}}{\partial CH_{cm}} - \sum_{cm=1}^{NC} GK_{na,cm} \cdot (2a_{cm} + b_{cm}) \tag{3.28}$$

Based on (3.3)-(3.8), we would calculate the partial derivative of natural gas flow of each branch with respect to the corresponding pressure and horsepower of compressor. The detailed formulations of $\frac{\partial Gf_{na \to nb}}{\partial \pi_{na}}, \frac{\partial Gf_{na \to nb}}{\partial \pi_{nb}}, \frac{\partial Gf_{na \to nb}}{\partial CH_{cm}}$ given in (B.1)-(B.8) in Appendix B. If π, CH, GP, GL represent the variables, the modified Jacobian matrix is $\left[J_{\pi}^{(k)} \quad J_{CH}^{(k)} \quad \boldsymbol{GA} \quad -\boldsymbol{GB}\right]$. The iterative formulation is represented in (3.29). The Jacobian matrix is highly sparse and sparse matrix techniques including sparse storages, triangular factorization, fast forward (backward) substitution are used to solve (3.29) which results from the Newton-Raphson method.

$$\left[J_{\pi}^{(k)} \quad J_{CH}^{(k)} \quad \boldsymbol{GA} \quad -\boldsymbol{GB}\right] \begin{bmatrix} \Delta\boldsymbol{\pi}^{(k)} \\ \Delta\boldsymbol{CH}^{(k)} \\ \Delta\boldsymbol{GP}^{(k)} \\ \Delta\boldsymbol{GL}^{(k)} \end{bmatrix} = -\boldsymbol{g}(\boldsymbol{\pi}, \boldsymbol{CH}, \boldsymbol{GP}, \boldsymbol{GL})$$

$$\begin{bmatrix} \boldsymbol{\pi}^{(k+1)} \\ \boldsymbol{CH}^{(k+1)} \\ \boldsymbol{GP}^{(k+1)} \\ \boldsymbol{GL}^{(k+1)} \end{bmatrix} = \begin{bmatrix} \boldsymbol{\pi}^{(k)} \\ \boldsymbol{CH}^{(k)} \\ \boldsymbol{GP}^{(k)} \\ \boldsymbol{GL}^{(k)} \end{bmatrix} + \begin{bmatrix} \Delta\boldsymbol{\pi}^{(k)} \\ \Delta\boldsymbol{CH}^{(k)} \\ \Delta\boldsymbol{GP}^{(k)} \\ \Delta\boldsymbol{GL}^{(k)} \end{bmatrix} \tag{3.29}$$

The natural gas transmission feasibility check problem (3.30)-(3.37) would check whether the available gas resources and controllable compressors could satisfy natural gas transmission limits as well as natural gas demands of gas-fired units committed by the master UC problem. The non-negative natural gas load shedding variables $\boldsymbol{SL}$ are added to ensure that the optimization problem is feasible. From a physical viewpoint, such slack variables represent virtual natural gas load shedding at each delivery point to eliminate mismatches.

The objective is to minimize the sum of slack variables. Constraints (3.31)-(3.37) represent pressure limits on each node, maximum/minimum gas delivery mass of each node, horsepower limit, and pressure ratio range of compressors, respectively. It is noted that $\boldsymbol{GSL}_{\max} = 0$ for firm gas load and gas load from power plants. We use the successive LP to solve the problem iteratively. The Jacobian matrix is the same as (3.23). Hence

$$Min \quad \omega(\boldsymbol{G\hat{L}}) = \sum_{gl=1}^{NGL} (SL_{gl}) \tag{3.30}$$

$$s.t. \quad \begin{bmatrix} \boldsymbol{J}_{\pi} & \boldsymbol{J}_{CH} & \boldsymbol{GA} & \boldsymbol{GB} \end{bmatrix} \begin{bmatrix} \Delta\boldsymbol{\pi} \\ \Delta\boldsymbol{CH} \\ \Delta\boldsymbol{GP} \\ \Delta\boldsymbol{GSL} \end{bmatrix} + \boldsymbol{GB} \cdot \boldsymbol{SL} = -\boldsymbol{g}(\boldsymbol{\pi}, \boldsymbol{CH}, \boldsymbol{GP}, \boldsymbol{G\hat{L}} - \boldsymbol{GSL}) \quad \boldsymbol{\mu} \tag{3.31}$$

$$0 \le \boldsymbol{GSL} + \Delta\boldsymbol{GSL} \le \boldsymbol{GSL}_{\max} \le \boldsymbol{G\hat{L}} \tag{3.32}$$

$$0 \le \boldsymbol{SL} \tag{3.33}$$

$$\boldsymbol{\pi}_{\min} \le \boldsymbol{\pi} + \Delta\boldsymbol{\pi} \le \boldsymbol{\pi}_{\max} \tag{3.34}$$

$$\boldsymbol{GP}_{\min} \le \Delta\boldsymbol{GP} + \boldsymbol{GP} \le \boldsymbol{GP}_{\max} \tag{3.35}$$

$$\boldsymbol{CH}_{\min} \le \boldsymbol{CH} + \Delta\boldsymbol{CH} \le \boldsymbol{CH}_{\max} \tag{3.36}$$

$$\boldsymbol{PR}_{\min} \cdot (\boldsymbol{\pi}_{inlet} + \Delta\boldsymbol{\pi}_{inlet}) \le \boldsymbol{\pi}_{outlet} + \Delta\boldsymbol{\pi}_{outlet} \le \boldsymbol{PR}_{\max} \cdot (\boldsymbol{\pi}_{inlet} + \Delta\boldsymbol{\pi}_{inlet}) \tag{3.37}$$

The iterative solution process of natural gas transmission feasibility check subproblem is discussed as follows.

1) Calculate modified Jacobian matrix $\boldsymbol{J}$ and initial natural gas node mismatch vector $-\boldsymbol{g}(\boldsymbol{\pi}, \boldsymbol{CH}, \boldsymbol{GP}, \boldsymbol{G\hat{L}} - \boldsymbol{GSL})$ based on the initial gas load, system states, and generation schedules of natural gas providers.

2) Use LP to minimize the objective function (3.30) and calculate changes in state and control variables of the natural gas transmission system $\Delta\pi$, ΔCH, ΔGP, and ΔGSL. If the difference between current and previous iterative changes is less than a specified threshold ε, stop the process. Otherwise, go back to Step 3.

3) Update state and control variables. Calculate elements of Jacobian matrix and $\boldsymbol{SL}$.

$$\begin{bmatrix} \boldsymbol{\pi}^{(k+1)} \\ \boldsymbol{CH}^{(k+1)} \\ \boldsymbol{GP}^{(k+1)} \\ \boldsymbol{GSL}^{(k+1)} \end{bmatrix} = \begin{bmatrix} \boldsymbol{\pi}^{(k)} \\ \boldsymbol{CH}^{(k)} \\ \boldsymbol{GP}^{(k)} \\ \boldsymbol{GSL}^{(k)} \end{bmatrix} + \begin{bmatrix} \Delta\boldsymbol{\pi}^{(k)} \\ \Delta\boldsymbol{CH}^{(k)} \\ \Delta\boldsymbol{GP}^{(k)} \\ \Delta\boldsymbol{GSL}^{(k)} \end{bmatrix}$$

Once the above iterative process is completed, a non-negative objective function (3.30) that is larger than the specified tolerance means that nodal gas suppliers and loads cannot provide a feasible natural gas flow solution. In this case, an energy constraint (Benders cut) given in (3.38) will be formed.

$$\omega(\boldsymbol{GL}) = \omega(\boldsymbol{G\hat{L}}) + \sum_{gl} GB^{T}_{gl,na} \cdot \mu_{na} \cdot (GL_{gl} - \hat{GL}_{gl}) \le 0 \tag{3.38}$$

$$\omega(F_{ef,\eta}) = \omega(\hat{F}_{ef,\eta}) + \sum_{\eta} B^{T}_{gl,na} \cdot \mu_{na} \cdot (F_{ef,\eta} - \hat{F}_{ef,\eta}) \le 0 \tag{3.39}$$

Here, $\omega(\boldsymbol{G\hat{L}})$ is equal to the sum of slack variables in the current iteration. A positive $\omega(\boldsymbol{G\hat{L}})$ corresponds to a positive natural gas node mismatch $-\boldsymbol{g}(\boldsymbol{\pi}, \boldsymbol{CH}, \boldsymbol{GP}, \boldsymbol{G\hat{L}} - \boldsymbol{GSL})$. $\boldsymbol{\mu}$ is the dual variable corresponding to (3.30). $\boldsymbol{\mu}$ captures the sensitivity of $\omega(\boldsymbol{G\hat{L}})$ to right

hand mismach $-g(\pi, CH, GP, G\hat{L} - GSL)$ which is derived by solving the dual problem of successive LP. So μ can capture the mismatch of natural gas node and feed the information back to the UC problem. By substituting (3.14) into (3.38), we derive energy constraints (3.39) which is added to the master UC problem for the next iterative solution of UC.

Here, Benders cuts are generated from the solution of a successive approximation of a nonlinear equation. Pipeline equations may make the subproblems non-convex in feasible sets. So if the initial operating point of natural gas problem is not close enough to the global optimal points, the final solution of SCUC with natural gas constraints may result in a local optimal solution. However, we may try different initial points of natural gas flow to find the best possible solution. Reference [Tom07] introduces a set of initial points (π_{na}, π_{nb}) to linearize (3.3) which can replace the nonlinear function with linear inequality for each pipeline. For any given pipeline flow, only one of the inequality constraints, namely the one that approximates the flow best, will be binding. For a pipeline network without compressors, (3.30)-(3.37) represent a LP problem, rather than a successive LP, when applying linearized inequality constraints [Tom07]. The improvement can potentially enhance the quality of optimal solution with the same computing time.

3.5 Case Studies

We apply two case studies consisting of a 6-bus power system with 7-node gas system and the IEEE 118-bus system with 14-node natural gas system to illustrate the performance of our SCUC with natural gas transmission constraints. We assume that 1 kilo-cubic feet of natural natural gas can generate 1 MBtu of energy in both cases.

3.5.1 6-Bus system. The 6-bus system, depicted in Figure 3.5, has three gas-fired units, five transmission lines, and two tap-changing transformers. The characteristics of generators, buses, transmission lines, and tap-changing transformers and the hourly load distribution over the 24-h horizon are given in Tables A.1 through A.6 in Appendix A, respectively. The unit startup and shutdown costs are assumed negligible and equal to zero in this case. The 7-node natural gas system is given in Figure 3.6, which has 1 compressor, 5 pipelines, 2 natural gas suppliers, and 5 natural gas loads. The natural gas transmission parameters are listed in Tables A.7 through A.11 in Appendix A.

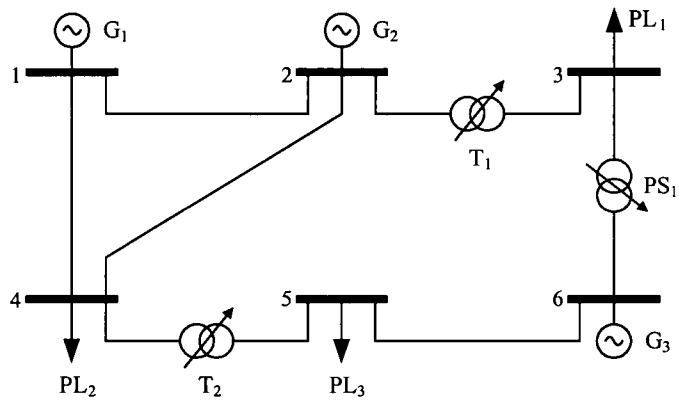

Figure 3.5. 6-Bus Power System

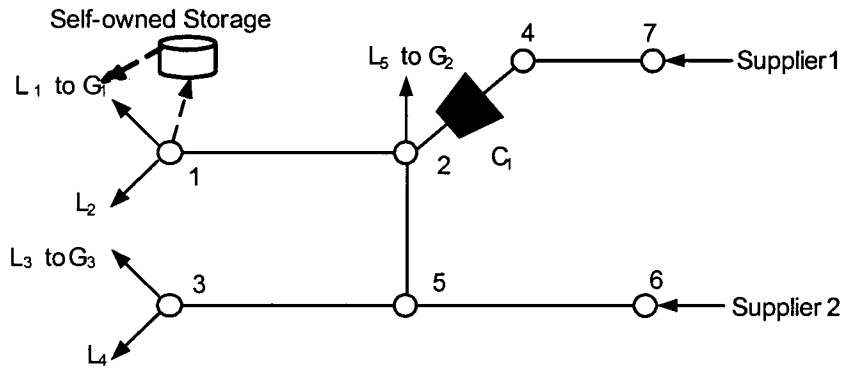

Figure 3.6. 7-Node Natural Gas System

According to Figure 3.6, natural gas loads 1, 5, 3 correspond to the gas-fired units 1, 2, 3, which are determined by the hourly generation dispatch of generating units. The units have interruptible contracts with the natural gas company. Gas loads 2 and 4 represent equivalent loads consumed by other natural gas users. Here, we assume that natural gas loads 2 and 4 have a higher priority than gas-fired power plants, which means any natural gas transmission infeasibility will lead to the natural gas load shedding of gas-fired power plants. The hourly sums of natural gas loads 2 and 4 are given in Table A.13 and A.14.

In order to discuss the efficiency of the proposed approach as well as the impact of natural gas transmission system on SCUC results, we consider the following five cases:

- Case 1: SCUC without natural gas transmission constraints
- Case 2: SCUC with natural gas transmission constraints
- Case 3: Impact of fluctuating natural gas loads
- Case 4: Impact of natural gas pipeline outages
- Case 5: Impact of natural gas storage on power plants

Theses cases are discussed as follows.

Case 1: SCUC without natural gas transmission constraints.

We calculate the hourly UC solution in 24 hours by considering dc transmission constraints and ignoring gas transmission constraints. The hourly commitment schedule is shown in Table I in which the hour 0 represents the initial condition. The peak electricity load is at hour 17 when units 1, 2, 3 are dispatched at 204.11 MW, 37.01 MW and 20 MW, respectively. The daily operating cost is $509,572. In this Case, expensive generating units 2 and 3 are not committed at certain hours in order to minimize the daily

operating cost.

Case 2: SCUC with natural gas transmission constraints.

We apply the SCUC schedule given in Case 1 and incorporate natural gas transmission constraints. When we ignored natural gas constraints, the gas demand of unit 1 was 2,952 kcf/h at hour 17, and the gas load 2 at the same node was 4,000 kcf/h. However, the natural gas transmission limit of pipeline 1 which is 6,765 kcf/h is violated because the minimum pressure at the natural gas node 1 and the maximum pressure at the natural gas node 2 are 105 and 170 Psig, respectively. Since the gas load 2 at hour 17 has the higher priority, the natural gas load 1 corresponding to unit 1 is slacked and the dual variable μ is calculated after solving the successive LP. According to (3.38), a Benders cut (energy constraints) given by (3.40) is created which indicates that a gas load shedding of 187.1 kcf/h will take place at the natural gas load 1. The new UC solution in the master problem results in a new generation dispatch of 190.43 MW for unit 1 at hour 17.

$$\omega(\hat{GL}) = 187.1 + [1 \cdot GL_{1,t=17}(P_{1,t=17})] - 1 \cdot 2952 \leq 0 \tag{3.40}$$

In this case, the natural gas transmission feasibility check subproblem also encounters natural gas flow violations at hours 8-16 and 18-24. SCUC, with a single iteration between the master UC problem and natural gas transmission feasibility check subproblem, commits the expensive unit 2 at hours 10, 11, and 22 as well as the expensive unit 3 at hours 8 and 9. Figure 3.7 shows that the generation dispatch of cheaper unit 1 at hours 8-24 is curtailed. Table II shows that the daily operating cost of $550,399 is higher than that of Case 1.

Table 3.1. Hourly Schedule of Case 1 of 6 Bus System

Daily production cost: $509,572	
Unit	Hours (0-24)
1	1 1 1 1 1 1 1 1 1 1 1 1 1 1 1 1 1 1 1 1 1 1 1 1
2	1 0 0 0 0 0 0 0 0 0 0 0 1 1 1 1 1 1 1 1 1 1 0 0 0
3	0 0 0 0 0 0 0 0 0 0 1 1 1 1 1 1 1 1 1 1 1 1 1 0 0

Table 3.2. Hourly Schedule of Case 2 of 6-Bus System

Daily production cost: $550,399	
Unit	Hours (0-24)
1	1 1 1 1 1 1 1 1 1 1 1 1 1 1 1 1 1 1 1 1 1 1 1 1
2	1 0 0 0 0 0 0 0 0 0 1 1 1 1 1 1 1 1 1 1 1 1 0 0
3	0 0 0 0 0 0 0 0 1 1 1 1 1 1 1 1 1 1 1 1 1 1 1 1

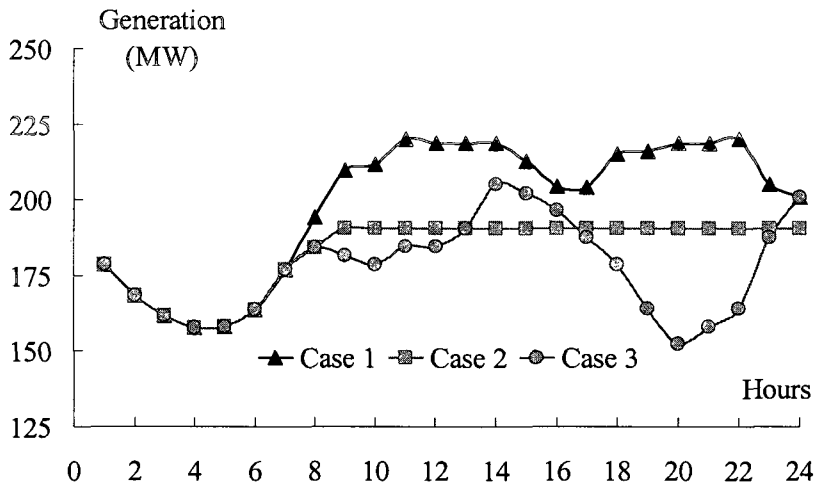

Figure 3.7. Hourly Dispatch of Unit 1 in Cases 1-3

Case 3: Impact of fluctuating natural gas loads.

There is a higher chance of natural gas flow congestion or pressure loss if the residential gas load and electricity generation would peak simultaneously. In this case and thereafter, we use the natural gas load data given in Table A.14 in Appendix A instead of a constant load presented in Case 2. New SCUC scheduling results are given

in Table 3.3 with an operating cost of $553,850 which is higher than those in Cases 1 and 2. The SCUC solution resorts to 62.63 MW of electric load shedding during hours 17-21 to deal with natural gas shortages. The total load shedding cost is $62,650 since the load shedding price is $1000/MW. Figure 3.8 demonstrates that both electric and natural gas loads are high when load shedding is deemed necessary. Accordingly, hourly variations of residential and industrial natural gas load can affect the security and economics of power systems.

Table 3.3. Hourly Schedule of Case 3 of 6-Bus System

Daily production cost: $553,850																									
Electric load shedding: 62.63 MW														Load shedding cost: $62,630											
Unit	Hours (0-24)																								
1	1	1	1	1	1	1	1	1	1	1	1	1	1	1	1	1	1	1	1	1	1	1	1	1	1
2	1	0	0	0	0	0	0	0	0	1	1	1	1	1	1	1	1	1	1	1	1	1	1	0	0
3	0	0	0	0	0	0	0	0	1	1	1	1	1	1	1	1	1	1	1	1	1	1	1	1	0

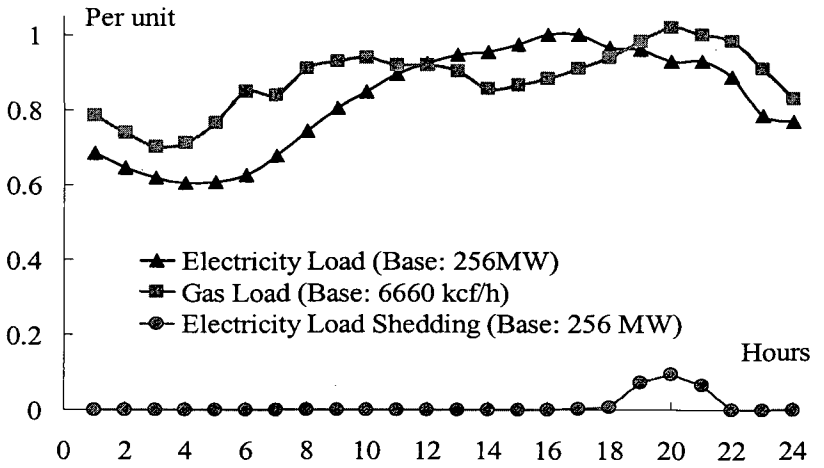

Figure 3.8. Electricity load shedding in Case 3

Case 4: Impact of natural gas pipeline outages.

The potential outages of natural gas system will become a critical issue when the

total installed capacity of natural gas-fired generating units increases. In this case, the outage of natural gas pipeline 2 between nodes 2 and 5 at hours 21-24 will lead to the curtailment of generation unit 1 as shown in Table 3.4.

Table 3.4. Hourly Schedule of Case 4 of 6-Bus System

Daily production cost: $496,873																									
Electric load shedding: 737 MW														Load shedding cost: $737,000											
Unit	Hours (0-24)																								
1	1	1	1	1	1	1	1	1	1	1	1	1	1	1	1	1	1	1	1	1	0	0	0	0	
2	1	0	0	0	0	0	0	0	0	1	1	1	1	1	1	1	1	1	1	1	1	1	1	1	
3	0	0	0	0	0	0	0	0	1	1	1	1	1	1	1	1	1	1	1	1	1	1	1	1	

Here unit 1 is the cheapest one; however, unit 2 is more likely to stay on-line longer than unit 1 during outage hours. In this case, the minimum generation of unit 1 is 100 MW which cannot be sustained when there is a natural gas shortage. At the same time, unit 1 is larger than other generating units which makes it impossible for other units to compensate the generation gap when unit 1 is on outage at hours 21-24. Accordingly, a 737 MW of electric load shedding will occur, which is an undesirable option in power systems. This case shows that natural gas pipeline outages may have a significant impact on the power system security and economics.

Case 5: Impact of natural gas storage on power plants.

We consider an additional storage facility owned by gas-fired power unit 1 as shown in Figure 3.6. The storage parameters are listed in Table A.15. With storage, the additional natural gas transported through pipeline 1 during off-peak hours is stored for peak hours or when pipeline outages occur. Table 3.5 gives the new daily UC schedule

with a production cost of $557,351. This new schedule will not require any curtailments of electric loads at hours 21-24. The reasons are given as follows. First, after the 7-node natural gas transmission is divided into two subsystems, the supplier 2 cannot provide gas fuels to units 2 and 1. By comparing with Case 4, we learn that unit 3 is kept on-line to make use of supplier 2 by decreasing the production of generating units 1 and 2. Meanwhile, the most expensive unit 2 is not committed at hours 9-11 and 22-24, which indicates that the additional available gas can be used to produce power by the most efficient unit 1 or stored in storage. Figure 3.9 shows the hourly natural gas transmission through pipeline 1 in Cases 4 and 5, respectively. It is clear that pipeline 1 transports more gas to the storage and unit 1 at hours 1-8 and 21-24. Figure 3.10 shows the hourly dispatch of unit 1 in Cases 4 and 5. Figure 3.11 shows the hourly gas volume in storage. The natural gas storage can improve the security and economics of constrained power systems by supplying additional gas reserves to power plants. The information on cuts and CPU times is given in Table 3.6.

Table 3.5. Hourly Schedule of Case 5 of 6-Bus System

Daily production cost: $557,351																									
Electric load shedding: 0 MW															Load shedding cost: $0										
Unit	Hours (0-24)																								
1	1	1	1	1	1	1	1	1	1	1	1	1	1	1	1	1	1	1	1	1	1	1	1	1	1
2	1	0	0	0	0	0	0	0	0	0	0	0	0	1	1	1	1	1	1	1	1	1	0	0	0
3	0	1	1	1	1	1	1	1	1	1	1	1	1	1	1	1	1	1	1	1	1	1	1	1	1

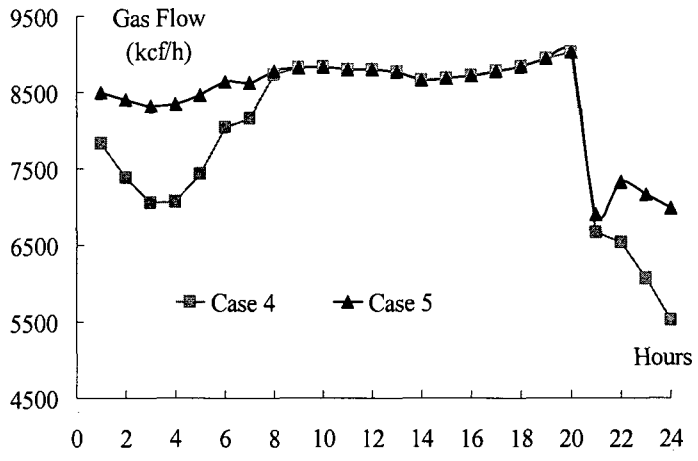

Figure 3.9. Natural Gas Pipeline Flows in Cases 4 and 5

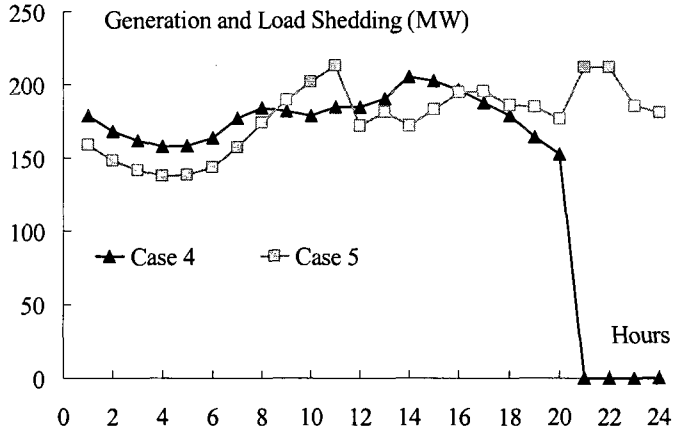

Figure 3.10. Hourly Dispatch of Unit 1 in Cases 4 and 5

Table 3.6. Information of Generated Cuts and Iteration of 6 Bus System

Number of Cuts and Interations	Case 1	Case 2	Case 3	Case 4	Case 5
Total Electric Network Cuts	10	10	10	10	10
Total Gas Cuts	0	16	21	21	25
Number of Iterations of Electric Network Loop	2	3	4	4	6
Number of Iterations of Gas Loop	0	2	3	3	5

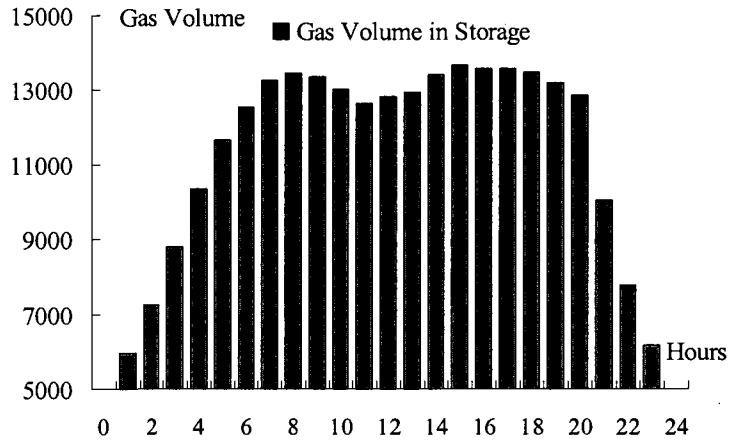

Figure 3.11. Hourly Gas Volume of Storage in Case 5

3.5.2 IEEE 118-Bus System. A modified IEEE 118-bus system is used to study the SCUC with natural gas transmission constraints. The system has 54 fossil units, 12 gas-fired combined cycle units, 7 hydro units, 186 branches, 14 capacitors, nine tap-changing transformers, and 91 demand sides. The peak load of 7,300 MW occurs at hour 21. The power transmission topology is shown in Figure 3.12.

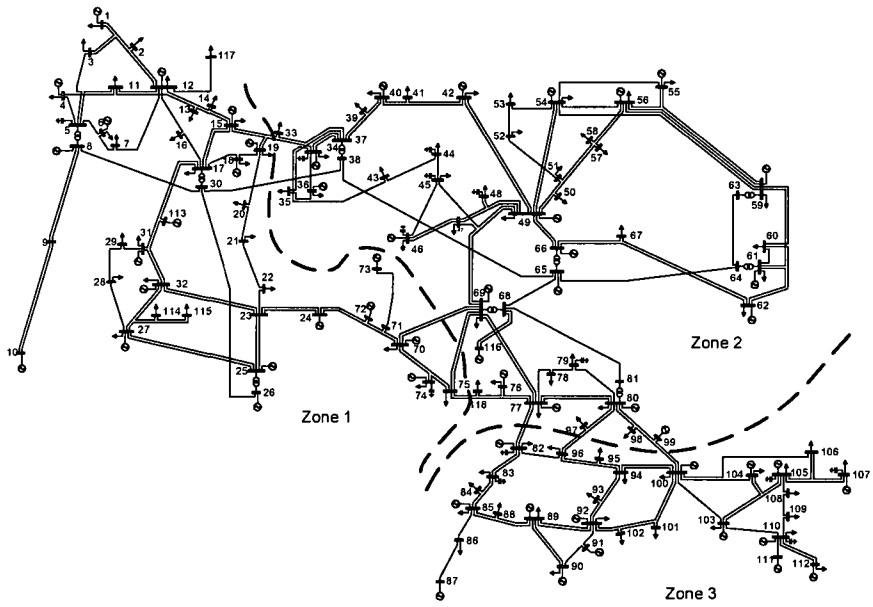

Figure 3.12. 118-Bus Power System

The natural gas transmission is composed of 14 nodes, 12 pipelines, and 2 compressors as shown in Figure 3.13. The test data for the 118-bus power system and 14-node gas system are given in http://motor.ece.iit.edu/data/Gastranssmion_118_14test.xls.

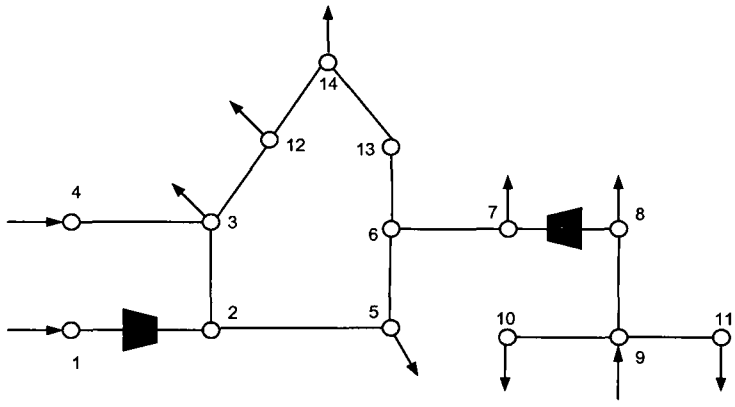

Figure 3.13. 14-Node Gas Transmission System

Table 3.7 presents the base case SCUC without natural gas transmission constraints with a daily operating cost of $1,936,329. The execution time is 60 sec on a 2.6 GHz personal computer. Since combined-cycle gas units demonstrate a better efficiency, generating units 4001-4012 are committed at certain hours to serve the hourly load while the expensive fossil units such as 1013, 1047, and 1052 are not committed.

In order to check if the gas flow is feasible, we use the initial UC solution to examine the hourly natural gas transmission feasibility check subproblem (3.30)-(3.37). In the subproblem, gas load violations occur in nodes 5, 10-11, 14, which show that the natural gas required by combined-cycle units cannot be transported to related nodes by the gas transmission system in base case operating conditions. Accordingly, natural gas demands are slacked and energy constraints are fed back to the master UC problem. The information on generated cuts and iterations of natural gas and power transmission loops are listed in Table 3.8. After six iterations between SCUC and natural gas feasibility

check subproblems, we obtain the generation dispatch and hourly UC results shown in Table 3.9. In Table 3.9, combined-cycle units 4003, 4005 and 4010 are off because of gas shortages. Furthermore, the distribution of combined-cycle units has changed as compared to that in the base case. The daily operating cost is $1,965,738 which is higher than that of the base case.

Table 3.7. Hourly Unit Commitment of Case 1 for the 118 Bus System

Daily production cost: $ 1936329																									
Unit	Hours (0-24)																								
1013	1	0	0	0	0	0	0	0	0	0	0	0	0	0	0	0	0	0	0	0	0	0	0	0	0
1034	1	0	0	0	0	0	0	0	0	0	0	0	0	0	0	1	1	1	1	1	1	1	1	1	1
1047	1	0	0	0	0	0	0	0	0	0	0	0	0	0	0	0	0	0	0	0	0	0	0	0	0
1048	1	1	1	1	1	1	1	1	1	1	1	1	1	1	1	1	1	1	1	1	1	1	1	1	0
1051	1	1	1	1	1	1	1	1	1	1	1	1	1	1	1	1	1	1	1	1	1	1	0	0	0
1052	1	0	0	0	0	0	0	0	0	0	0	0	0	0	0	0	0	0	0	0	0	0	0	0	0
4001	0	1	1	3	3	3	3	4	4	4	4	4	4	4	4	4	4	4	4	4	4	4	4	4	4
4002	0	0	0	0	0	2	2	4	4	4	4	4	4	4	4	4	4	4	4	4	4	4	4	4	4
4003	0	0	0	0	0	0	0	1	1	3	3	4	4	4	4	4	4	4	4	4	4	4	4	4	4
4004	0	0	0	0	0	0	0	0	0	0	0	0	0	0	0	1	1	3	3	4	4	4	4	4	4
4005-4006	0	2	2	4	4	4	4	4	4	4	4	4	4	4	4	4	4	4	4	4	4	4	4	4	4
4007-4009	0	2	2	2	4	4	4	4	4	4	4	4	4	4	4	4	4	4	4	4	4	4	4	4	4
4010-4011	0	2	2	4	4	4	4	4	4	4	4	4	4	4	4	4	4	4	4	4	4	4	4	4	4
4012	0	2	2	2	2	4	4	4	4	4	4	4	4	4	4	4	4	4	4	4	4	4	4	4	4

Table 3.8. Generated Cuts and Iterations of 118 Bus System

Iteration Index of Gas Transmission Loop	1	2	3	4	5	6
Number of Iterations of Power Transmission Loop in Each Iteration of Natural Gas Loop	8	2	3	1	1	1
Power Transmission Cuts in Each Iteration of Natural Gas Transmission Loop	68	2	2	0	0	0
Gas Cuts in Each Iteration of Natural Gas Transmission Loop	24	22	17	15	4	0

Table 3.9. Hourly Unit comiitment of Case 2 for the 118 Bus System

Daily production cost: $ 1965738																									
Unit	Hours (0-24)																								
1013	1	1	1	1	1	1	1	1	1	1	1	1	1	1	1	1	1	1	1	1	1	0	0	0	
1034	1	0	0	0	0	0	0	0	0	1	1	1	1	1	1	1	1	1	1	1	1	1	1	1	
1047-1048	1	0	0	0	0	0	0	0	0	0	0	0	0	0	0	1	1	1	1	1	1	1	1	1	
1051-1052	1	0	0	0	0	0	0	0	0	0	0	0	0	0	0	1	1	1	1	1	1	1	1	1	
4001	0	1	1	3	3	3	3	4	4	4	4	4	4	4	4	4	4	4	4	4	4	4	4	4	
4002	0	0	0	0	2	2	4	4	4	4	4	4	4	4	4	4	4	4	4	4	4	4	4	4	
4003	0	0	0	0	0	0	0	0	0	0	0	0	0	0	0	0	0	0	0	0	0	0	0	0	
4004	0	0	0	0	0	2	2	4	4	4	4	4	4	4	4	4	4	4	4	3	3	4	4	4	
4005	0	1	1	0	0	0	0	0	0	0	0	0	0	0	0	0	0	0	0	0	0	0	0	0	
4006	0	2	2	4	4	4	4	4	4	4	4	4	4	4	4	4	4	4	4	4	4	4	4	4	
4007-4009	0	2	2	2	4	4	4	4	4	4	4	4	4	4	4	4	4	4	4	4	4	4	4	4	
4010	0	0	0	0	0	0	0	0	0	0	0	0	0	0	0	0	0	2	2	1	1	0	0	0	
4011	0	2	2	4	4	4	4	4	4	4	4	4	4	4	4	4	4	4	4	4	4	4	4	4	
4012	0	2	2	2	2	4	4	4	4	4	4	4	4	4	4	4	4	4	4	4	4	4	4	4	

3.6 Conclusions

This chapter proposes a mathematical model and its solution for SCUC with natural gas transmission constraints. At the base case, natural gas transmission is modeled by a group of nonlinear equations. Benders decomposition is applied to separate the natural gas transmission subproblem from the master UC problem and the power transmission subproblem. The decomposition would avoid the computational complexity when solving the proposed large-scale optimization problem. Successive LP is applied to solve the natural gas transmission feasibility check subproblem. The LP duality theory is applied to generate energy constraints corresponding to natural gas transmission violations, which are added to the master UC problem for rescheduling the hourly UC. The tests on the 6-bus power system linking with the 7-node gas system and the IEEE 118-bus systems with the 14-node gas system demonstrate the effectiveness of the proposed scheduling approach.

CHAPTER 4

LEAST SOCIAL COST OF SCHEDULING COORDINATION OF HYDROTHERMAL POWER SYSTEM AND NATURAL GAS SYSTEM BY AUGMENTED LAGRANGIAN RELAXATION

4.1 Introduction

The previous chapter presented a security-constrained unit commitment model incorporating with nonlinear gas transmission constraints and natural gas contracts. The natural gas usage limits of gas-fired units are implicitly determined by the feasible adjustment range of gas network and priority orders of gas load contracts shared by gas operators. Benders decomposition was used to apply the hourly unit commitment (UC) results to separate blocks of electric power and natural gas transmission constraints. However, our previous model considered the viewpoints of the ISO and vertically integrated utility operators. Furthermore, operating costs of compressors and natural gas wells, and residual gas load models were not directly considered in the objective function.

In this chapter we propose a coordinated scheduling model from a joint operator's viewpoint as shown in Fig. 1. The coordination model is a mixed-integer nonlinear optimization problem in which the objective function will minimize the social cost of electric power and natural gas systems. In our proposed model, the joint operator is an independent organization which could operate outside the traditional jurisdictions of gas and electric power operators and would pursue the overall interest of coordinated energy systems. Natural gas resources will be allocated optimally to either supply gas loads or gas-fired generating units. The two systems have a decomposable structure and we consider the LR method as the decomposition strategy of the coordination problem. The coupling constraints between the electric power system and the natural gas transmission

system is relaxed by Lagrangian multipliers and dualized into the objective function. The LR method is divided into two phases. The first phase is to solve the dual problem. However, the solution of phase one may not be feasible when considering the primal problem. Thus, the phase two of the dual problem will seek a feasible solution based on the solution of phase one as shown in Fig. 1. The relaxed primal problems are decomposed into security-constrained unit commitment subproblem with the hydro coordination (SCUC) and gas allocation subproblems which can be solved independently but in coordination. The methodologies for SCUC and natural gas allocation problems were developed in [Sha02, Woo96, Ric79], which incorporate the LR framework in our proposed model to solve the mixed-integer nonlinear subproblems individually.

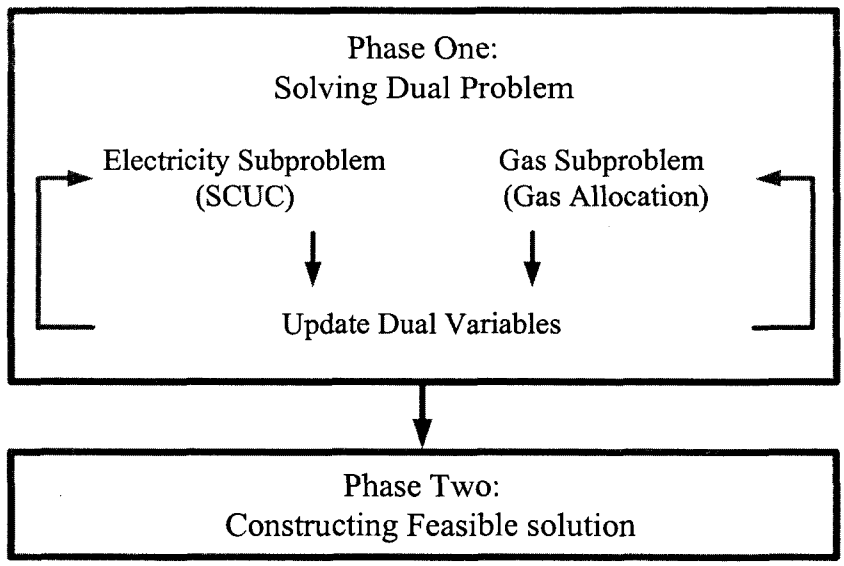

Figure 4.1. LR Based Electricity-Gas Dcheduling Coordination

We demonstrate that the LR approach in our coordination model will not exhibit a satisfactory convergence. The nonconvex characteristics of the coordinated problem will result in the oscillation of dual solution which is due to integer variables and network constraints. Moreover, with slight changes in the multipliers, the linear price function of

the natural gas well may lead to a cycling behavior of gas well output between its max and min values. Accordingly, the violation of relaxed constraints cannot be alleviated iteratively. Hence, the augmented LR method with piecewise linear approximation of quadratic penalty term is used for preventing numerical oscillations and improving the quality of dual solution. The Lagrangian dual will no longer be decomposable after introducing inseparable penalty terms. So we use the block descent coordination (BDC) technique to deal with this problem and solve the decomposed SCUC and gas allocation subproblems sequentially.

The proposed model can be used by combination natural gas and electric utilities for the commitment and dispatch of power units, gas wells, compressors, and gas storage together. It can also be a theoretic foundation of forming regional joint-operators to coordinate operation of coupled power and natural gas systems.

The rest of the chapter is organized as follows. Section 4.2 proposes formulations of integrated scheduling model. Section 4.3 presents the standard LR and augmented LR based methodology to implement coordination procedures. Numerical cases are studied in section 4.4. The conclusion is drawn in Section 4.5.

4.2 Scheduling Coordination Model

4.2.1 Modeling Details. Our proposed model mainly focuses on the steady state (i.e., algebraic equalities and inequalities) analyses of the two systems. Both of them include integer variables and nonlinear constraints. Furthermore, our coordination model does not lay any particular emphasis or preference on either natural gas or electric power system. The outline of our proposed model is described as the following optimization problem:

Max Social welfare or *Min* Social cost

s.t.

- Power balance and reserve requirements
- Individual generator constraints (including min on/off time, min/max generation capacity, startup/ shutdown characteristics, ramp rate limits, etc)
- Power transmission constraints
- Gas source limits and gas storage constraints
- Natural gas network constraints
- Electricity-gas coupling constraints

4.2.2 Objective Function. The objective function is to minimize the social cost, which is the sum of electricity and gas operating costs over the scheduling period as shown in (4.1).

$$Min\ (EC + GC) \tag{4.1}$$

In our proposed model, gas-fired units do not need to directly concern their fuel costs but other operating costs such as maintenance and crew costs. Therefore, EC in (4.2) represents all operating costs of non-gas-fired units, electricity load not serve penalty as well as non-fuel operating costs of gas-fired units. The fuel cost of gas-fired units, which depends on the individual unit consumptions, will be implicitly considered in the natural gas allocation cost GC.

$$\begin{aligned} EC = \sum_t [\sum_{i \notin GU} F_{ec,i}(P_{it}) \cdot I_{it} + SU_{it} + SD_{it}] + \sum_t \sum_{el} \sigma_{el} \cdot ELS_{elt} \\ + \sum_t [\sum_{i \in GU} F_{ec,i}(P_{it}) \cdot I_{it} + SU_{it} + SD_{it}] \end{aligned} \tag{4.2}$$

GC is represented in (4.3) which includes operating costs of gas wells, liquefied natural gas (LNG), and gas storage as well as penalty costs for the residual natural gas load not served. σ_{gl} is the penalty price corresponding to residual gas loads, indicating their

incremental costs and priority orders.

$$GC = \sum_{t} \sum_{gi} F_{gc,gi}(\cdot) + \sum_{t} \sum_{gl \notin GU} \sigma_{gl} \cdot GLS_{glt} \tag{4.3}$$

The joint operator will coordinate the operation schedule to pursue the overall interests of coupled electricity and natural gas systems. The optimal allocation of natural gas to residual loads or gas-fired generating units is determined by market demands and relative incremental costs. For instance, joint operators will supply more natural gas to power plants, if the proposed supply of fuel to gas-fired generating units will result in the additional commitment of expensive generators. Also, higher penalty costs for not supplying the residual gas loads will lead to a larger supply of natural gas to such loads. Here, we may consider gas-fired units to provide a generation service to the coordinated electricity and natural gas systems while being compensated for their maintenance or crew costs. The joint operator will then deal with coordination of the fuel consumed by electric and natural gas systems.

4.2.3 Power System Constraints.

1) Power balance and reserve constraint

$$\sum_{i} P_{it} + \sum_{el} ELS_{elt} = \sum_{el} EL_{elt} + P_{Loss,t} \tag{4.4}$$

$$\sum_{i} SR_{it} \geq SR_{D,t} \tag{4.5}$$

2) Individual unit constraints

Min on/off time

$$[X^{on}_{i(t-1)} - T^{on}_{i}] \cdot [I_{i(t-1)} - I_{it}] \geq 0 \tag{4.6}$$

$$[X^{off}_{i(t-1)} - T^{off}_{i}] \cdot [I_{it} - I_{i(t-1)}] \geq 0 \tag{4.7}$$

Ramping rate limits

$$P_{it} - P_{i(t-1)} \le Y_{it} \cdot P_{\min,i} + (1 - Y_{it}) \cdot UR_i \tag{4.8}$$

$$P_{i(t-1)} - P_{it} \le Z_{it} \cdot P_{\min,i} + (1 - Z_{it}) \cdot DR_i \tag{4.9}$$

Max/Min power generation

$$P_{\min,i} \cdot I_{it} \le P_{it} \le P_{\max,i} \cdot I_{it} - R_{it} \tag{4.10}$$

A more detailed formulation of such constraints including emission and fuel constraints are given in [Fu05]. Either a mode or a component model [Liu09a] can be used for combined-cycle generating units. The model for fuel switching units is provided in [Li05].

3) Hydro unit and reservoir constraints.

For cascaded hydro systems, the reservoir operation is very complex, which is coupled in time. It is also coupled in spatial extent, how a single reservoir is operated may affect other reservoirs downstream.

Power-water discharge conversion relationship:

$$P_{it} = F_{h,i}(q_{it}, I_{it}) \tag{4.11}$$

Water discharge limits:

$$q_{i,\min} \cdot I_{it} \le q_{it} \le q_{i,\max} \cdot I_{it} \tag{4.12}$$

Reservoir volume limits:

$$HV_{i,\min} \le HV_{it} \le HV_{i,\max} \tag{4.13}$$

Initial and terminal reservoir volume:

$$HV_{i,t=0} = HV_{0,i} \qquad HV_{i,t=NT} = HV_{NT,i} \tag{4.14}$$

Water balance constraint for cascaded hydro units:

$$HV_{it} = HV_{i,t-1} - q_{it} - s_{it} + w_{it} + RC_{ij} \cdot q_{j(t-\tau_j)} \quad \backslash \tag{4.15}$$

where $q_{j(t-\tau)}$ represents the delayed water discharge to hydro unit i from other hydro units j.

4) Power transmission constraints.

$$\begin{aligned} &\boldsymbol{C}\cdot\boldsymbol{Pf} = \boldsymbol{A}\cdot\boldsymbol{P} - \boldsymbol{B}\cdot(\boldsymbol{EL}-\boldsymbol{ESL}) \\ &Pf_l = \frac{\theta_a - \theta_b - \gamma_{ab}}{x_{ab}} \quad (a,b \in l) \\ &\left|Pf_l\right| \le Pf_{l,\max} \\ &\gamma_{\min} \le \gamma \le \gamma_{\max} \\ &\theta_{ref} = 0 \end{aligned} \tag{4.16}$$

4.2.4 Natural Gas Constraints.

1) Gas well and storage constraints. The natural gas source is represented by gas well, gas storage, and LNG tank, which demonstrate distinct prices and operating characteristics.

The cost of gas well is given as follows

$$F_{gc,gi}(\cdot) = \rho_{gas,git}\cdot GP_{git} \qquad \forall gi \notin GS \tag{4.17}$$

Gas well and LNG source satisfy the following constraint:

$$GI_{git}\cdot GP_{gi,\min} \le GP_{git} \le GI_{git}\cdot GP_{gi,\max} \qquad \forall gi \notin GS \tag{4.18}$$

Natural gas storage or LNG tanks are supplemental gas sources. Gas storage can operate and switch among three exclusive modes, i.e., releasing gas, charging gas, and off. When charging or releasing gas, additional operating costs will be considered as in (4.19).

$$F_{gc,gi}(\cdot) = \rho^I_{git}\cdot GP^I_{git} + \rho^O_{gas,git}\cdot GP^O_{git} \qquad \forall gi \in GS \tag{4.19}$$

Max/Min flow rate while releasing or charging gas

$$GI^I_{git}\cdot GP^I_{gi,\min} \le GP^I_{git} \le GI^I_{git}\cdot GP^I_{gi,\max} \qquad \forall gi \in GS \tag{4.20}$$

$$GI_{git}^{O} \cdot GP_{gi,\min}^{O} \le GP_{git}^{O} \le GI_{git}^{O} \cdot GP_{gi,\max}^{O} \quad \forall gi \in GS \tag{4.21}$$

The net output of gas storage is the difference between releasing and charging gas flow as (4.22)

$$GP_{git}^{O} - GP_{git}^{I} = GP_{git} \qquad \forall gi \in GS \tag{4.22}$$

In addition, there is a volume balance constraint for each storage (e.g., hydro reservoir):

$$SV_{git} - SV_{gi(t+1)} = GP_{git} \quad \forall gi \in GS \tag{4.23}$$

The volume of gas storage is restricted as

$$SV_{gi,\min} \le SV_{git} \le SV_{gi,\max} \quad \forall gi \in GS \tag{4.24}$$

$$SV_{i,t=0} = SV_{0,i} \qquad SV_{i,t=NT} = SV_{NT,i} \tag{4.25}$$

2) Gas transmission constraints

A steady-state gas transmission model is built based on the nodal gas mass balance that indicates that the gas flow injected to a node is equal to the gas flowing out of the node as shown in (4.27). The natural gas pressure is associated with each node while the natural gas flow rate is associated with each branch.

$$\begin{aligned} &\sum_{gi} GA_{na,gi} \cdot GP_{gi} - \sum_{gl} GB_{na,gl} \cdot (GL_{gl} - GLS_{gl}) \\ &- \sum_{nb} GK_{na,nb} \cdot Gf_{na \to nb} + \sum_{cm} GD_{na,cm} \cdot F_{cf,cm}(\cdot) = 0 \end{aligned} \tag{4.27}$$

The Weymouth equation is mostly used to optimize the natural gas flow system [Mer02, Ber78]. It indicates the flow in a pipeline extending from gas node *na* to gas node *nb* is modeled as

$$Gf_{nanb} = \mathrm{sgn}(\pi_{na}, \pi_{nb}) \cdot C_{mn} \sqrt{\left| \pi_{na}^2 - \pi_{nb}^2 \right|} \tag{4.27}$$

$$\pi_{\min,na} \le \pi_{na} \le \pi_{\max,na} \tag{24.8}$$

where C_{mn} is the pipeline constant that depends on temperature, length, diameter, friction, and gas composition.

As described in the previous chapter, for driving the natural gas flow from gas provider to gas load, compressors are built at intervals along the gas pipeline to compensate the pressure loss. The gas flow through centrifugal compressor is governed by (4.29)-(4.31):

$$Gf_{na\to nb} = \mathrm{sgn}(\pi_{na}, \pi_{nb}) \cdot \frac{CH_{cm}}{k1_{cm} - k2_{cm} \cdot PR_{cn}^{k3_{cm}}} \tag{4.29}$$

$$CH_{\min,cm} \le CH_{cmt} \le CH_{\max,cm} \tag{4.30}$$

$$PR_{\min} \le \frac{\max(\pi_{na}, \pi_{nb})}{\min(\pi_{na}, \pi_{nb})} \le PR_{\max} \tag{4.31}$$

where $k1_{cm}$, $k2_{cm}$ and $k3_{cm}$ are empirical parameters corresponding to the compressor design.

4.2.5 Electricity-Natural Gas Coupling Constraints. A gas-fired power plant is the linkage between natural gas and electricity systems. The gas consumption of a generation unit is a function of its hourly power generation as

$$GL_{glt} = \sum_i GE_{gli} \cdot F_{ef,i}(P_{it}, I_{it}) \qquad \forall i \in GU \tag{4.32}$$

The coupling equations are considered as complicating constraints that if relaxed, the integrated optimization problem will be decomposed into two simpler subproblems. We will discuss the decomposition procedures and the solution of coordination problem in Section 4.3.

4.3 Solution of Coordinated Scheduling Model by Lagrangian Relaxation and Augmented Lagrangian Relaxation

4.3.1 A Coordinated Scheduling by LR. A group of equations in the form (4.32)

would associate the two systems in our electricity-gas coordination problem. The two systems have a decomposable structure and we consider the LR method as the decomposition strategy of the coordination problem (4.1)–(4.32). The LR method is divided into two phases as shown in Figure 4.1. The first phase is obligatory to solve the dual problem. However, the solution of phase one may not be feasible in the primal problem. Thus, the second phase of the LR-based algorithm will seek a feasible solution based on the solution of phase one.

For the sake of clarity, we use vectors $\boldsymbol{x}$ and $\boldsymbol{y}$ to represent power system and natural gas system variables respectively in Section IV. The coupling constraints are expressed as (4.33) instead of (4.32), in which $\boldsymbol{x}_c$, $\boldsymbol{y}_c$ are subvectors of $\boldsymbol{x}$ and $\boldsymbol{y}$, representing variables appeared in coupling constraints.

$$\boldsymbol{e}(\boldsymbol{x}_c) - \boldsymbol{g}(\boldsymbol{y}_c) = 0 \tag{4.33}$$

Coupling constraints in (4.33) are relaxed and incorporated into the objective function using Lagrangian multipliers to obtain the Lagrangian function (4.34)

$$\mathcal{L}(\boldsymbol{x}, \boldsymbol{y}, \boldsymbol{\lambda}) = EC(\boldsymbol{x}) + GC(\boldsymbol{y}) + \boldsymbol{\lambda}^T \boldsymbol{e}(\boldsymbol{x}_c) - \boldsymbol{\lambda}^T \boldsymbol{g}(\boldsymbol{y}_c) \tag{4.34}$$

The relaxed primal problem (4.35) is formulated in terms of minimizing the Lagrangian function subject to constraints (4.4)–(4.32). $\phi(\boldsymbol{\lambda})$ in (4.35) is defined as the Lagrangian dual function with respect to $\boldsymbol{\lambda}$.

$$\phi(\boldsymbol{\lambda}) = \underset{\boldsymbol{x},\boldsymbol{y}}{Min}\{\mathcal{L}(\boldsymbol{x}, \boldsymbol{y}, \boldsymbol{\lambda}) \mid (4) - (31)\} \tag{4.35}$$

The resulting max–min problem is the following dual problem

$$\underset{\boldsymbol{\lambda}}{Max}\ \underset{\boldsymbol{x},\boldsymbol{y}}{Min}\{\mathcal{L}(\boldsymbol{x}, \boldsymbol{y}, \boldsymbol{\lambda}) \mid (4) - (31)\} \tag{4.36}$$

The difference between the optimal value of objective function of primal problem and

dual problems (4.36) is the duality gap.

In the convex case, the duality gap will be zero. In practice, most of the mathematical programming problems are nonconvex [Con06] such as hydrothermal coordination problem, LR-DP based unit commitment problem, and maintenance scheduling problem. The proposed gas-electricity coordination problem is also nonlinear which is due to integer variables and transmission constraints.

For a given $\lambda^{(k)}$, the Lagrangian dual (4.35) of the primal problem is decomposed into independent SCUC and gas allocation subproblems as shown in (4.37) and (4.38).

$$\underset{x}{Min}\left\{ EC(x) + \lambda^{(k)} \cdot e(x_c) \mid (4)-(16) \right\} \tag{4.37}$$

$$\underset{y}{Min}\left\{ GC(y) - \lambda^{(k)} \cdot g(y_c) \mid (17)-(31) \right\} \tag{4.38}$$

Since $\lambda^{(k)}$ may not be the optimal solution of the dual problem (4.36), the dual cost $\phi(\lambda^{(k)})$ resulted from the solution of subproblems (4.37) and (4.38) would produce a lower bound for the optimal solution of the dual problem (4.36). According to the weak duality theory, (4.39) is satisfied where x^*, y^* is the optimal solution of primal problem and λ^* is the optimal solution of the dual problem.

$$\phi(\lambda^{(k)}) \le \phi(\lambda^*) \le EC(x^*) + GC(y^*) \tag{4.39}$$

The phase one procedure of LR is to update Lagrangian multipliers a λ nd then solve the resulting small-scale optimization problem (4.37)-(4.38) iteratively so that the dual cost increases gradually until changes of λ or x_c y_c are relatively small.

The Lagrangian multipliers would be updated in the direction of the dual cost increment. The subgradient method shown in (4.40) is the most popular one. The parameter $s^{(k)}$ in (40) represents the step size which would need to satisfy (4.41) for

convergence [Zha99, Ber95]. Since $\phi(\lambda^*)$ is generally not known before the dual problem is solved, we use the estimated value of $\phi(\lambda^*) - \phi(\lambda^{(k)})$.

$$\lambda^{(k+1)} = \lambda^{(k)} + \tau^{(k)} \cdot [e(x_c) - g(y_c)] \tag{4.40}$$

$$0 < \tau^{(k)} < \frac{\phi(\lambda^*) - \phi(\lambda^{(k)})}{\|e(x_c) - g(y_c)\|^2} \tag{4.41}$$

where $\|\cdot\|$ represents Euclidian norm.

4.3.2 Coordinated scheduling by augmented LR. The proposed LR method demonstrated a few drawbacks as follows. The nonconvex characteristics of our coordination problem with integer variables and nonlinear network constraints will create a large duality gap and make it difficult to find a good dual solution. Based on our experience, a better dual solution with a lower degree of violation would result in a good optimal primal solution. Furthermore, the LR application in our case will cause oscillations in the solution of dual problem which is due to the linearity of the price function of gas wells, storage, or contracts. A similar phenomenon is recognized in the solution of hydrothermal coordination problem [Gua95, Coh88, Zha93]. In the following, the augmented LR is used which introduces penalty terms to smooth out the dual function and alleviate numerical oscillations.

We relax the coupling constraint (4.33) in an augmented Lagrangian fashion in (4.42), where ω is a positive penalty factor.

$$\mathcal{A}(x, y, \omega, \lambda) = EC(x) + GC(y) + \lambda^T [e(x_c) - g(y_c)] + \omega \|e(x_c) - g(y_c)\|^2 \tag{4.42}$$

Note that the augmented Lagrangian function (4.42) cannot be decomposed as it contains the inseparable cross penalty term, whose variables belong to both power and gas constraints. To make this term separable, [Coh80] uses the Auxiliary Problem

Principle (APP) to linearize the penalty term. An alternative is to use the block coordinate descent (BCD) method, which is a kind of nonlinear Gauss–Seidel method [Ber95]. The BCD would solve the subproblems (4.43) and (4.44) sequentially. Here, when minimizing one of the subproblem, the coupling variables of the other one appears in a inseparable penalty term which will be fixed based on the latest solution $\tilde{x}_c, \tilde{y}_c$ of subproblems. In this chapter, BCD method is adopted.

$$\begin{aligned} &\underset{x}{Min}\left\{ EC(x) + \lambda^{(k)^T} \cdot e(x_c) + \frac{1}{2}\omega^{(k)} \left\| e(x_c) - g(\tilde{y}_c) \right\|^2 \right\} \\ &s.t.\ \ (4)-(16) \end{aligned} \tag{4.43}$$

$$\begin{aligned} &\underset{y}{Min}\left\{ GC(y) - \lambda^{(k)^T} \cdot g(y_c) + \frac{1}{2}\omega^{(k)} \left\| e(\tilde{x}_c) - g(y_c) \right\|^2 \right\} \\ &s.t.\ \ (17)-(31) \end{aligned} \tag{4.44}$$

This procedure may create high order terms for subproblems (4.43) and (4.44). The absolute penalty terms are proposed in [Coh80] to replace the quadratic penalty terms. In this chapter, a piece-wise linearly approximations with respect to quadratic penalty terms is used which is illustrated in Figure 4.2.

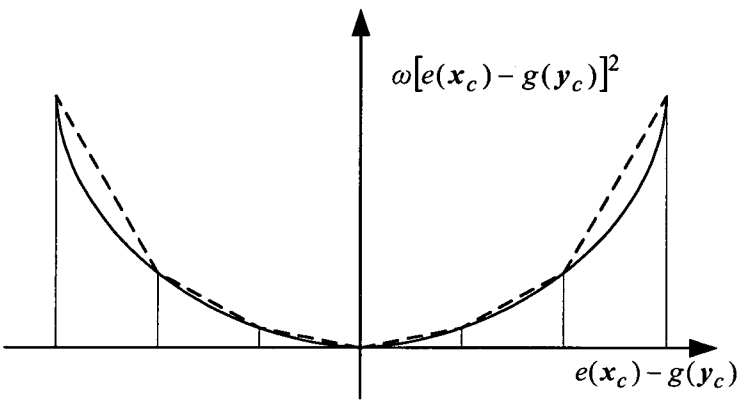

Figure 4.2. Piece-Wise Linear Approximation of Quadratic Penalty Terms Ecomposition of the Midterm Stochastic Problem

The dual problem is formulated as:

$$\phi_{\omega}(\lambda^{*}) = \underset{\lambda}{Max}\left\{\underset{x,y}{Min}\, \mathcal{A}(x, y, \omega, \lambda) \middle| (4)-(31)\right\} \tag{4.44}$$

The updating of Lagrangian multipliers can still use (4.40). The iterative solution steps for the augmented LR based coordination algorithm is discussed as follows"

Step 1. Initiate the Lagrangian multipliers $\lambda^{(0)}$ and penalty factors $\omega^{(0)}$, $k = 0$

Step 2. For the given $\lambda^{(k)}$ $\omega^{(k)}$ $\tilde{y}_c$, solve the electricity subproblem (4.43). Update $\tilde{x}_c = x_c^{(k)}$.

Step 3. Solve the gas subproblem (4.44) based on $\lambda^{(k)}$, $\omega^{(k)}$ and $\tilde{x}_c$. Update $\tilde{y}_c = y_c^{(k)}$

Step 4. Update the Lagrangian multipliers λ based on the subgradient method (4.40).

Step 5. If $\left\|e(x_c^{(k)}) - g(y_c^{(k)})\right\| > \alpha \left\|e(x_c^{(k-1)}) - g(y_c^{(k-1)})\right\|$ Update $\omega^{(k+1)} = \beta\omega^{(k)}$, $\beta > 1$

Step 6. If $\left\|x_c^{(k)} - y_c^{(k)}\right\| \le \varepsilon$, the final primal-dual solution is calculated as $(x^{(k)}, y^{(k)}, \lambda^{(k)})$. Otherwise $k = k+1$.

Step 7. If the iteration number k is larger than the pre-specified number, go to Step 8. Otherwise go to Step 2.

Step 8. Construct the final feasible solution to the primal problem based on the obtained best solution to the dual problem.

4.3.3 Solution of SCUC and Gas Allocation Subproblems. The objective of SCUC is to minimize the operating cost of power systems while satisfying the prevailing constraints [Sha02, Woo95]. The gas allocation is to commit and schedule natural gas resources while satisfying gas transmission constraints [Ric79].

The common points of the two optimization subproblems are their types and structures. First, both are mixed-integer programming problems. Second, both have transmission network constraints and hold L-shaped structure. Once dispatch of power and gas resources is determined, the network constraints become uncoupled among different hours. For large-scale applications, the network security check is usually separated from the economic resource dispatch by either the Benders decomposition or the sensitivity analysis (i.e., power transfer distribution factor (PTDF)). The framework for the solution of SCUC or gas allocation subproblems is given in Figure 4.3. More detailed formulations are provided in [Liu09b,Fu05]. The methodologies for the solution of SCUC or natural gas allocation subproblem do not change the overall framework of the LR based coordination strategy. Other techniques can also be incorporated into our program to solve the subproblems [Wol00, Tom07].

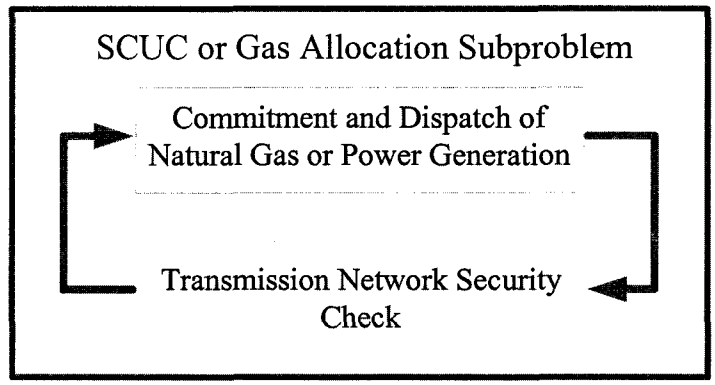

Figure 4.3 Framework for the Solution of SCUC/Gas Allocation Subproblem

4.3.4 Calculation of Feasible Solution. In some cases, the convergence of dual problem is quick and fairly reliable, while in other cases the solution tends to exhibit a cycling behavior, especially when using the LR approach. Usually, the iterative process is terminated after a pre-specified number of iterations. However, even the dual solution

resulted from the last iteration may still be infeasible in the primal case due to smaller violations of coupling constraints. Accordingly, we need to construct a feasible solution in the phase two of dual solution shown in Figure 4.1. The feasible solution process could be heuristic or based on the approximate programming. In this chapter, we adopt two steps to construct a feasible solution. First, based on the dual solution $\tilde{y}_c$, we solve the SCUC problem (45) to obtain the power system schedule plan x^*. In (45), $e(x_c) \le g(\tilde{y}_c)$ represents energy constraints or gas usage limits of gas-fired generating units. Then, we obtain a feasible solution (x^*, y^*) by solving (46) based on the power system schedule x^*.

$$\begin{aligned} x^* &= \arg\min EC(x) \\ &s.t. \quad (4)-(16) \\ &\quad e(x_c) \le g(\tilde{y}_c) \end{aligned} \tag{4.45}$$

$$\begin{aligned} y^* &= \arg\min GC(y) \\ &s.t. \quad (17)-(31) \\ &\quad g(y_c) = e(x_c^*) \end{aligned} \tag{4.46}$$

4.4 Case Studies

We illustrate effectiveness of proposed model and performance of the proposed algorithm by two cases. In the 6 bus power system and 7 node gas system, we mainly study impact of gas storage and network congestions on coordinated scheduling results. 118 bus 14 node case show impact of price incentives on least social cost and coordinated schedule. The comparison of ALR and SLR methods are given in both case.

4.4.1 6-Bus Power System and 7-Node Natural Gas System. The 6-bus system and the 7-node natural gas system are depicted in Figures 3.5 and 3.6. Two gas wells supply natural gas to 2 non-power gas users and 3 gas-fired units through pipelines. Parameters

of the coupled power system and natural gas system can be found in the Table A.1-Table A.14 in Appendix A. The cost information for gas well and gas storage is given in Tables 4.1 and 4.2. The penalty prices for electricity and natural gas load not serve are large and listed in Table 4.3.

Table 4.1. Parameters of Gas Well of 7 Node Gas System

Gas Well	Node No.	Wellhead price ($/kcf)	Min output (kcf/h)	Max output (kcf/h)
1	7	5.6	2000	5300
2	6	6	1000	6000

Table 4.2. Parameters of Gas Storage of 7 Node Gas System in Case 3

Storage Node No.	Gas Injection cost ($/kcf)	Min. Input (kcf/h)	Max. Input (kcf/h)	Min. Output (kcf/h)	Max. Output (kcf/h)
1	2.5	150	2500	0	2000

Table 4.3. Electricity and Gas Load not Serve Penalty Price of 7 Node Gas System

Electricity load not serve penalty price ($/MWh)	2000
Gas load not serve penalty price ($/kcf)	100

We apply the augmented LR and the standard LR methods to solve the following three cases. The augmented LR method is first applied to solve the three cases listed above.

- Case 1: Base case without network or gas storage constraints
- Case 2: Including network constraints
- Case 3: Including network constraints and gas storage

In Case 1, we ignore both electricity and natural gas transmission network constraints. Hence, there are no congestion impacts on the scheduling of electricity and

natural gas systems. The hourly commitment of three gas-fired units is given in Table 4.4. Figure 4.4 shows the hourly schedule of gas well 2 which is the marginal gas well because of its higher wellhead price. The social cost is $1,322,422 which is the lowest of all three cases.

In Case 2, we consider electricity and natural gas transmission network constraints. The flow limits of power transmission line and pressure limits of gas nodes through pipelines will cause the commitment of expensive units at additional hours. Compared to Table 4.4, Table 4.5 shows that unit 2 is committed at hours 10-11, 22, and unit 3 is on at hours 8-9 and 23-24. The most efficient unit G1 would generate less in Case 2 as shown in Figure 4.5. The social cost is $1,366,196 which is higher than that in the Case 1.

In Case 3, the simulation includes a gas storage which draws natural gas from pipeline into the gas reservoir at off-peak hours 2-7, and releases the natural gas during peak hours 8-24 as illustrated in Figure 4.6. By using the stored gas, the efficient generation unit 1 would generate more during hours 1-24 as indicated in Figure 4.6. The hourly schedule of generation units is given in Table 4.6. The social cost is $1,350,932 which includes the cost of gas well and the operating cost of gas storage.

Table 4.4. Hourly Commitments of Case 1 Based on Augmented LR

Unit	Hours (0-24)
1	1 1 1 1 1 1 1 1 1 1 1 1 1 1 1 1 1 1 1 1 1 1 1 1
2	1 0 0 0 0 0 0 0 0 0 0 0 1 1 1 1 1 1 1 1 1 1 0 0 0
3	0 0 0 0 0 0 0 0 0 0 1 1 1 1 1 1 1 1 1 1 1 1 1 0 0

Table 4.5. Hourly Commitments of Case 2 Based on Augmented LR

Unit	Hours (0-24)
1	1 1 1 1 1 1 1 1 1 1 1 1 1 1 1 1 1 1 1 1 1 1 1 1
2	1 0 0 0 0 0 0 0 0 0 0 1 1 1 1 1 1 1 1 1 1 1 1 0 0
3	0 0 0 0 0 0 0 0 0 1 1 1 1 1 1 1 1 1 1 1 1 1 1 1 1

Table 4.6. Hourly Commitments of Case 3 Based on Augmented LR

Unit	Hours (0-24)
1	1 1 1 1 1 1 1 1 1 1 1 1 1 1 1 1 1 1 1 1 1 1 1 1 1
2	1 0 0 0 0 0 0 0 0 0 0 0 0 1 1 1 1 1 1 1 1 1 1 0 0 0
3	0 0 0 1 0 0 0 0 0 0 1 1 1 1 1 1 1 1 1 1 1 1 1 1 0

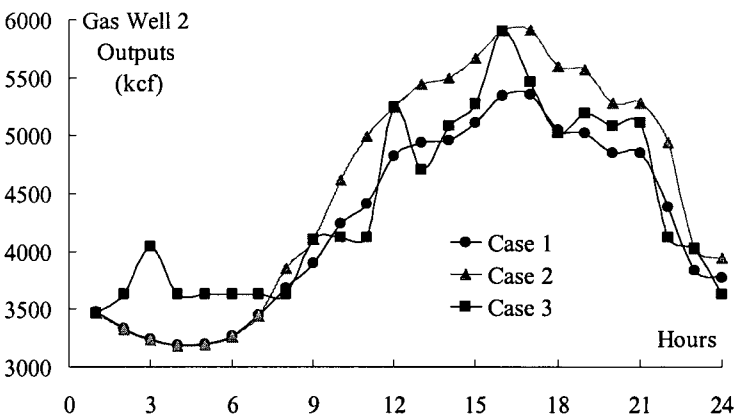

Figure 4.4. Gas Well 2 in Cases 1, 2 and 3 Based on Augmented LR

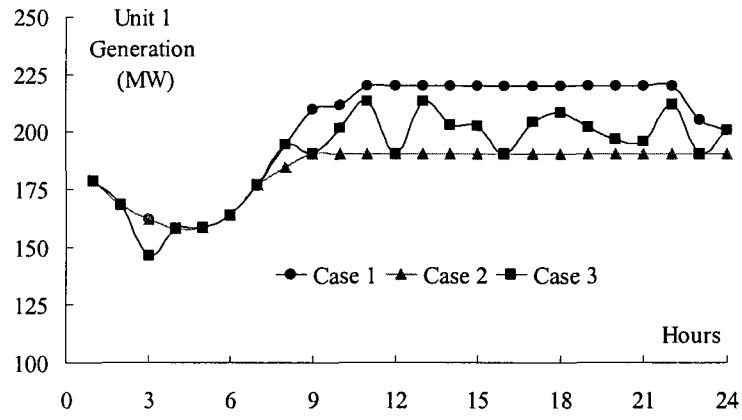

Figure 4.5. Unit 1 in Cases 1, 2 and 3 Based on Augmented LR

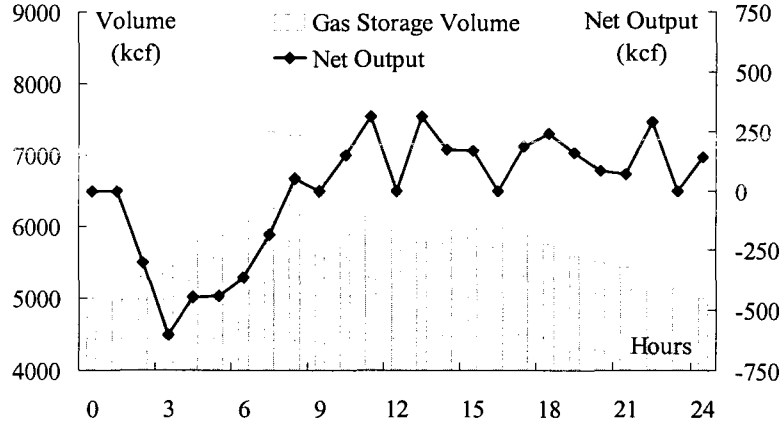

Figure 4.6. Gas Storage Volume and Output Based on Augmented LR

We also solve the three cases by the standard LR in order to compare the performances of the two methods. The results of standard LR are listed in Table 4.7. As presented in Section 4.3, using the standard LR algorithm would cause dual solution oscillations. A feasible solution based on the dual solution of standard LR by (4.45) would lead to electricity load shedding. The augmented LR algorithm, on the other hand, can avoid the oscillation and will result in a better solution.

To further illustrate the worst convergence of the dual problem by the standard LR, the dual cost and the violation degree of constraints (4.32) versus iterations are plotted in Figure 4.7 and 4.8. Here, the violation degree of (4.32) is defined by the Manhattan norm $\|e(x_c)-g(y_c)\|_1$ of $e(x_c)-g(y_c)$. Obviously, the violation of constraints by the standard LR method cannot be mitigated. The violations will approach zero by increasing the number of iterations in the augmented LR.

Table 4.7. Comparison of Augmented LR and Standard LR Based Results

	Case Index	Case 1	Case 2	Case 3
ALR	Dual cost ($)	1,322,408	1,366,196	1,350,931
	Violation degree (kcf)	2.3	3.1	3.6
	Feasible social cost ($)	1,322,422	1,366,196	1,350,932
	Electricity load not serve (MWh)	0	0	0
	Gas load not serve (kcf)	0	0	0
SLR	Dual cost ($)	1,319,070	1,343,842	1,344,346
	Violation degree (kcf)	14,642	12,162	12,491
	Feasible cost ($)	1,525,986	2,0743,44	1,935,640
	Electricity load not serve (MWh)	76.2	396.4	319.2
	Gas load not serve (kcf)	0	0	0

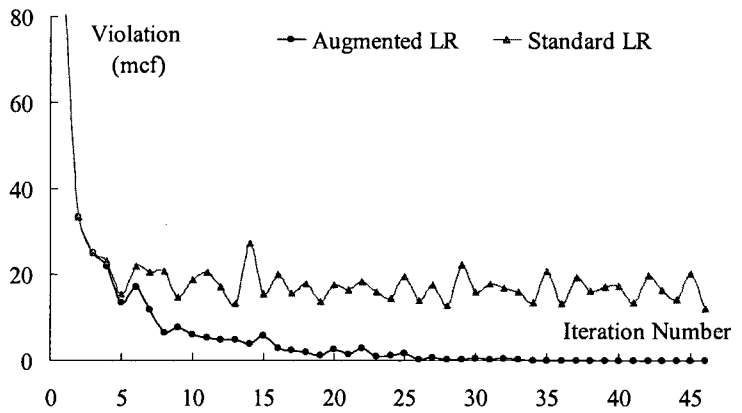

Figure 4.7. Violation Degree against Dual Iterations in Case 2

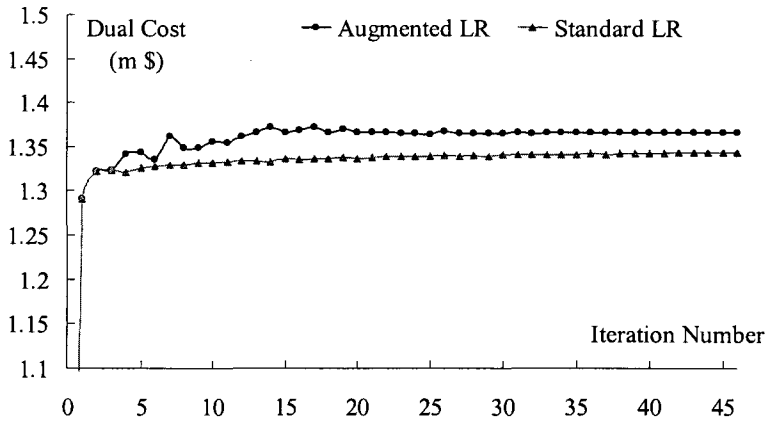

Figure 4.8. Dual Cost versus Dual Iterations in Case 2

4.4.2 118-Bus power system and 14-node natural gas system. A modified IEEE 118-bus power system and 14-node gas system is used to study the least social cost of interdependent power and natural gas system coordinated scheduling. The power system has 54 fossil units, 12 gas-fired combined cycle units, 7 hydro units, 186 branches, 14 capacitors, 9 tap-changing transformers, and 91 demand sides. The natural gas transmission system is composed of 14 nodes, 12 pipelines, and 2 compressors. The electricity and natural gas transmission system data are found in http://motor.ece.iit.edu/data/Gastranssmion_118_14test.xls. Table 4.8 lists the well head prices of natural gas as well as penalty price of residual natural gas loads not serve in all three cases.

Case 1: Base case

We solve the coordination scheduling problem as we presented in this chapter to obtain least social cost schedules for coupled power and natural gas system. The daily social cost based on ALR in this case is $2,350,957. Here, for reason of limited space, we will not give the hourly generation and commitment for each unit. Instead, we present

daily generation and resource information in Table 4.9, as well as hourly generation in Figure 4.9 for further analysis and comparison with other cases. Congestion in gas transmission system occurred in 24 hours. Residual gas loads 1-5 will be fully supplied by joint-operator due to their higher penalty price. However, gas consumption of gas-fired units and residual gas loads 6-8 are curtailed through optimization iterations.

Table 4.8. Well Head Prices and Gas Loads Price Incentives in Cases 1-3

Price incentives	Case 1	Case 2	Case 3
Gas Well 1	0.95	0.95	1.66
Gas Well 2	0.90	0.90	1.58
Gas Well 3	1.00	1.00	1.75
Penalty price of Residual Gas Loads 1-3 not serve	3.00	1.20	3.00
Penalty price of Residual Gas Loads 4-5 not serve	2.50	1.10	2.50
Penalty price of Residual Gas Loads 6-8 not serve	1.10	0.90	1.80

Case 2: Impact of penalty price of residual gas load

We assume the penalty price of residual gas loads not serve in case 2 are decreased as shown in Table 4.9. It represents that residual gas loads can be interrupted or not supplied, with just adding less social cost compared to case 1. In this situation, joint-operator prefer to dispatch more natural gas to gas-fired units for power generation rather than supply residual gas loads in order to mitigate the integrated social cost. In another word, benefits of supplying gas-fired units is higher than providing natural gas to residual gas loads from social welfare point of view. As shown in Table 4.9, 21,178 MWh generation fueled by natural gas in case 2 is higher than that in case 1. Natural gas fed to residual gas load is reduced to 148,015 kcf from 229,126 kcf in case 1. The social

cost in case 2 is $2,303,216. From Figure 4.9, it is clear that the hourly coal generation in Case 1 is higher than that in Case 2.

Table 4.9. Summarized Daily Generation and Resource Based on ALR

Daily Resource Results	Case 1	Case 2	Case 3
Generation by Coal (MWh)	120,796	114,312	131,724
Generation by Natural Gas (MWh)	14,689	21,178	3783
Generation by Water (MWh)	8,308	8,302	8,286
Supplied Gas to Residual Loads (kcf)	229,126	148,015	305,526
Supplied Gas to Gas-fied units (kcf)	190,270	275,309	48,907
Consumed Gas by Compressors (kcf)	6,374	6,472	6,186

Case 3: Impact of wellhead price of natural gas

In this case, we consider to increase wellhead price of natural gas wells by round 75% in comparison with that in case 1. We solve the coordination scheduling problem by ALR again. From the result indicated in Table 4.9, power generation by natural gas in case 1 is replaced largely by coal generation because of soaring natural gas. Natural gas is no longer a economic choice to generate electricity compared to coal fuel. So natural gas units only generate power on some peak hours as marginal units in case 3 as shown in Figure 4.9. Moreover, joint-operator can dispatch more natural gas to residual gas loads. The daily social cost in case 3 is $2,710,834 which is much higher than that in case 1.

Daily and hourly hydro generation in three cases are closed, but different. Because optimization process will coordinate water resource to generate more power during peak load hours or avoid committing more coal or gas-fired units while satisfying hydro reservoir constraints.

We also solve the base case and other two cases by standard LR methods. The social costs are given in Table 4.10. We can draw a conclusion that the standard LR algorithm would result in higher feasible solution, while the augmented LR algorithm, on the other hand, can avoid the oscillation and will lead to a better solution.

Table 4.10. Social Costs Based on Augmented LR and Standard LR in Cases 1-3

Daily Resource Results		Case 1	Case 2	Case 3
Social Cost ($)	ALR	2,350,957	2,303,216	2,710,834
	SLR	2,424,892	2,384,547	2,823,916

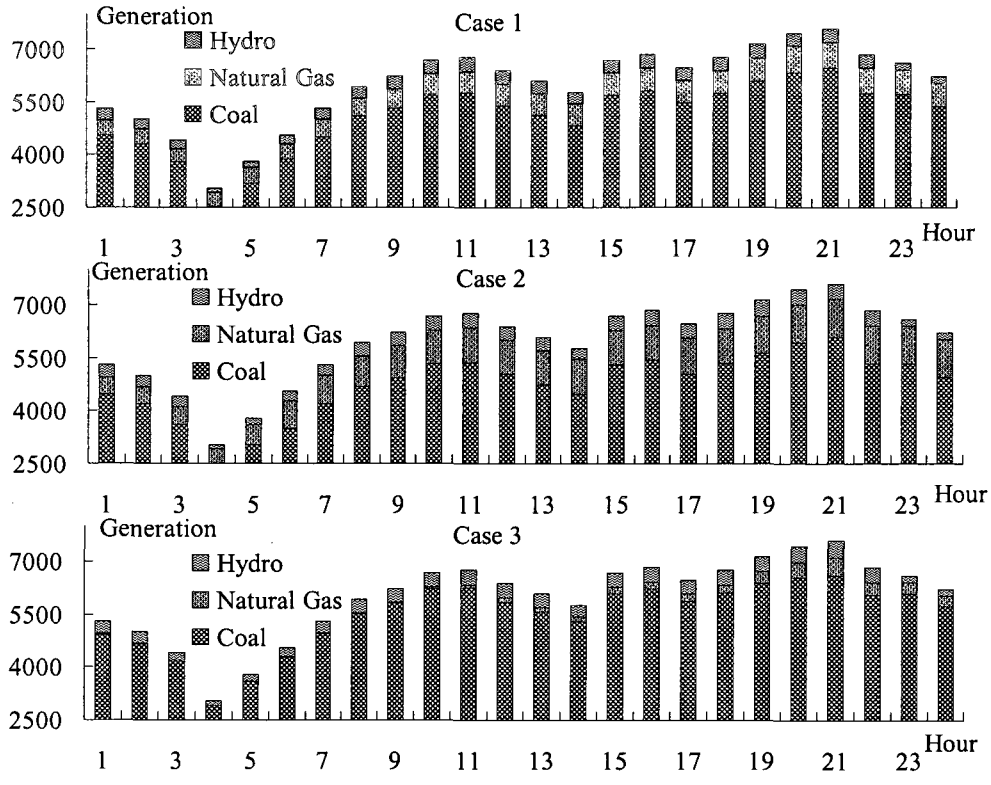

Figure 4.9. Hourly Generation Composition in Case 1-3 Based on ALR

4.5 Conclusions

This chapter proposes new model for scheduling coordination of coupled power systems and natural gas transmission systems from joint-operator point of view. The integrated operator will coordinate scheduling resources to pursue least social cost of coupled energy system. Meanwhile, gas-fired units do not need to concern about their fuel cost and amount. Therefore, they can avoid risks caused by natural gas fuel without coordination between power operator and gas operator. In this chapter, LR based method are proposed to solve the problem. Moreover, to avoid numerical oscillation caused by linear price function of gas well and improve local convexity of relaxed primal problem, the augmented LR with piecewise linear approximation of quadratic penalty terms is adopted in this chapter. To make the added penalty term separable, SCUC and gas allocation subproblems are solved in a sequential way by using block descent coordination technique. Case studies with two systems verify that our new method is effective for solving the proposed coordination model. Moreover, compared to standard subgradient LR, case study also shows augmented LR can avoid oscillations of dual solution and improve quality of dual solution.

CHAPTER 5

COORDINATED SCHEDULING OF SECURITY-CONSTRAINED POWER AND NATURAL GAS INTRASTRCTURES WITH TRANSIENT NATURAL GAS FLOW MODEL

5.1 Introduction

It is of paramount necessity to incorporate the natural gas transmission system model into the operation planning and optimization of electric power systems. In the last decade, references [Uns07a Uns07b An03 Hec01 Mor03 Urb07] and our previous chapter proposed several state of the art strategies to model the two systems together. However all of them focus on steady-state formulations for both electric power and natural gas transmission systems. They neglect significant distinctness on travelling speeds of natural gas flow and power flow as well as line-pack capacities of interstate pipelines. Line pack relates to the amount of additional gas that is stored in a pipeline as a result of maintaining above-normal pressure in the pipeline [Nor02 Mer02]. By analogy with the important function of reserve in power systems, line pack is essential for a pipeline to handle large swing in gas load such as ramp up of gas-fired units during peak hours or called reserve of gas-fired units to react contingencies in power systems. It is well recognized that natural gas flow in high-pressure interstate pipelines is governed by some dynamic laws based on distributed parameters in short-term periods such as several hours.

This chapter concentrates on the development of a methodology for the coordinated scheduling of interdependent power and natural gas transmission systems based on a transient state model of natural gas flow. In the proposed model, interstate natural gas pipelines are described by a set of partial differential equations (PDEs) instead of the steady-sate Weymouth equations. Implicit finite difference method will be

adopted in this chapter to approximate PDEs into algebraic difference equations. As a result, the natural gas flow model will be coupled not only in space but also in time.

This chapter further presents a bi-level programming model based on our previous model "SCUC with steady state natural gas transmission constraints" in Chapter 3 and [Liu09b]. The proposed coordination scheme between gas system operators and Independent System Operator (ISO) of power systems is shown in Figure 5.1. Constraints related to natural gas supply contracts are directly included in the UC problem. When an optimal UC schedule is obtained without violating power transmission constraints, hourly natural gas demands of gas-fired units are then submitted to the gas system operators for checking the feasibility of natural gas transmission constraints. If any violations of natural gas transmission constraints are detected, corresponding constraints (Benders cuts) are formed and fed back to the ISOs for the next iteration of calculation. The cut which represents shortages of natural gas supply or gas transmission congestions would limit the fuel consumption of gas-fired units. In the last stage when the natural gas transmission check is feasible, gas consumptions of gas-fired units as well as SCUC solution is firmed. Natural gas transmission system operator will schedule gas compressors by minimizing their energy consumptions.

The rest of this chapter is organized as follows. Section 5.2 proposes the transient state model of natural gas transmission systems. Section 5.3 presents a bilevel formulation of the coordinated scheduling model. Algorithms for solving the proposed model will be discussed in Section 5.4. Numerical studies will be given in Section 5.5. The conclusion is drawn in Section 5.6

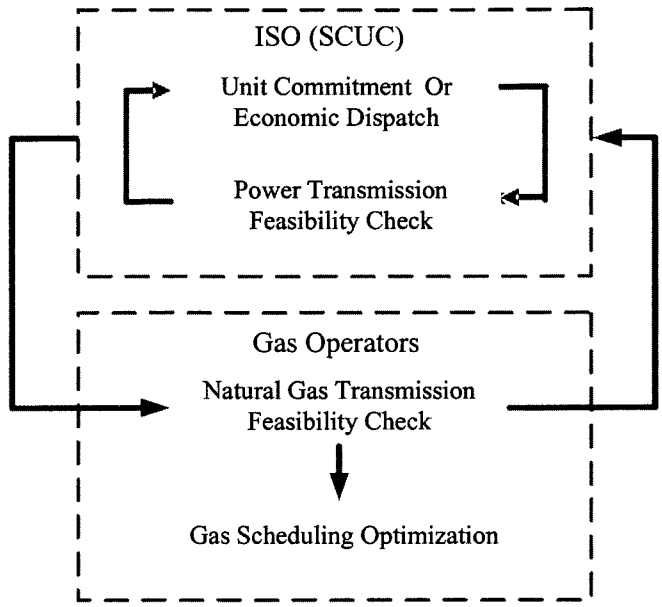

Figure 5.1. Coordination scheme of electric power and natural gas systems

5.2 Modeling of Transient Gas Flows in Natural Gas Transmission Systems

Energy infrastructure dynamics vary from milliseconds to a couple of hours, which indicates the fact that the transportation of energy via different infrastructures happen over different time frames. It is well known that electrical energy travels via the current electrical transmission systems almost instantaneously and cannot be stored in large amount. Once power injection and load on each bus is given, power flows in transmission system satisfy steady state algebraic equations and are independent from hour to hour. Therefore, in the operation planning stage, traditional security-constrained unit commitment (SCUC) and security-constrained economic dispatch (SCED) commonly ignore electrical transient process of electricity infrastructure and instead focus on steady state analysis [Sha02 Woo96 Fu05].

Unlike the instantaneous delivery of energy over electric power systems, the natural gas flow travelling via pipeline represents much slower phenomenon. When gas

load or gas supply changes, natural gas transmission system will take longer time to respond to disturbances. In particular, the dynamics for high pressure interstate pipelines are much slower and large amount of gas stored in the pipelines cannot be neglected. In this case, steady-state assumption and corresponding algebraic Weymouth equation of pipeline might be inappropriate and inaccurate for numerical simulation of unsteady gas flows. Rigorous gas flow simulation requires pipeline distributed-parameters and the transient state model.

5.2.1 Modeling of Natural Gas Pipelines. Natural gas flows through pipelines, driven by pressures, are dependent on factors such as the length and the diameter of pipelines, operating temperatures, composition of natural gas, altitude change over the transmission path, roughness of pipelines, and boundary conditions. The transient state natural gas flow through a gas pipeline is usually described as one dimensional dynamic alongside the axis of natural gas pipeline. Dynamic simulation requires the use of distributed parameters and the consideration of time-varying state variables. A set of partial differential equations is obtained by applying laws regarding conservation of mass, momentum, and conservation of energy. Equations (5.1)-(5.4) represent time and space dependent gas density, mass flow, flow velocity and pressure [Her09 Osi96]:

$$\frac{\partial(\rho \cdot v)}{\partial z} = -\frac{\partial \rho}{\partial t} \tag{5.1}$$

$$\frac{\partial(\pi + \rho \cdot v^2)}{\partial z} + \frac{2 f_c \cdot \rho \cdot v^2}{d} + \frac{\partial(\rho \cdot v)}{\partial t} + \rho \cdot g_e \cdot \sin\alpha = 0 \tag{5.2}$$

$$\frac{\partial[\rho \cdot (e + \frac{1}{2} v^2)]}{\partial t} + \frac{\partial[\rho \cdot v \cdot (h + \frac{1}{2} v^2)]}{\partial z} - \rho \cdot \Omega + \rho \cdot g_e \cdot v \cdot \sin\alpha = 0 \tag{5.3}$$

$$\pi = \rho \cdot Z \cdot R_g \cdot T \tag{5.4}$$

Where,

π: Gas pressure

z: Space index of pipeline

d: Diameter of pipeline

v: Gas axial velocity

ρ: Gas density

h: Specific enthalpy

e: Specific internal energy of gas pipeline

Ω: Rate of heat transfer per unit time and unit mass of the gas

Z: Compressibility factor

T: Temperature of gas in pipeline

α: Elevation angle of gas pipeline

R_g: Gas constant

f_c: Fenning friction factor of gas pipeline

g_e: Gravitation acceleration

The law of conservation of mass states that mass can neither be created nor disappeared. Equation (5.1) represents the fact that the net mass rate of flow out of a differential volume of fluid is equal to the time rate of decrease of mass within the differential volume.

Equation (5.2) derived from Newton's second law (momentum law) indicates that the sum of forces acting on gas system of particles is equal to the time rate of increase of momentum of gas particles at a time instant. In equation (5.2), terms $2f_c \cdot \rho \cdot v^2 / d$, $\rho \cdot g_e \cdot \sin\alpha$, $\partial(\rho \cdot v)/\partial t$, and $\partial(\rho \cdot v^2)/\partial z$ define the hydraulic friction force, force of gravity, gas inertia, and flowing gas dynamic pressure, respectively.

Equation (5.2) is considered for a high pressure gas pipeline, where the dynamic variation takes longer time (hours) to complete a significant change. In hourly analysis, the convective acceleration terms $\partial(\rho \cdot v)/\partial t$, $\partial(\rho \cdot v^2)/\partial z$ and $\rho \cdot g \cdot \sin\alpha$, compared to the other term $2f_c \cdot \rho \cdot v^2 / d$ in equation (5.2), contribute less than one percent to the sum of all terms under normal operating conditions [Her09 Osi96]. In most engineering applications, those terms are neglected for simplicity [Won68 Ehr03]. In this chapter, since we focus on the slow transient process in terms of hours caused by gas load swings, those three terms can also be ignored without sacrificing calculation accuracy.

Equation (5.3) is derived from the law of conservation of energy. In order to solve Equations equations (5.1)-(5.4) it is required to know the value of Ω. Rigorously, when $\Omega \neq 0$, there is no thermal equilibrium between gas pipeline and the surroundings and we will need more equations to model the heat conduction process. However, in the case of slow transients caused by fluctuations in gas demand and gas injection, the assumption of isothermal flow is valid and can be found in most literatures [Won68 Ehr03 Her09 Osi87 Osi96 Ke00]. Under this assumption, the pipeline has sufficient time to reach thermal equilibrium. The gas temperature changes caused by compression and expansion of natural gas can be neglected and the temperature of natural gas (T) is assumed to remain constant at surrounding earth temperature. Accordingly, the energy equation (5.3) becomes redundant if Ω is deemed to be zero.

In the state equation (5.4), gas pressure is a function of the gas density, compressibility factor, and gas temperature. In this chapter, we use equation (5.5) instead of (5.4) under an isothermal process [Her09 Osi96], where average temperature T_{avg} and average compressor factor Z_{avg} is given as an input constant.

$$\pi = \rho \cdot Z_{avg} \cdot R_g \cdot T_{avg} \tag{5.5}$$

After ignoring Equations (5.3) and making reasonable approximations as described above, we can substitute gas flow $Gf = \rho \cdot v \cdot S$ and (5.5) into (5.1) and (5.2) and obtain (5.6) and (5.7) which are used in the remaining sections of this chapter [Won68 Ehr03].

$$\frac{\partial(\pi_{zt})}{\partial t} + K_1 \frac{\partial(Gf_{zt})}{\partial z} = 0 \tag{5.6}$$

$$\frac{\partial(\pi_{zt}^2)}{\partial z} + K_2 \cdot Gf_{zt}^2 = 0 \tag{5.7}$$

where K_1, K_2 are parameter in transient state model of natural gas pipeline and are determined by $K_1 = \frac{Z_{avg} R_g T_{avg,t}}{S}$ and $K_2 = \frac{4 f_c Z_{avg} R_g T_{avg,t}}{dS^2}$.

It is noted that the steady state Weymouth equation as follow can be obtained by integrating (5.7) along the length of pipeline.

$$Gf_t^2 = C \cdot \sqrt{\left| \pi_{z=0,t}^2 - \pi_{z=L,t}^2 \right|}$$

where, $C = \sqrt{\frac{1}{K_2 \cdot L}}$.

It is also assumed that the boundary conditions of PDE (5.6) and (5.7) are known. At t = 0, the initial values can be given by various measurements in the natural gas transmission system. At the beginning point and terminal end of a pipeline, gas flows satisfy nodal gas flow balance constraint as indicated in the Section 5.2.3.

5.2.2 Modeling of Compressors. Please see Chapter 3 and 4.

$$CH_{cmt} = Gf_{cmt} \cdot (k2_{cm} \cdot PR_{cmt}^{\ k3_{cm}} - k1_{cm}) \tag{5.8}$$

$$CH_{\min,cm} \le CH_{cmt} \le CH_{\max,cm} \tag{5.9}$$

$$PR_{\min,cm} \le PR_{cmt} = \frac{\pi_{nat}}{\pi_{nbt}} = \le PR_{\max,cm} \tag{5.10}$$

where π_{nat} and π_{nb} represent pressures at outlet and inlet of compressor cm at t. The amount of consumed gas is related to the power of the compressors $F_{cf,cm}(CH_{cmt})$.

5.2.3 Nodal Gas Flow Balance. Gas nodes are defined as junctions of pipelines and compressors where gas wells inject gas into network or gas loads withdraw natural gas flow from network respectively. The natural gas pressure associated with each node has to be limited within a reasonable range (5.11). Output of gas well and gas load shedding amount are restricted by (5.12)-(5.13).

$$\pi_{\min,na} \le \pi_{nat} \le \pi_{\max,na} \tag{5.11}$$

$$GP_{gi,\min} \le GP_{git} \le GP_{gi,\max} \tag{5.12}$$

$$0 \le GSL_{glt} \le GSL_{\max,gl} \le GL_{gl} \tag{5.13}$$

The nodal gas flow balance is modeled by (5.14), indicating that the natural gas flow injected into a node is equal to the natural gas flowing out of the node.

$$\begin{aligned} g_{na}(\boldsymbol{\pi}, \boldsymbol{CH}, \boldsymbol{GP}, \boldsymbol{GSL}, \boldsymbol{GL}) = &-\sum_{nb} GK_{na,nb} \cdot Gf_{na\to nb,na} + \sum_{gi=1}^{NGS} GA_{na,gi} \cdot GP_{gi} \\ &- \sum_{gl=1}^{NGL} GB_{na,gl} \cdot (GL_{gl} - GSL_{gl}) - \sum_{cm=1}^{NC} GD_{na,cm} \cdot F_{cf,cm}(CH_{cm}) = 0 \end{aligned} \tag{5.14}$$

where $GK_{na,nb}$ is the element of matrix $\boldsymbol{GK}$ in row na and column nb. $Gf_{na\to nb,na}$ is the gas flow injected into node na through the branch between na and nb. If the gas flow from na to nb in a pipeline is defined as positive, the boundary conditions for PDE of pipeline are given in (5.15)-(5.16).

$$\pi_{t,z=0} = \pi_{nat}, \pi_{t,z=L} = \pi_{nbt} \tag{5.15}$$

$$Gf_{t,z=0} = -Gf_{na\to nb,na}, Gf_{t,z=L} = Gf_{na\to nb,nb} \tag{5.16}$$

5.3 Formulation of Integrated Scheduling of Electricity and Natural GAS Systems

5.3.1 Individual Scheduling Model. Traditionally, electric power system and natural gas transmission system are scheduled independently without coordination.

In power system, the ISO execute SCUC to to minimize the operating cost of power systems while satisfying prevailing unit commitment constraints and power transmission network constrains.

$$Min\sum_{\eta}W_{o,\eta}+\sum_{t}\sum_{\eta}W_{\eta t}+\sum_{t}\sum_{i\notin GU}[F_{ec,i}(P_{it})\cdot I_{it}+SU_{it}+SD_{it}]+\sum_{t}\sum_{el}\sigma\cdot ELS_{elt} \tag{5.17}$$

st.

Take-or-pay natural gas supply contracts are associated with a constant cost $W_{o,\eta}$ if natural gas usage is less than $F_{o,\eta}$.

$$\sum_{t}F_{ef,\eta t}\le F_{o,\eta} \tag{5.18}$$

Cost of flexible natural gas supply contract:

$$W_{\eta t}=\rho_{gas,\eta}\cdot F_{ef,\eta t} \tag{5.19}$$

Natural gas-fired power plants usually hold several different gas contracts in their gas supply portfolio. Each gas contract will be considered as a gas load in natural gas transmission system.

$$\sum_{i\in GU(\xi)}F_{ef,it}=\sum_{\eta=1}^{N\eta(\xi)}F_{ef,\eta t} \tag{5.20}$$

Power balance and reserve requirements:

$$\sum_{i}P_{it}\cdot I_{it}=P_{Loss,t}+\sum_{t}\sum_{el}(EL_{elt}-ELS_{elt})\quad\forall t \tag{5.21}$$

$$\sum_{i}SR_{it}\cdot I_{it}\ge SR_{D,t}\quad\forall t \tag{5.22}$$

Individual generator constraints include individual constraints for restricting ramp up/down limits, min on/off time, emission limits, max/min capacities and so on. The detailed modeling of individual generating unit constraints is discussed in [Woo96 Liu09a Fu05].

DC power transmission network constraints are given in (5.23). AC constraints can be modeled similarly 0 and do not alter the proposed solution framework.

$$\begin{aligned} &\boldsymbol{C}\cdot\boldsymbol{Pf} = \boldsymbol{A}\cdot\boldsymbol{P} - \boldsymbol{B}\cdot(\boldsymbol{EL}-\boldsymbol{ELS}) \\ &Pf_l = \frac{\theta_a - \theta_b - \gamma_{ab}}{x_{ab}} \quad (a,b \in l) \\ &|Pf_l| \le Pf_{l,\max} \\ &\gamma_{\min} \le \gamma \le \gamma_{\max} \\ &\theta_{ref} = 0 \end{aligned} \tag{5.23}$$

The natural gas supply and transportation sectors have been unbundled since 1980s. A variety of gas purchase patterns and transportation contracts appeared during market evolutions as shown in Table 5.1. Transportation services with different priority orders can be described in Chapter 1.

Table 5.1. Natural Gas Transportation and Supply Contracts

Transportation Contract			Supply Contract	
No-notice	Firm	Interruptible	Take or pay	Flexible

Gas transmission scheduling problem is to minimize operating cost of compressors (5.24) while satisfying transient transmission natural gas constraints and respecting natural gas transportation contracts and pressure requirements at receiving points.

$$Min \sum_t \sum_{cm} \rho_{gas,cm} \cdot F_{cf,cm}(CH_{cmt}) \tag{5.24}$$

s.t. Transient-state natural gas transmission constraints (5.6)-(5.16)

5.3.2 Bilevel Program Formulations for Integrated Model. The electric power systems, with the gas-fired units, can be viewed as the demand side of the natural gas transmission system, so we consider that electric power sectors have upper level pulling power to determine the amount of natural gas consumption. In this chapter, we assume that natural gas transmission operators have to respect the transportation contracts if their physical gas infrastructures can afford them. Mathematically, the proposed scheduling coordination problem can be described by a bi-level programming formulation as follows:

$$\underset{x}{Min}\ EC(\boldsymbol{x}) \tag{5.25}$$

$$s.t. \qquad \boldsymbol{EU}(\boldsymbol{x}) \le 0 \tag{5.26}$$

$$\boldsymbol{EN}(\boldsymbol{x}) \le 0 \tag{5.27}$$

$$\underset{y}{Min}\ GC(\boldsymbol{y}) \tag{5.28}$$

$$s.t. \quad \boldsymbol{GN}(\boldsymbol{x}_c, \boldsymbol{y}) \le \boldsymbol{0} \tag{5.29}$$

where $\boldsymbol{x}$ and $\boldsymbol{y}$ represent state and decision variables in power system and gas system optimization respectively. $\boldsymbol{x}_c$ is subvector of $\boldsymbol{x}$ for representing natural gas consumptions by power plants. (5.26), (5.27) and (5.29) denote unit commitment constraints, power transmission network constraints and transient natural gas transmission constraints, respectively. The lower-level problem (5.28)-(5.29) represents gas scheduling optimization problem which is a constraint embedded into the upper-level optimization problem for generation scheduling.

By ignoring (5.28), bilevel programming problem will be transferred into (5.30). Obviously, LB provides a lower bound for primal problem (5.25)-(5.29).

$$LB = EC(\boldsymbol{x}^*, \boldsymbol{y}^\#) = \underset{x}{Min}\ \{EC(\boldsymbol{x}) \mid (5.25), (5.26), (5.29)\} \tag{5.30}$$

It is noted that x_c are not part of the decision variables in the lower-level problem. Based on fixed x_c^* from (5.30), we can solve (5.31) and obtain an optimal solution y^*. Since (x^*, y^*) is a feasible solution of the bi-level optimization problem (5.25)-(5.29), $EC(x^*, y^*)$ is an upper bound for (5.25)-(5.29).

$$y^* = Arg \min_{y} \{GC(y) \mid (5.29)\} \tag{5.31}$$

$$UB = EC(x^*, y^*) = EC(x^*, y^\#) = LB \tag{5.32}$$

(x^*, y^*) is an optimal solution for the original bi-level programming problem (5.25)-(5.29).

Generalized L-shaped decomposition (Benders) is applied to decompose the optimization problem (5.30) into UC master problem (5.33), power transmission network constraints (5.27) check subproblem and gas transmission network constraints (5.29) check subproblem.

$$Min_{x} \{EC(x) \mid (5.26)\} \tag{5.33}$$

It should be noted that the above conclusion can only be obtained under the fact that the x_c is not a decision variable in the lower-level optimization problem. That means natural gas transmission operator cannot shed gas loads requested from power plants just for the purpose of reducing compressors' cost. Gas loads can only be bumped by other gas loads with higher transportation priority when there is congestion. However, if x_c is also a decision variable of lower-level optimization problem, the primal bi-level optimization problem will be more complicated and can be solved by employing Kuhn–Tucker conditions of the lower-level problem. This will be a topic for further research in the future.

)

5.3.3 Coordination Schemes. Figure 2 depicts the flowchart for coordinating the electricity and natural gas infrastructure scheduling. The whole process can be divided into two parts: the ISO part and the gas system operator part.

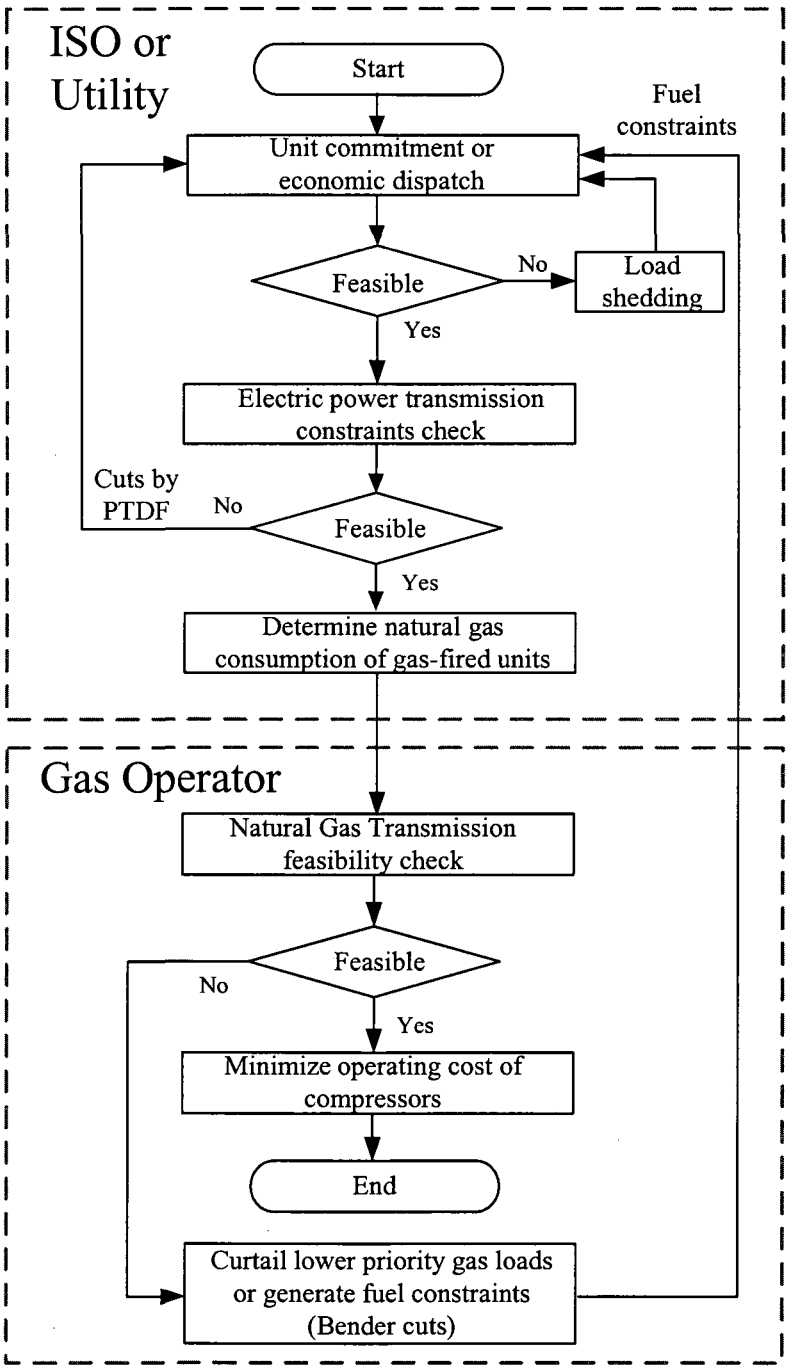

Figure 5.2. Flowchart of coordination schemes between ISO and gas operator

The ISO or the utility operator would execute the unit commitment to determine the UC schedule and hourly dispatch that would satisfy the forecasted electric load. If generation facilities are not able to provide enough power to match electricity demands, load shedding scheme will be employed. Based on the UC and dispatch solutions, the ISO conducts the security analysis for network constraints. The power transmission check mitigates transmission violations and iterates with the UC via power transfer distribution factors (PTDFs) or Benders cuts [Sha02 Fu05]. If there is no violation in the power transmission network, the ISO can then determine the natural gas amount consumed by gas-fired units and submit the gas demands to the gas system operator.

Meanwhile, natural gas transmission system operator collect the information on requested gas demands, gas contracts, gas transmission parameters, initial pressures and planned outage of gas pipelines. The gas feasibility check problem will examine the feasibility of the gas transmission system for serving expected gas loads. If the outcome of the gas transmission check is infeasible, gas fuel constraints using cutting-plane method for gas-fired power plants will be formed and fed back to the ISO for rescheduling. The iterative process between SCUC and gas transmission feasibility check will continue until the feasibility of transient gas transmission flow is obtained. It is noted that gas flow obtained during the feasibility check is not necessarily the optimal results for gas transmission network operation in the next day. Gas transient flow feasibility check only verifies whether there are enough line pack resources and transportation capacities to support the ISO's committed gas-fired units. If the gas transmission feasibility check is feasible, the solution of SCUC will be firmed and the gas transmission

system operator will continue to schedule compressors, storages, and line pack resources by minimizing operating cost of compressors.

5.4 Solution of Scheduling Coordination

5.4.1 Solution of SCUC. In this chapter, the UC problem is a mixed-integer nonlinear program which will be linearized and solved based on branch and cut method [Sha02 Wol98 Jer80]. The power transmission feasibility check subproblems including either DC or AC constraints can be solved by linear programs, iterating with UC via power transfer distribution factor (PTDF) or Benders decomposition method. Refer to [Sha02 Fu05] for more details.

5.4.2 Implicit Finite Difference Approximation of Partial Differential Equations. There are many methods to solve the PDEs. Analytical methods can provide a continuous solution by compact mathematic expression if the region and boundary values of dependent variables are defined. Compared to analytical methods, numerical methods are more popular for engineering computation of gas pipeline dynamics. They are used to evaluate the dependent variables at discrete points in a spanning region of time and space as shown in Figure 5.3.

In this chapter, we adopt the Euler finite difference numerical method to approximate PDE (5.6) and (5.7) by replacing derivative expressions in space and time with equivalent difference quotients. Generally, implicit methods have better numerical stability than explicit methods, because explicit methods calculate dependent variables at a later time from those at the current time while implicit methods find a solution by solving an equation involving dependent variables in both the current and the future times.

Equations (5.34) and (5.35) are obtained by applying backward Euler method and midpoint Euler method which belong to implicit methods.

$$\frac{\pi_{t,n}-\pi_{t-1,n}}{\Delta t}=\frac{K_1}{2\Delta z}(Gf_{t,n-1}-Gf_{t,n+1}) \qquad (5.34)$$
$$t\in\{1,2,...NT\}, n\in\{1,2,...,N-1\}$$

$$\frac{\pi^2_{t,n-1}-\pi^2_{t,n+1}}{2\Delta z}=K_2\cdot Gf^2_{t,n} \qquad (5.35)$$
$$t\in\{0,1,...NT\}, n\in\{1,2,...,N-1\}$$

In (5.34) and (5.35), different pairs of n and t index correspond to different grid points. Obviously, increasing the number of points on the grid in Figure 5.3 can enhance the numerical accuracy, but may also lead to longer computing time. The number of grid points can be increased or decreased by adjusting the step size Δz and Δt.

On the time boundary, state variables at t = 0 are all given as known initial values. On the space boundary, (5.34) are replaced by (5.36)-(5.37).

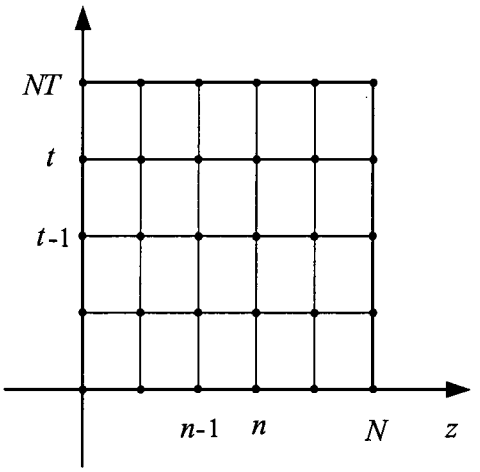

Figure 5.3. Grid points in the finite difference scheme

$$\frac{\pi_{t,n}-\pi_{t-1,n}}{\Delta t}=\frac{K_1}{\Delta z}(Gf_{t,n}-Gf_{t,n+1}) \qquad (5.36)$$
$$t\in\{1,2,...NT\}, n=0$$

$$\frac{\pi_{t,n}-\pi_{t-1,n}}{\Delta t}=\frac{K_1}{\Delta z}(Gf_{t,n-1}-Gf_{t,n}) \qquad t\in\{1,2,...NT\}, n=N \tag{5.37}$$

So far, PDEs are transformed into a set of algebraic equations as shown in (5.34)-(5.37). For the sake of simplicity, we denote them by (5.38).

$$\boldsymbol{h}(\boldsymbol{Gf}^T,\boldsymbol{\pi}^T)=0 \tag{5.38}$$

5.4.3 Solution of Natural Gas Transmission Feasibility Check. The gas transmission feasibility check subproblem is to minimize the sum of slack variables on all gas nodes while satisfying transient gas pipelines constraints, pressure constraints, and compressors constraints as well as respecting natural gas transportation contracts for submitted gas loads $\boldsymbol{G\hat{L}}$. Gas load shedding can be implemented on the load whose priority is even lower than the load used for power generation. For a gas load with firm transportation contract, $GSL_{\max}=0$. We use the successive LP to solve the optimization problem iteratively.

$$Min\ \ \omega(\boldsymbol{G\hat{L}})=\sum_{na=1}^{NN}(SL) \tag{5.39}$$

s.t.

$$\nabla\boldsymbol{h}(\boldsymbol{Gf}^T,\boldsymbol{\pi}^T)\cdot\begin{bmatrix}\Delta\boldsymbol{Gf}\\ \Delta\boldsymbol{\pi}\end{bmatrix}=-\boldsymbol{h}(\boldsymbol{Gf}^T,\boldsymbol{\pi}^T) \tag{5.40}$$

$$\begin{aligned}&[\frac{\partial\boldsymbol{g}}{\partial\boldsymbol{\pi}}\quad\frac{\partial\boldsymbol{g}}{\partial\boldsymbol{CH}}\quad\boldsymbol{GA}\quad\boldsymbol{GB}]\cdot\begin{bmatrix}\Delta\boldsymbol{\pi}\\ \Delta\boldsymbol{CH}\\ \Delta\boldsymbol{GP}\\ \Delta\boldsymbol{GSL}\end{bmatrix}+\boldsymbol{GB}\cdot\boldsymbol{SL} \qquad \boldsymbol{\mu}\\ &=-\boldsymbol{g}\ (\boldsymbol{\pi}^T,\boldsymbol{CH}^T,\boldsymbol{GP}^T,\boldsymbol{G\hat{L}}^T-\boldsymbol{GSL}^T)\end{aligned} \tag{5.41}$$

$$0\le\boldsymbol{GSL}+\Delta\boldsymbol{GSL}\le\boldsymbol{GSL}_{\max}\le\boldsymbol{G\hat{L}} \tag{5.42}$$

$$\pi_{\min} \le \pi + \Delta\pi \le \pi_{\max} \tag{5.43}$$

$$GP_{\min} \le \Delta GP + GP \le GP_{\max} \tag{5.44}$$

$$CH_{\min} \le CH + \Delta CH \le CH_{\max} \tag{5.45}$$

$$PR_{\min}(\pi_{inlet} + \Delta\pi_{inlet}) \le \pi_{inlet} + \Delta\pi_{outlet} \le PR_{\max}(\pi_{in} + \Delta\pi_{in}) \tag{5.46}$$

$$0 \le SL \tag{5.47}$$

In each iteration, the linear programming problem (5.39)-(5.47) is solved and variables are updated based on (5.48). The iterative process will continue until $\Delta\pi^{(k)}$, $\Delta CH^{(k)}$, $\Delta GP^{(k)}$, $\Delta GSL^{(k)}$ is less than a specified threshold ε

$$\begin{bmatrix} \pi^{(k+1)} \\ CH^{(k+1)} \\ GP^{(k+1)} \\ GSL^{(k+1)} \end{bmatrix} = \begin{bmatrix} \pi^{(k)} \\ CH^{(k)} \\ GP^{(k)} \\ GSL^{(k)} \end{bmatrix} + \begin{bmatrix} \Delta\pi^{(k)} \\ \Delta CH^{(k)} \\ \Delta GP^{(k)} \\ \Delta GSL^{(k)} \end{bmatrix} \tag{5.48}$$

Once the iterative process is completed, a non-negative objective function (39) that is less than the specified tolerance indicates that natural gas transmission network can support gas loads from the power system. Otherwise, a gas fuel constraint (Benders cut) given in (5.49) will be generated and added to the SCUC formulation.

$$\omega(GL) = \omega(\hat{GL}) + \mu^T \cdot GB \cdot (GL - \hat{GL}) \le 0 \tag{5.49}$$

where μ is dual variable vector which is obtained by solving LP in the latest iteration.

It should be noted that the gas transmission system feasibility check subproblem based on the transient model of gas transmission system is coupled between hours, but that based on the steady-state model is de-coupled between hours and can be solved in parallel. In addition, equation (5.40) may include a great number of constraints and variables if the number of grid points in Figure 5.3 is large. Thus, the computing time of the transient model is usually much higher than that of steady-state model.

5.4.4 Solution of natural gas scheduling problem. The natural gas scheduling problem is also solved by successive linear programming in this chapter. The natural gas transmission feasibility check subproblem provides an initial value for the solution of natural gas scheduling problem. In general, $F_{cf,cm}()$ is convex, so the objective function (5.39) can be replaced by (5.50). However, pipeline equations and compressor equations may make the feasible sets of the subproblem non-convex. So if the initial operating point of the gas scheduling problem is not close enough to the global optimal points, the final solution may just be a local optimal solution. Heuristic methods may be used to find the best possible solution. This is outside the scope of this chapter.

$$Min \sum_{t=1}^{NT} \sum_{cm=1}^{NC} \rho_{gas,cm} \cdot \frac{\partial F_{cf,cm}(CH_{cmt})}{\partial CH_{cmt}} \cdot \Delta CH_{cmt} \tag{5.50}$$

5.5 Case Studies

A modified IEEE 118-bus system is used to study coordinated scheduling of interdependent electricity and natural gas infrastructures. The power system has 54 fossil units fueled by coal, 12 combined cycle units, 7 hydro units, 186 branches, 14 capacitors, 9 tap-changing transformers, and 91 demand sides. All 12 combined-cycle gas turbine units are supplied by an interstate pipeline and a compressor as shown in Figure 5.4. Parameters of pipeline, compressor and gas well are given in Table 5.2 and Table 5.3. The generating fuel prices are 1.4$/MBtu for natural gas and 1$ MBtu for coal. Power system data can be found in motor.ece.iit.edu/data/Gastranssmion_118_14test.xls.

Three cases are studied to show the effectiveness of the proposed approach as well as the impact of transient state natural gas flow model on SCUC and gas scheduling

results. The program is coded in C++ and solved by CPLEX 9.0 on a 2.6 GHz personal computer.

Table 5.2. Parameters of Interstate Pipeline

Max pressure (psig)	Min pressure (psig)	Parameter K_1	Parameter K_2	Parameter C	Length L (miles)
500	400	0.05	2*10-6	50	200

Table 5.3. Parameters of Compressor and Gas Well

Compressor	k1	k2	K3	Min power (hp)	Max power (hp)	af (MBtu/ hp2h)	bf (MBtu/hph)	cf (MBtu/h)
	0.1	0.17	0.15	500	2000	0.0001	0.15	25
Gas well			Max output (MBtu/h)			Min output (MBtu/h)		
			5000			20000		

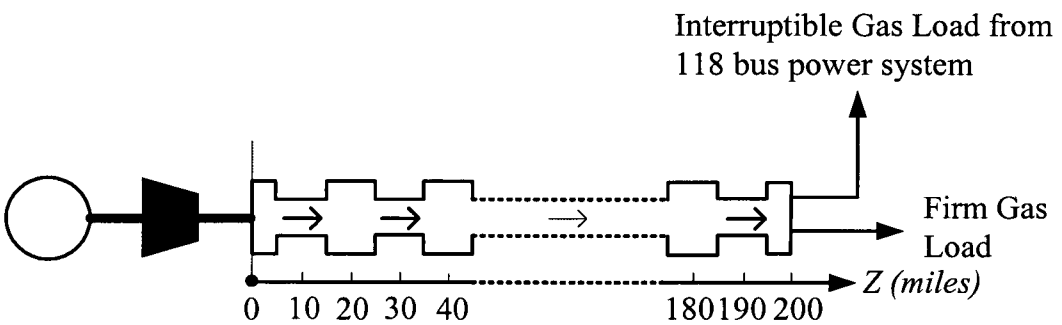

Figure 5.4. Interstate Pipeline

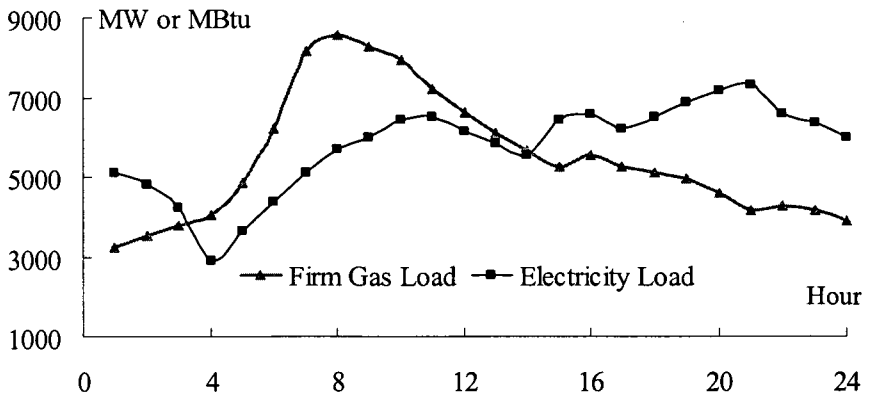

Figure 5.5. Hourly Electricity and Gas Load

Case 1: Scheduling coordination with steady-state gas transmission constraints

We calculate the hourly UC solution in 24 hours by considering dc transmission constraints and steady-state gas transmission constraints. Under steady-state gas flow assumption, the maximum natural gas flow through the pipeline is 15,000MBtu/h based on the Weymouth equation. Natural gas usages of combined cycle units 4001-4012 are curtailed at certain hours because of gas transmission congestions during hour 8 to hour 24. The hourly commitment schedule is shown in Table 5.4 in which hour 0 represents the initial condition. Due to space limit, only those units with different hourly unit commitments in Table 5.4 and Table 5.7 are listed. The daily operating cost of the power system is $2,046,006. After power system schedule is set, we minimize the operation cost of the compressor still based on the steady-state gas transmission constraints. Compressor will consume 8965 MBtu in the next operating day. Other daily results are shown in Table 5.5. Hourly natural gas amount withdrawn from the pipeline, hourly gas well output, and hourly natural gas amount consumed by the compressor are shown in Figure 5.6, Figure 5.7 and Figure 5.8, respectively.

Table 5.4. Unit Commitments of Generating Units in Case 1

Unit	Hours (0-24)																								
1013	1	0	0	0	0	0	0	0	0	0	0	0	0	0	0	0	0	0	0	0	0	1	0	0	0
1014	1	0	0	0	0	0	0	1	1	1	1	1	1	1	1	1	1	1	1	1	1	1	1	1	1
1019	1	0	0	0	0	0	0	0	0	1	1	1	1	1	1	1	1	1	1	1	1	1	1	1	1
1022-1023	1	0	0	0	0	0	0	0	0	1	1	1	1	1	1	1	1	1	1	1	1	1	1	1	1
1026	1	0	0	0	0	0	0	0	0	1	1	1	1	1	1	1	1	1	1	1	1	1	1	1	1
1034-1035	1	0	0	0	0	0	0	0	0	1	1	1	1	1	1	1	1	1	1	1	1	1	1	1	1
1047-1048	1	0	0	0	0	0	0	0	0	0	0	0	0	0	0	0	0	0	0	0	0	0	0	0	0
1051	1	0	0	0	0	0	0	0	0	0	0	0	0	0	0	0	0	0	1	1	1	1	1	1	0
1052	1	0	0	0	0	0	0	0	0	0	0	0	0	0	0	0	0	0	1	1	1	1	1	1	0
4001	0	0	0	0	0	0	0	0	0	0	0	0	0	0	0	0	0	0	1	1	3	3	1	1	0
4002	0	0	0	0	0	0	2	2	4	4	4	4	4	4	4	4	4	4	4	4	4	4	4	4	4
4003	0	1	1	0	0	0	1	1	3	3	4	4	4	4	4	4	4	4	4	4	4	4	4	4	4
4004	0	0	0	0	0	0	0	0	0	0	0	0	0	0	0	0	1	1	3	3	4	4	4	4	3
4005	0	0	0	0	0	0	2	2	4	4	4	4	4	4	4	4	4	4	4	4	4	4	4	4	4
4006	0	1	1	1	1	3	3	4	4	4	4	4	4	4	4	4	4	4	4	4	4	4	4	4	4
4007	0	2	2	2	4	4	4	4	4	4	4	4	4	4	4	4	4	4	4	4	4	4	4	4	4
4008-4009	0	1	1	1	3	3	3	4	4	4	4	4	4	4	4	4	4	4	4	4	4	4	4	4	4
4010	0	0	0	0	0	1	1	3	3	4	4	4	4	4	4	4	4	4	4	4	4	4	4	4	4
4011	0	0	0	1	1	3	3	3	4	4	4	4	4	4	4	4	4	4	4	4	4	4	4	4	4
4012	0	1	1	1	1	3	3	3	3	4	4	4	4	4	4	4	4	4	4	4	4	4	4	4	4
6002	0	1	1	0	0	0	0	1	1	1	1	1	1	1	0	1	1	1	1	0	0	0	1	0	0
6006	0	0	0	0	0	0	0	0	1	0	1	1	0	0	0	1	1	0	1	1	1	1	1	0	0

Table 5.5. Daily Scheduling Coordination Results in Case 1-3

Daily Results	Case 1	Case 2	Case 3
Daily operating cost ($) of electric power system	2,046,006	2,044,479	2,037,255
Daily natural gas amount consumed by compressor (MBtu)	8,965	12,273	5,056
Daily gas well output (MBtu)	322,031	408,621	201,383
Daily natural gas amount delivered to power plants (MBtu)	181,766	163,200	220,649
Daily electric power generated by natural gas plants (MW)	13,962	12,995	17,316

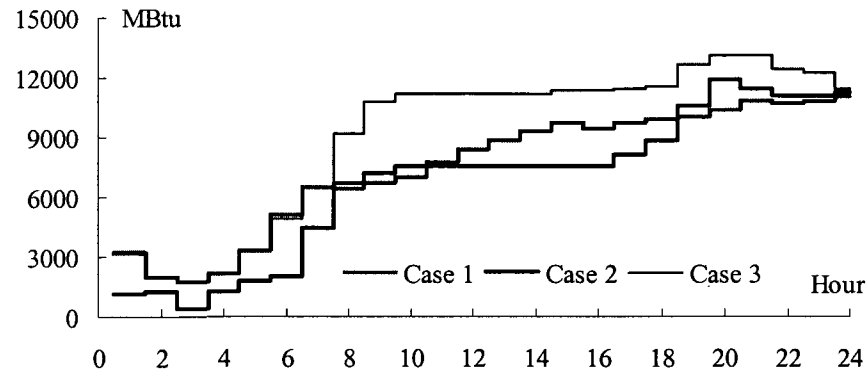

Figure 5.6. Hourly Gas Amount Delivered to Power Plants in Case 1-3

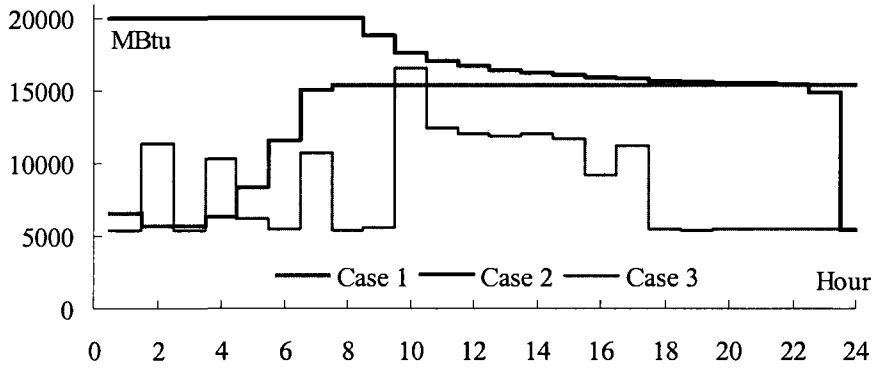

Figure 5.7. Hourly Gas Well Outputs in Case 1-3

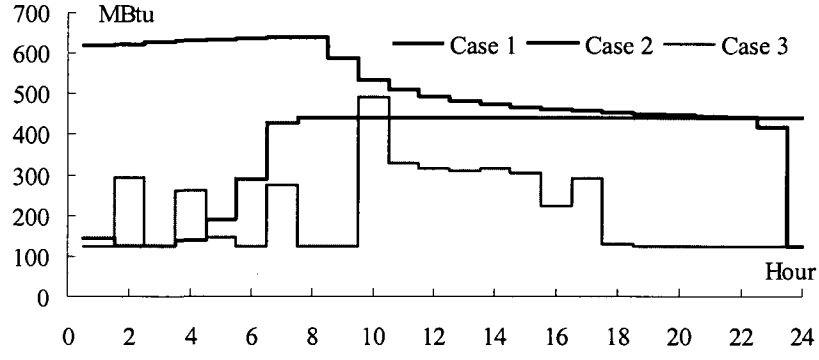

Figure 5.8. Hourly Gas Amount Consumed by the Compressor in Case 1-3

Case 2: Scheduling coordination with transient gas flow model based on lower initial line pack

Table 5.6. Initial Parameters of Interstate Pipeline

Initial Status of Pipelines	Initial Pressure (Psig)		Mass Gas Flow (MBtu)	
	Starting Point	Ending Point	Starting Point	Starting Point
Case 2	448	500	10088	10088
Case 3	400	458	10029	10029

We solve generation scheduling problem again by considering transient state gas flow model proposed in this chapter. The 200-miles long pipeline will be partitioned into several segments. The time interval is 1 hour and the length interval is 10 miles. Thereafter, partial differential equations of pipeline with boundary conditions will be transformed into a set of difference equations by the proposed implicit finite difference methodology. The initial pressures of pipeline are given in Table 5.6. Lower initial pressures in Case 2 indicate that a smaller amount of natural gas remians in the pipeline after previous day's operation. Hourly unit commitment results are given in Table 5.7 in which combined-cycle units 4001-4012 generate less at most hours and more coal units are committed compared to Case 1. However, from Figure 5.6, more natural gas is delivered to combined-cycle units in Case 2 at hours 19-23 when the electricity load is peak. As a result, the daily operating cost of power system is $2,044,476 in Case 2 which is still less than that in Case 1. In order to satisfy gas demands in peak hours at the ending point of the pipeline, the gas compressor has to charge the pipeline at beginning hours of the planning period. Pressure level at starting point of the pipeline gradually increases as shown in Figure 5.9.

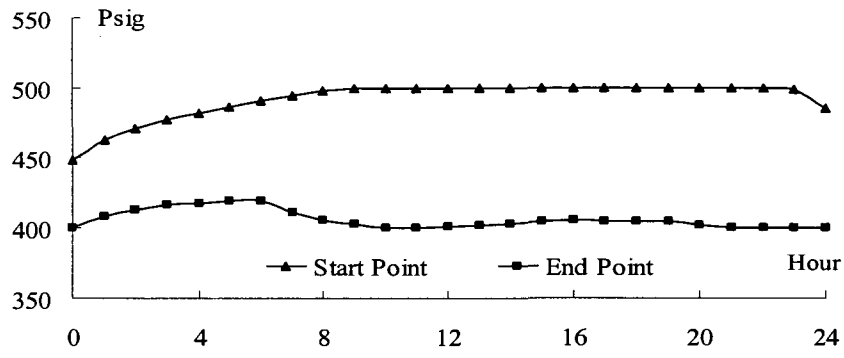

Figure 5.9. Hourly Pressure at Starting and Ending Points of the Pipeline in Case 2

Table 5.7. Unit Commitments of Generating Units in Case 2

Unit	Hours (0-24)																								
1013	1	1	1	1	1	1	1	1	1	1	1	1	1	1	1	1	1	1	1	1	1	0	0	0
1014	1	1	1	1	1	1	1	1	1	1	1	1	1	1	1	1	1	1	1	1	1	1	1	1
1019	1	0	0	0	0	0	0	0	1	1	1	1	1	1	1	1	1	1	1	1	1	1	1	1
1022-1023	1	0	0	0	0	0	0	0	1	1	1	1	1	1	1	1	1	1	1	1	1	1	1	1
1026	1	0	0	0	0	0	0	0	1	1	1	1	1	1	1	1	1	1	1	1	1	1	1	1
1034-1035	1	0	0	0	0	0	0	0	1	1	1	1	1	1	1	1	1	1	1	1	1	1	1	1
1047	1	0	0	0	0	0	0	0	0	0	1	1	1	1	1	1	1	1	1	1	1	1	1	0
1048	1	0	0	0	0	0	0	0	0	0	0	0	0	0	0	1	1	1	1	1	1	1	1	0
1051	1	0	0	0	0	0	0	0	0	0	0	0	0	0	0	1	1	1	1	1	1	1	1	0
1052	1	1	1	1	1	1	1	1	1	1	1	1	1	1	1	1	1	1	1	1	1	1	1	0
4001	0	0	0	0	0	0	0	0	0	0	0	0	0	0	0	0	0	0	0	0	1	1	0	0
4002	0	0	0	0	0	0	1	1	3	3	4	4	4	4	4	4	4	4	4	4	4	4	4	4
4003	0	1	1	0	0	0	0	2	2	4	4	4	4	4	4	4	4	4	4	4	4	4	4	4
4004	0	0	0	0	0	0	0	0	0	0	0	0	0	0	0	0	0	2	2	4	4	4	4	3
4005	0	0	0	0	0	0	0	0	0	0	0	0	0	0	2	2	4	4	4	4	4	4	4	4
4006	0	1	1	1	1	1	3	3	4	4	4	4	4	4	4	4	4	4	4	4	4	4	4	4
4007-4009	0	0	0	0	2	2	2	4	4	4	4	4	4	4	4	4	4	4	4	4	4	4	4	4
4010	0	0	0	0	0	0	0	0	0	0	0	0	0	0	0	0	0	0	0	0	0	0	0	0
4011	0	0	0	0	0	0	0	0	0	0	0	0	0	0	0	0	0	2	2	4	4	4	4	4
4012	0	0	0	2	2	2	2	4	4	4	4	4	4	4	4	4	4	4	4	4	4	4	4	4
6002	0	1	1	0	0	0	0	1	1	1	1	1	1	1	1	1	1	1	1	0	0	0	1	0	0
6006	0	0	0	0	0	0	0	0	0	0	1	1	1	0	0	0	1	1	0	1	1	1	1	1	0	0

Case 3: Scheduling coordination with transient gas flow model based on higher initial line pack

If the given initial pressure of pipeline is high, there is more natural gas contained in the pipeline before the current operation day. Thereby the pipeline can supply more natural gas to gas loads during hour 1 to hour 24. The hourly unit commitment results in Case 1 and Case 3 are exactly the same, but dispatch in Case 3 is more economical. The daily operating cost of the power system in Case 3 is $2,037,255, which is lower than that in Case 1 or Case 2. In fact, there is no violation in gas transmission feasibility check subproblem in Case 3. Figure 5.10 shows that pressures at starting and ending points of the pipeline gradually decline, releasing additional line pack resource to gas loads. The generations of combined-cycle units 4001-4012 are no longer limited by gas transmission congestion. Their total daily generating power is 17,316MW which is the highest in all three cases as shown in Table 5.5. From Figure 5.7 and Figure 5.8, we can observe that the operating cost of compressor and gas well output in Case 3 is much less than that in Case 1 or Case 2 primarily because of its higher initial line pack value.

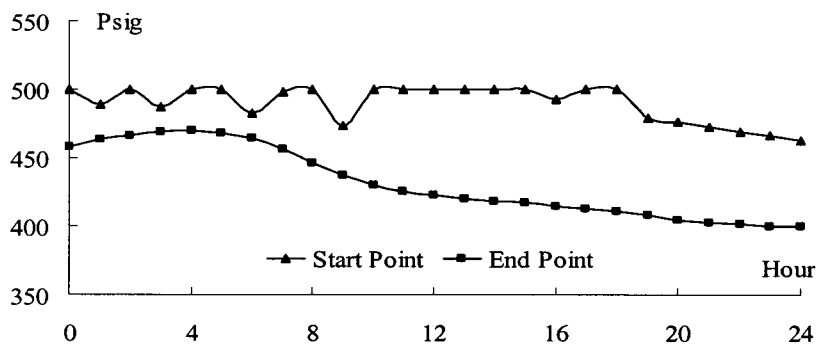

Figure 5.10. Hourly Pressure at Starting and Ending Points of the Pipeline in Case 3

By comparing the results of the above three cases, we notice that the steady-state model and the transient-state model may result in distinct results for coordinated scheduling of power and natural gas systems. The computing time of scheduling

coordination based on the transient-state model is higher that that based on the steady-state model as shown in Table 5.8.

Table 5.8. Computing Time in Case 1-3

Computing time	Case 1	Case 2	Case 3
	58s	115s	92s

5.6 Conclusions

This chapter develops a bilevel coordinated scheduling model for interdependent electricity and natural gas infrastructures. The transient nature of natural gas flow is considered in the proposed model. Natural gas pipeline are modeled as a set of partial differential equations. An implicit finite difference method is used to transform them into difference equations. It has been shown that the proposed decomposition methodology and coordination scheme can be applied to solve the proposed coordinated scheduling problem effectively. Through several numerical study cases, we demonstrate that the steady-state model and the transient-state model of natural gas flow may result in different results for coordinated scheduling of interdependent electricity and natural gas systems. The steady-state gas flow model that neglects the storage nature of pipeline and slower travelling speed of gas flow may result in impractical results and non-optimal schedule in short term operation. The proposed coordinated scheduling model with transient-state gas transmission formulations can be widely used in daily operation scheduling, real time operation scheduling, and post-contingency rescheduling.

CHAPTER 6

SUMMARY

The natural gas and electric power infrastructures are coupled with each other in time and space due to the increasing number of natural gas fired power plants. To ensure more economical and secure services are provided to electricity and natural gas customers, it is envisioned that interdependent power and natural gas infrastructures need to consider an integrated approach for their operation and planning.

This dissertation proposes mode and component models for scheduling of general combined cycle gas turbine units. Testing experience shows that it is convenient to represent CCGTs into integrated scheduling model of natural gas and electricity systems.

This dissertation adopts different coordination schemes between natural gas system and electric power system. By using different proposed coordination models, we can either minimize operating cost of individual system or pursue least integral social cost while satisfying both natural gas and power system security and network constraints. Extremely general system equations and performance criteria can be handled and multiple type constraints of a wide variety present no difficulties.

Discrete variables and nonlinear network formulations may bring difficulties to solution of integrated models. In this dissertation, it has been shown that decomposition methodologies can be applied to integrated optimization problems to avoid the computational complexity when solving the proposed large-scale optimization problem with complex coupled infrastructures.

Electricity and natural gas energy are transported through infrastructures by different ways and time frames. Both steady state and transient state formulations of

natural gas transmission system are applied in the integrated scheduling model. Compared to steady state model, transient state model can result in more accurate results especially for high pressure interstate pipelines, but requires longer computing time and more computing resources.

In the future, the focus would be on studying long term interdependency and reliability model of electricity and natural gas infrastructures on the foundation of short term models proposed in this dissertation.

APPENDIX A

6 BUS ELECTRIC POWER AND 7 NODE NATURAL GAS TESTING SYSTEMS

Table A.1. Parameters of Generators of 6 Bus System

Unit	Af (MBtu/MW2h)	Bf (MBtu/MWh)	Cf (MBtu/h)	Contract Gas Price ($/MBtu)	Initial MW
G1	0.0004	13.51	176.95	6.2345	150
G2	0.001	32.63	129.97	6.2305	50
G3	0.005	17.70	137.41	6.231	0

Table A.2. Parameters of Generators of 6 Bus System

Unit	Pmin (MW)	Pmax (MW)	Ramp (MW/h)	Min On (h)	Min Off (h)	Initial hour
G1	100	220	55	4	4	4
G2	10	100	50	2	3	2
G3	10	20	20	1	1	-1

Table A.3. Parameters of Power Transmission Branch of 6 Bus System

Branch	From Bus	To Bus	R (p.u.)	X (p.u.)	Flow Limit (MW)
Line 1	1	2	0.005	0.17	200
Line 2	1	4	0.003	0.258	100
Line 3	2	4	0.007	0.197	100
Line 4	5	6	0.002	0.14	100
TF1	2	3	0	0.037	100
TF2	4	5	0	0.037	100
PS1	3	6	0.0005	0.018	100

Table A.4. Parameters of Tap-changing Transformer and Phase-shifter of 6 Bus System

Line No.	From Bus	To Bus	Tap Min	Tap Max	Angle min	Angle Max
TF1	2	3	1.0204	1.0753	0	0
TF2	4	5	1.0204	1.0753	0	0
PS1	3	6	0	0	-30	30

Table A.5. Distribution Factor of Electricity load of 6 Bus System

Load	1	2	3
Bus No.	3	4	5
Factor	0.2	0.4	0.4
Price of Load Shedding ($/MW)	1000	1000	1000

Table A.6. Electricity Load Data of 24 Hour of 6 Bus System

Hour	Load (MW)	Hour	Load (MW)	Hour	Load (MW)	Hour	Load (MW)
1	175.19	7	173.39	13	242.18	19	245.97
2	165.15	8	190.40	14	243.60	20	237.35
3	158.67	9	205.56	15	248.86	21	237.31
4	154.73	10	217.20	16	255.79	22	227.14
5	155.06	11	228.61	17	256	23	201.05
6	160.48	12	236.10	18	246.74	24	196.75

Table A.7. Parameters of Nodes in Gas Transmission System of 6 Bus System

Node No.	Min-Pressure (Psig)	Max-Pressure (Psig)
1	105	150
2	140	170
3	150	195
4	70	100
5	150	200
6	160	240
7	100	140

Table A.8. Parameters of Gas Pipeline of 6 Bus System

Index	From Node	To Node	C (kcf/Psig)
Pipe 1	1	2	50.6
Pipe 2	2	5	37.5
Pipe 3	5	6	45.3
Pipe 4	3	5	43.5
Pipe 5	4	7	50.1

Table A.9. Parameters of Natural Gas Compressor of 6 Bus System

Index	Inlet Node	Outlet Node	α	K1	K2	Rmin	Rmax
C1	4	2	0.25	0.165	0.1	1.6	2.45

Table A.10. Parameters of Natural Gas Compressor of 6 Bus System

Index	a (MBtu/ MW^2h)	b (MBtu/MWh)	c (MBtu/h)	Node	Hmin	Hmax
C1	0	0.2	50	2	400	600

Table A.11. Parameters of Natural Gas Supplier of 6 Bus System

Supplier No.	Node No.	Min Output (kcf/h)	Max Output (kcf/h)
1	7	5300	5300
2	6	1000	6000

Table A.12. Parameters of Gas Load of 6 Bus System

Load No.	Node No.	Distribution Factor	Service Priority
1	1	Gas consumption of G1	low
2	1	2/3 of Residential gas load	high
3	3	Gas consumption of G3	low
4	3	1/3 of Residential gas load	high
5	2	Gas consumption of G2	low

Table A.13. Residential Gas Load Data in Case 2 of 6 Bus System

Hour	Gas Load (kcf)
1-24	6000

Table A.14. Residential Gas Load Data of 24 Hour in Case 5 of 6 Bus System

Hour	Gas Load (kcf/h)	Hour	Gas Load (kcf /h)	Hour	Gas Load (kcf /h)	Hour	Gas Load (kcf/h)
1	5220	7	5580	13	6000	19	6540
2	4920	8	6060	14	5700	20	6780
3	4680	9	6180	15	5760	21	6660
4	4740	10	6240	16	5880	22	6540
5	5100	11	6120	17	6060	23	6060
6	5640	12	6120	18	6240	24	5520

Table A.15. Parameters of Self-Owned Storage Facility of 6 Bus System

SV at hour 0 (kcf)	SVmin (kcf)	SVmax (kcf)	SV at hour 24 (kcf)
5000	5000	15000	5000

APPENDIX B

ELEMENTS OF JACOBIAN MATRIX IN CALCULATION OF NATURAL GAS STEADY STATE FLOW

For natural gas pipelines,

$$\text{If } \pi_{na} > \pi_{nb} > 0,\ Gf_{nanb} = C_{nanb}\sqrt{\pi_{na}^2 - \pi_{nb}^2} \text{ then, } \frac{\partial Gf_{nanb}}{\partial \pi_{na}} = \frac{C_{nanb}\pi_{na}}{\sqrt{\pi_{na}^2 - \pi_{nb}^2}}$$

$$\text{If } \pi_{nb} > \pi_{na} > 0,\ Gf_{nanb} = -C_{nanb}\sqrt{\pi_{nb}^2 - \pi_{na}^2} \text{ then, } \frac{\partial Gf_{nanb}}{\partial \pi_{na}} = \frac{C_{nanb}\pi_{na}}{\sqrt{\pi_{nb}^2 - \pi_{na}^2}}$$

$$\text{If } \pi_m = \pi_n > 0,$$

$$\left.\frac{\partial Gf_{nanb}}{\partial \pi_{na}}\right|_{\pi_{na}^+} = \lim_{\Delta\pi \to 0^+} \frac{C_{nanb}[\mathrm{sgn}(\pi_{na} + \Delta\pi, \pi_{nb})\sqrt{(\pi_{na} + \Delta\pi)^2 - \pi_{nb}^2} - \mathrm{sgn}(\pi_{na}, \pi_{nb})\sqrt{\pi_{na}^2 - \pi_{nb}^2}]}{\Delta\pi}$$

$$= \lim_{\Delta\pi \to 0^+} \frac{C_{nanb}\sqrt{2\pi_{na}\cdot\Delta\pi + \Delta\pi^2}}{\Delta\pi} = +\infty$$

$$\left.\frac{\partial Gf_{nanb}}{\partial \pi_{na}}\right|_{\pi_{na}^-} = \lim_{\Delta\pi \to 0^-} \frac{C_{nanb}[\mathrm{sgn}(\pi_{na} + \Delta\pi, \pi_{nb})\sqrt{\pi_{na}^2 - (\pi_{nb} + \Delta\pi)^2} - \mathrm{sgn}(\pi_{na}, \pi_{nb})\sqrt{\pi_{na}^2 - \pi_{nb}^2}]}{\Delta\pi}$$

$$= \lim_{\Delta\pi \to 0^-} \frac{-C_{nanb}\sqrt{-2\pi_{na}\cdot\Delta\pi - \Delta\pi^2}}{\Delta\pi} = \lim_{\substack{\Delta\delta \to 0^+ \\ \Delta\delta = -\Delta\pi}} \frac{C_{nanb}\sqrt{2\pi_{na}\cdot\Delta\delta - \Delta\delta^2}}{\Delta\delta} = +\infty$$

In order to avoid numerical instability, we assign a large constant M or –M when π_{na} and π_{nb} are very close. Hence,

$$\frac{\partial Gf_{nanb}}{\partial \pi_{na}} = \begin{cases} M, & \left|\pi_{na}^2 - \pi_{nb}^2\right| < \varepsilon \\ \dfrac{C_{nanb}\pi_{na}}{\sqrt{\left|\pi_{na}^2 - \pi_{nb}^2\right|}}, & \left|\pi_{na}^2 - \pi_{nb}^2\right| \geq \varepsilon \end{cases} \tag{B.1}$$

Similarly,

$$\frac{\partial Gf_{nanb}}{\partial \pi_{nb}} = \begin{cases} -M, & \left|\pi_{na}^2 - \pi_{nb}^2\right| < \varepsilon \\ \dfrac{-C_{nanb}\pi_{nb}}{\sqrt{\left|\pi_{na}^2 - \pi_{nb}^2\right|}}, & \left|\pi_{na}^2 - \pi_{nb}^2\right| \geq \varepsilon \end{cases} \tag{B.2}$$

For compressors, If node m is the inlet of compressor, then $\pi_{nb} > \pi_{na} > 0$ (or $1 < PR_{\min,cm} \le \frac{\pi_{nb}}{\pi_{na}} \le PR_{\max,cm}$), $Gf_{nanb} = \frac{CH_{cm}}{k1_{cm}\left[\frac{\pi_{nb}}{\pi_{na}}\right]^{k3_{cm}} - k2_{cm}}$

Therefore,

$$\frac{\partial Gf_{nanb}}{\partial \pi_{na}} = \frac{k1_{cm} \cdot k3_{cm} \cdot CH_j \cdot \frac{\pi_{nb}^{\,k3_{cm}}}{\pi_{na}^{\,k3_{cm}+1}}}{\left[k1_{cm}\left(\frac{\pi_{nb}}{\pi_{na}}\right)^{k3_{cm}} - k2_{cm}\right]^2} \tag{B.3}$$

$$\frac{\partial Gf_{nanb}}{\partial \pi_{nb}} = \frac{-k1_{cm} \cdot k3_{cm} \cdot CH_j \cdot \frac{\pi_{nb}^{\,k3_{cm}-1}}{\pi_{na}^{\,k3_{cm}}}}{\left[k1_{cm}\left(\frac{\pi_{nb}}{\pi_{na}}\right)^{k3_{cm}} - k2_{cm}\right]^2} \tag{B.4}$$

$$\frac{\partial Gf_{nanb}}{\partial CH_{cm}} = \frac{1}{k1_{cm}\left(\frac{\pi_{nb}}{\pi_{na}}\right)^{k3_{cm}} - k2_{cm}} \tag{B.5}$$

If node n is the inlet of compressor, then $\pi_{na} > \pi_{nb} > 0$ (or $1 < PR_{\min,cm} \le \frac{\pi_{na}}{\pi_{nb}} \le PR_{\max,cm}$), $Gf_{nanb} = \frac{-CH_{cm}}{k1_{cm}\left[\frac{\pi_{na}}{\pi_{nb}}\right]^{k3_{cm}} - k2_{cm}}$

Thus,

$$\frac{\partial Gf_{nanb}}{\partial \pi_{na}} = \frac{k1_{cm} \cdot k3_{cm} \cdot CH_j \cdot \frac{\pi_{na}^{\,k3_{cm}-1}}{\pi_{na}^{\,k3_{cm}}}}{\left[k1_{cm}\left(\frac{\pi_{na}}{\pi_{nb}}\right)^{k3_{cm}} - k2_{cm}\right]^2} \tag{B.6}$$

$$\frac{\partial Gf_{nanb}}{\partial \pi_{nb}} = \frac{-k1_{cm} \cdot k3_{cm} \cdot CH_j \cdot \frac{\pi_{na}^{k3_{cm}}}{\pi_{nb}^{k3_{cm}+1}}}{\left[k1_{cm}\left(\frac{\pi_{na}}{\pi_{nb}}\right)^{k3_{cm}} - k2_{cm}\right]^2} \tag{B.7}$$

BIBLIOGRAPHY

[Als90] Alsac, O., Bright, J., Prais, M., & Stott, B. (1990). Further Developments in LP-based Optimal Power Flow. *IEEE Trans. Power Syst.*, *5*(3), 697–711,

[An03] An, S., Li, Q., & Gedra, T. W. (2003). Natural Gas and Electricity Optimal Power Flow. In *Proceedings of IEEE/PES Transmission and Distribution Conference and Exposition* (Vol. 1, pp. 7-12).

[Ave72] Avery, W., Brown, G. G., Rosenkranz, J. A., & Wood, R. K. (1992). Optimization of Purchase, Storage and Transmission Contracts for Natural Gas Utilities. *Operation Research*, *40*(3), 446-462.

[Ber78] Berard, G.P., & Eliason, B.G. (1978). An Improved Gas Transmission System Simultor. *Society of Petroleum Engineerrs Journal*, 18(6), 389-398.

[Ber95] Bertsekas, D. P. (1995). *Nonlinear Programming*. Belmont, Massachusetts: Athena Scientific.

[Bix07] Bixby, R., & Rothberg, E. (2007). Progress in Computational Mixed Integer Programming - A Look Back from the Other Side of the Tipping Point. *Annals of Operations Research, 149*, 7–41.

[Bje00] Bjelogrlic, M. (2000). Inclusion of Combined Cycle Plants into Optimal Resource Scheduling. In *Proc. IEEE PES Summer Meeting* (pp. 189–195).

[Boy02] Boyce, M. (2002). *Handbook for Cogeneration and Combined Cycle Power Plants*. New York, NY: ASME.

[Car06] Carrion, M., & Arroyo, J. (2006). A Computationally Efficient Mixed-Integerlinear Formulation for the Thermal Unit Commitment Proble. *IEEE Trans. Power Syst., 21*(3), 1371-1378.

[Che07] Chen, H., & Baldick, R. (2007). Optimizing Short-Term Natural Gas Supply Portfolio for Electric utility Company. *IEEE Trans. Power Syst., 22*(1), 232-239.

[Coh80] Cohen, G. (1980). Auxiliary Problem Principle and Decomposition of Optimization Problems. *Journal of Optimization Theory and Applications*, *32* pp. 277–305.

[Coh88] Cohen G., & Zhu, D. L. (1988). Decomposition Coordination Methods in Large Scale Optimization problems: The nondifferentiable case and the use of Augmented Lagrangian. *Advances in Large Scale Systems, Theory and Application*, *1*, 203-266. CT, USA: JAI Press Inc.

[Coh96] Cohen, A., & Ostrowski, G. (1996). Scheduling Units with Multiple Operating Modes in Unit Commitment. *IEEE Trans. Power Syst., 11*(1), 497-503.

[Con06] Conejo, A. J., & et al. (2005). *Decomposition Techniques in Mathematical Programming*. Springer.

[Cha] Chase, D. *Combined-cycle Development, Evolution, and Future*. Retrieved http://www.gepower.com/prod_serv/products/tech_docs/en/downloads/ger4206.pdf

[Dep08] Department of Energy. (2008). *20% Wind Energy by 2030.*

[Ehr03] Ehrhardt, K., & Steinbach, M. (2003). Nonlinear Optimization in Gas Networks. In *Konrad-Zuse-Zentrum fur Informationstechnik.* Berlin.

[Eia] EIA. *http://www.eia.doe.gov/.*

[Fu05] Fu, Y., Shahidehpour, M., & Li, Z. (2005). Security-constrained Unit Commitment with AC Constraints. *IEEE Trans. Power Syst., 20*(2), 1001-1013.

[Fu07] Fu, Y., & Shahidehpour, M. (2007). Fast SCUC for Large-scale Power Systems. *IEEE Trans. Power Syst.*, vol. 22, pp.2214-2151, Nov. 2007.

[Gao05] Gao, F., & Sheble G. (2005). Economic Dispatch Algorithms for Thermal Unit System Involving Combined Cycle Units. In *Proc. 15th Power Systems Computation Conference* (pp. 1-6).

[Gei07] Geidl, M., & Andersson, G. (2007). Optimal power flow of multiple energy carriers. *IEEE Trans. Power Syst., 22*(1), 145-155.

[Geo72] Geoffrion, A. M. (1972). Generalized Benders Decomposition. *J. Optim. Theory Appl., 10*(4), 237–261.

[Gil03] Gil, E., Quelhas, A., & McCally J. (2003). Modeling Integrated Energy Transportation Networks for Analysis of Economic Efficiency and Network Interdependencies. In *Proc. of North American Power Symposium.* Rolla, USA.

[Gua95] Guan, X., Luh, P.B., & Zhang L. (1995). Nonlinear Approximation Method in Lagrangian Relaxation-Based Algorithms for Hydrothermal Scheduling. *IEEE Trans. Power Syst., 10*(2), 772-778.

[Hec01] Hecq, S., Bouffioulx, Y., Doulliez, P., & Saintes, P. (2001). The Integrated Planning of the Natural Gas and Electricity Systems Under Market Conditions. In *Proc. IEEE Porto Power Tech Conference,* Porto Porfuga.

[Her09] Herran-Gonzalez, A., De La Cruz, J. M., De Andres-Toro, B., & Risco-Martin, J. L. (2009). Modeling and simulation of a gas distribution pipeline network. *Applied Mathematical Modeling, 33*, 1584-1600.

[Iea07] International Energy Agency. (2007). *Natural gas market review 2007: Security in a Globalizing Market to 2015*. Paris.

[Iso08a] ISO New England, (2008). *CIGRE 2008 Case Study: Electric & Natural Gas Market Interdependencies within New England.*

[Iso08b] ISO New England. (2008). *2007 Assessment of the Electricity Markets in New England.*

[Jer80] Jeroslow, R. G. (1980). A cutting-plane game for facial disjunctive programs. *SIAM J. Control and Opt., 18*(3), 264-281.

[Jon] Jones, C., & Jacobs III, J. *Economic and Technical Considerations for Combined-cycle Performance-enhancement Options.* Retrived http://www.gepower.com/prod_serv/products/tech_docs/en/downloads/ger4200.pdf

[Ke00] Ke, S. L., & Ti, H. C. (2000). Transient analysis of isothermal gas flow in pipeline network. *Chemical Engineering Journal, 76*, 169–177.

[Keh91] Kehlhofer, R. (1991). *Combined-Cycle Gas and Steam Turbine Power Plants*. Lilburn: Fairmont.

[Li05] Li, T., & Shahidehpour, M. (2005). Price-Based Unit Commitment: A Case of Lagrangian Relaxation Versus Mixed Integer Programming. *IEEE Trans. Power Syst., 20*(4), 2015-2025.

[Li08] Li, T., Eremia, M., & Shahidehpour, M. (2008). Interdependency of Natural Gas Network and Power System Security. *IEEE Trans. Power Syst., 23*(3), 1817-1824.

[Liu09a] Liu, C., Shahidehpour, M., Li, Z., & Fotuhi-Firuzabad, M. (2009). Component & Mode Models for Short-term Scheduling of Combined- Cycle Units. *IEEE Trans. Power Syst., 24*(2), 976-990.

[Liu09b] Liu, C., Shahidehpour, M., Fu, Y., & Li, Z. (2009). Security-Constrained Unit Commitment with Natural Gas Transmission Constraints. *IEEE Trans. Power Syst., 24*(3), 1523-1536.

[Lu05] Lu, B., & Shahidehpour, M. (2005). Unit Commitment with Flexible Generating Units. *IEEE Trans. Power Syst., 20*(2), 1022-1034.

[Mel06] Mello, O.D., & Ohishi, T. (2006). An integrated dispatch model of gas supply and thermoelectric generation with constraints on the gas supply. In *Proc. of X SEPOPE*. Florianopolis, SC, Brazil.

[Mer02] Mercado, R. R. (2002). *Natural Gas Pipeline Optimization, Handbook of Applied Optimization*. Oxford University Press.

[Mor03] Morais, M. S., & Marangon Lima, J. W. (2003). Natural Gas Network Pricing and Its Influlence on Electricity and Gas Marketis. In *2003 IEEE Bologna PowerTech Conference*. Bologna, Italy.

[Mun03] Munoz, J., Jimenez-Redondo N., Perez-Ruiz, J., & Barquin J. (2003). Natural gas Network Modeling for Power Systems Reliability Studies. In *Proceedings of IEEE/PES General Meeting* (Vol. 4, pp. 23-26).

[Nor02] North American Electric Reliability Council. (2002). *Reliability Assessment 2001-2011: The Reliablity of bulk Electric Systems in North America*.

[Nor04] North American Electric Reliability Council. (2002). *Gas/Electricity Interdependencies and Recommendations*.

[Nor07] North American Electric Reliability Council. (2007). *2007/2008 Winter Reliability Assessment*.

[Osi87] Osiadacz, A. J. (1987). *Simulation and Analysis of Gas Pipeline Networks*. London: E.& F.N. Spon.

[Osi96] Osiadacz, A. J. (1996). Different transient models- limitations, advantages and disadvantages. In *Proc. of the PSIG 28th Annual Meeting*. San Francisco,USA.

[Ouy96] Ouyang, L., & Aziz, K. (1996). Steady-state Gas Flow in Pipes. *Journal of Petroleum Science and Engineering*, *14*(3), 137-158.

[Pad08] Padberg, U., & Haubrich, H. (2008). Stochastic Optimization of Natural Gas Portolios. In *European Electricity Market, 2008 5th International Conference*.

[Pou03] Pourbeik, P. (2003). Modeling of Combined-cycle Power Plants for Power System Studies, In *Proc. 2003 IEEE PES General Meeting* (Vol. 3, pp. 1308-1313).

[Que06] Quelhas, A., Gil, E., & McCalley, J. D. (2006). Modal Prices in an Integrated Energy System. *International Journal of Critical Infrastructures*, *2*(1), 50-69.

[Que07] Quelhas, A., Gil, E., McCalley, J. D., & Ryan, S. M. (2007). A Multipeirod Generalized Network Flow Model of the U.S. Integrated Energy System: Part I-Model Despription. *IEEE Trans. Power Syst., 22*(2), 829-836.

[Ric79] O'Neill, R. P., Williard, R., Wilkins, B., & Pike, R. (1979). A Mathematical Programming Model for Allocation of Natural Gas. *Operation Research, 27*(5), 857-875.

[Rub08] Rubio, R., Ojeda-Esteybar, D., Añó, O., & Vargas, A. (2008). Integrated natural gas and electricity market: A Survey of the State of the Art in Operation Planning and Market Issues. In *IEEE/PES Transmission and Distribution Conference and Exposition*. Chicago, USA.

[Sha01] Shahidehpour, M., & Alomoush, M. (2001). *Restructured Electrical Power Systems*. New York: Marcel Dekker.

[Sha02] Shahidehpour, M., Yamin, H., & Li., Z. Y. *Market Operations in Electric Power Systems*. New York: Wiley.

[Sha03] Shahidehpour, M., & Wang, Y. (2003). *Communication and Control of Electric Power Systems*. New York: Wiley.

[Sha05] Shahidehpour, M., Fu, Y., & Wiedman, T. (2005). Impact of Natural Gas Infrastructure on Electric Power Systems. *Proc. of the IEEE, 93*, 1042-1056.

[Sto72] Stoner, M. A. (1972). Sensitivity Analysis Applied to A Steady-state Model of Natural Gas Transmission System. *Society of Petroleum Engineerrs Journal, 12*(2), 115-125.

[Str05] Streeiffert, D., Philbrick, P., & Ott, A. (2005). A Mixed Integer Programming Solution for Market Clearing and Reliability Analysis. In *IEEE PES General Meeting* (Vol. 3, pp.2724-2731).

[Tom07] Tomasgard, A., Rømo, F., Fodstad, M., & Midthun, K. (2007). Optimization Models for the Natural Gas Value Chain. In *G. Hasle, K.-A. Lie and E. Quak, Geometric Modeling, Numerical Simulation, and Optimization: Applied Mathematics at SINTEF.* Springe.

[Urb07] Urbina, M., & Li, Z. (2007). A Combined Model for Analyzing the Interdependency of Electrical and Gas System. In *Power Symposium, NAPS '07. 39th North American.*

[Uns07a] Unsihuay, C., Marangon Lima, J. W., & Zambroni de Souza, A. C. (2007). Modeling the Integrated Natural Gas and Electricity Optimal Power Flow. In *Proceedings of IEEE/PES General Meeting* (pp. 24-28).

[Uns07b] Unsihuay, C., Marangon Lima, J. W., & Zambroni de Souza, A.C. (2007). Short-term Operation Planning of Integrated Hydrothermal and Natural Gas Systems. In *Proceedings of IEEE/PES Power Tech Conferenc.*

[Uns07c] Unsihuay, C., Marangon Lima, J. W., & Zambroni de Souza, A.C. (2007). Integrated power generation and natural gas expansion planning. In *Proc. IEEE Power Eng. Soc. PowerTech.* Lausanne, Switzerland.

[Wil99] Williams, H. (1999). *Model Building in Mathematical Programming* (4th edition). Wiley.

[Wol98] Wolsay, L. A. (1998). *Integer Programming.* Wiley.

[Wol00] Wolf, D., & Smeers, Y. (2000). The Gas Transmission Problem Solved by an Extension of the Simplex Algorithm. *Management Science, 46*(11), 1454-1465.

[Won68] Wong, P. J., & Larson, R. E. (1968). Optimization of Natural-Gas Pipeline Systems via Dynamic Programming. *IEEE Trans. Automatic Control, 13*(5), 475-481.

[Woo96] Wood. A. J., & Wollenberg, B. F. (1996). *Power Generation, Operation and Control* (2nd edition). John Wiley & Sons.

[Zha02] Zhai, Q., Guan, X., & Cui, J. (2002). Unit Commitment With Identical Units: Successive Subproblem Solving Method Based on Lagrangian Relaxation. *IEEE Trans. Power Syst., 17*(4), 1250-1257.

[Zha93] Zhang, L., Luh, P. B., Guan, X., & Merchel, G. (1993). Optimization-Based Inter-Utility Power Purchase. In *Proceedings of 1993 IEEPPICA Conference* (pp. 285-291). Scottsdale, Arizona.

[Zha99] Zhao, X., Luh, P.B., & Wang, J. (1999). Surrogate Gradient Algorithm for Lagrangian Relaxation. *Journal of Optimization Theory and Applications, 100*(3), 857-875.